CENTER FOR INFRASTRUCTURE ENGINEERING STUDIES

Anchorage System for Externally Bonded FRP Laminates Using Near Surface Mounted FRP Rods

by

Stephen C. Gose

Antonio Nanni

University of Missouri-Rolla

DRAFT 2, February 2000

CIES 99-7

Disclaimer

The mission of CIES is to provide leadership in research and education for solving society's problems affecting the nation's infrastructure systems. CIES is the primary conduit for communication among those on the UMR campus interested in infrastructure studies and provides coordination for collaborative efforts. CIES activities include interdisciplinary research and development with projects tailored to address needs of federal agencies, state agencies, and private industry as well as technology transfer and continuing/distance education to the engineering community and industry.

Center for Infrastructure Engineering Studies (CIES)
University of Missouri-Rolla
223 Engineering Research Lab
1870 Miner Circle
Rolla, MO 65409-0710
Tel: (573) 341-6223; fax -6215
E-mail: cies@umr.edu
www.umr.edu/~cies

ABSTRACT

As the worlds infrastructure begins to age, it is becoming more and more necessary to rehabilitate these structures, it has also become necessary to retrofit structures so that they meet new seismic design codes. Traditional materials such as concrete and steel have been used to perform these upgrades, but recently with increases in technology, fiber reinforced polymers (FRP) have been leading the field in the rehabilitation and retrofit of in-situ structures.

Recently the use of FRP for the external reinforcement of concrete has become widely used. The system has proven to be effective, but the bond length and anchorage of the end of the sheets has been a concern when strengthening structures in shear or flexure. To address the end anchorage, test have been conducted using steel plates to anchor the sheets but they are only effective in the laboratory, because of corrosion problems.

This report looks at an anchorage system using all FRP materials. A system that is totally composite removes the possibility of corrosion problems with the environment and electrical incompatibility between steel anchors and Carbon FRP materials. The system looked at in this report also reduces the amount of stress concentration at the anchor location.

For this experiment, the goal was to characterize the anchor by looking at anchor bar size, groove size, location, and bar width. A total of eighteen (18) specimens were tested with parameters changing to represent all the variables. The specimens were all prepared by the same method and tested in the same testing apparatus. During the tests, load, strain, and center deflection were measured using a computerized data collection system.

The results of the tests show that the anchor system increases the ultimate capacity of the FRP system by as much as 48%. The results show that this anchorage system is effective and can easily be transferred to conditions in the field.

ACKNOWLEDGEMENTS

I would like to thank the National Science Foundation Industry/University Cooperative Research Center, for providing an environment to do undergraduate research. Special thanks also goes out to those companies who have provided the financial assistance and supplies to make a project like this possible, Master Builders, Inc., Marshall Industries Composites, Inc.

I would also like to express my appreciation to Dr. Antonio Nanni for his guidance and the opportunity to complete this research. The following individuals at the Center for Infrastructure Engineering Studies, have also put in numerous hours, and without them this project would not have been a success; Ahmed Khalifa, Steve Gabel, Tarek Alkhrdaji, Brian Miller, Steve Schiebel, Matt Mettemeyer, Charles Strauss, Laura DeLorenzis and Davide Tinazzi.

TABLE OF CONTENTS

LIST OF FIGURES

LIST OF TABLES

1. INTRODUCTION

1.1 BACKGROUND AND PROBLEM STATEMENT

As a response to corrosion problems in reinforcing steel, and to increase the efficiency of strengthening work in terms of time and ease of application, professionals have turned to alternative materials such as fiber reinforced polymer (FRP) composites. FRP materials can be produced in many shapes; the most popular are FRP reinforcing bars and FRP unidirectional continuous fiber sheets. FRP sheets may be used to provide additional flexural strength in beams or slabs, additional shear strength in beams or columns, or confinement and additional ductility in columns. Among many other applications, concrete and masonry walls may be strengthened to better resist seismic and wind loads (Nanni et al., 1998). Although the use of these materials has been implemented in many strengthening projects all around the world, there has always been the concern of the end anchorage of FRP sheets. This is particularly important when the length of the sheets is restricted, and the bonded length beyond the critical section is not sufficient to achieve the ultimate strength of the FRP sheet. Some of the possible field applications of FRP with an end anchor are studied in this project, are shown in Figure 1.1. Anchorage problem is a major concern when using FRP sheets for shear strengthening of T- sections. In this case, FRP sheets are applied to the sides of the web with the fibers being perpendicular to the axis of the beam. It has been shown that the anchorage of the ends of the sheets with steel plates and bolts is effective and can increase the shear capacity of RC members (Katasumata and Kobatake, 1997). In fact, it was observed that the shear capacity of members can be increases by more that 50% when the reinforcement is anchored (Sato et al., 1997). Mechanical anchorage with steel materials, although effective in the laboratory, is not practical for field applications due to certain drawbacks such as: steel corrosion, electrical incompatibility between steel and Carbon FRP materials, stress concentrations, and in the case of bolting, discontinuity of the FRP at drilling locations. A more effective sheet anchoring system could be achieved if FRP materials were used to anchor the sheets. The design and lab verification of such a system is the subject of this proposal.

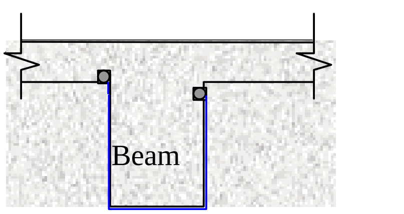

(a) Two options for anchorage of web shear strengthening of beams.

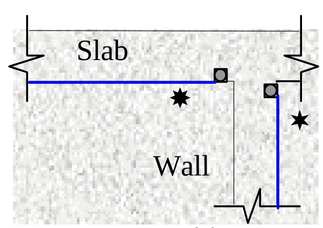

(b) ✶Anchorage of flexural or shear strengthening in walls and ✸ Anchorage of flexural strengthening in slabs or beams

Figure 1.1. Examples of Applications for the Proposed Anchorage System, further detail shown in Figure 1.2

1.2 PREVIOUS WORK

Experimental work has been carried out previously to determine the effectiveness of such an anchor system. One example is work done by Ahmed Kalifa to determine to feasibility of the system (Kalifa, et al, 1999). The results of the experiment showed that the anchorage system increased the ultimate capacity of Reinforced Concrete Beams strengthened in shear with CFRP. An increase of 145% was shown over a beam with no shear reinforcement, and a 45% increase compared to a beam strengthened with CFRP but no anchor. Testing of the anchor system has also been completed on a building in St. Louis, Missouri in which floor joists were strengthened. The joists with a single wrap of FRP and the anchor system showed an increase in capacity of 2.5% a joist without the anchor system, the joists with a double wrap of FRP had an increase of 2.2% (Annaiah, et al, 1999).

1.3 OBJECTIVES

The objective of this project is to verify the feasibility of a system for anchoring FRP sheets to concrete using FRP materials. This anchorage system will be included in the development of design guidelines for concrete structures strengthened with FRP sheets. The following variables will be examined in order to determine the effectiveness of the proposed anchorage system: location of anchor, groove size, and diameter of FRP bar. For this study, only static load will be addressed. Other types of loading (e.g., repeated and sustained) can be pursued in future studies.

1.4 PROPOSED ANCHORAGE SYSTEM

The anchorage system consists of a groove perpendicular to the longitudinal axis of the fiber, located at the end of the FRP sheet, as shown in Figure 1.2. The groove is typically made by making two parallel saw cuts on the concrete surface and then chipping out the concrete in between. One corner of the groove is rounded to a minimum radius of 0.5 in (12.7 mm). This will reduce the stress concentration at the corner and hence prevent premature breakage of the FRP sheet. The groove is then cleaned with pressured air to remove all loose materials. After the FRP sheet is attached to the concrete surface and in the groove, the groove is filled half way with epoxy paste. Then an FRP bar, with a length equal to the width of the sheet, is placed in the groove and slightly pressed in place, allowing the paste to flow around the bar and cover the inside of the groove. The groove is then filled with the same epoxy paste to improve the anchorage mechanism.

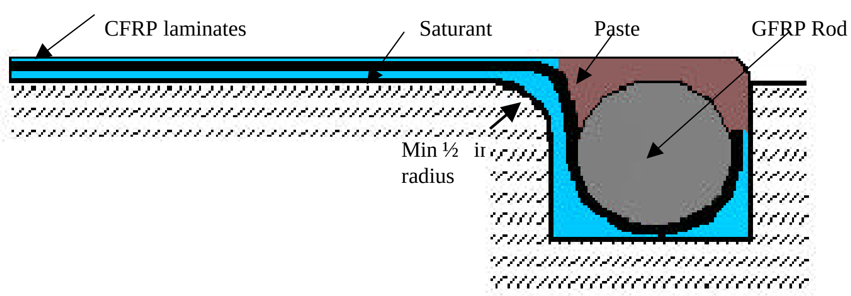

Figure 1.2. Anchorage Mechanism cross-section

2. CONSTITUENT MATERIALS

Four primary materials were used in the construction of the test specimen. The beam was made from plain concrete, CFRP sheets were used to reinforce the beam, GFRP rods were used to anchor the sheets, and epoxy based paste was used to bond the rods. Also, a primer and putty were used to prepare the concrete surface Each of the constituent materials along with the concrete beam will be discussed in this chapter.

2.1 CONCRETE BEAM

A local contractor prepared the concrete beams used in this study. A ready-mix concrete company supplied the concrete. The specified strength of the concrete to be used was 3000psi (20.68 Mpa). Concrete compression cylinders were made according to ASTM C 31 each time a set of beams was poured in order to determine the compressive strength of the concrete. All cylinders were tested in accordance with ASTM C 39, within two days of testing of the corresponding specimens. A minimum of three cylinders was tested for each batch, and the compressive strength of the concrete was taken as the average of the obtained values, these values ranged between 4010 psi (27.65 MPa) and 5475 psi (37.72 MPa). After the beams had cured for 10-14 days, the surface on which the CFRP was to be applied was sandblasted to remove the top layer of mortar, just until the aggregate was visible. The approximate depth of sandblasting was 0.06 in. (1.5 mm). Next, the beams were saw cut at midspan in order to force the beam to crack.

It was necessary to test two different anchor locations. The original specimen was used to test the anchor before the corner of a T-beam. To represent the anchor after the corner, a bump out was cast to the beam. The following sections discuss the dimensions of each beam configuration.

2.1.1 Flat Beams The dimensions of the specimen can be seen in Figure 2.1.

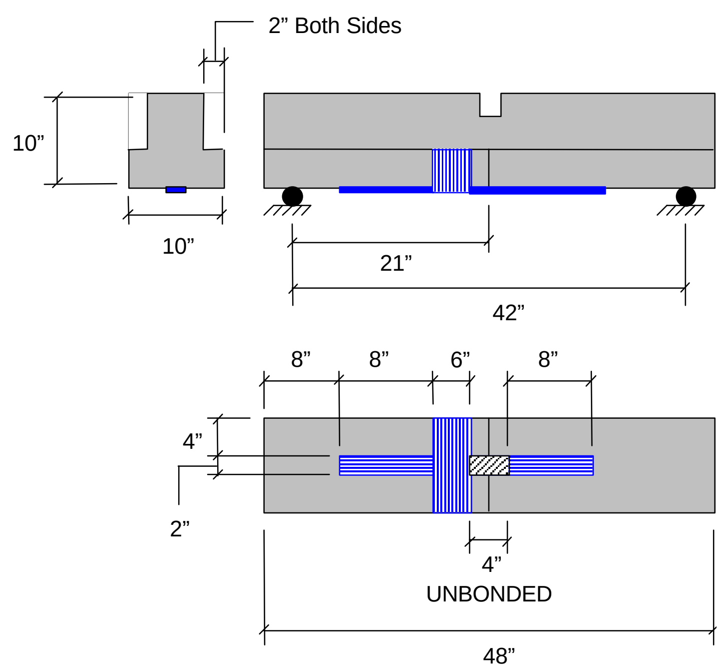

Figure 2.1. Dimensions and orientation of CFRP on flat beam (1 in = 25.4 mm)

2.1.2 Bump-Up Beams To modify the original specimen, a 3 in (76.2 mm) by 3 in (76.2 mm) by 10 in (254 mm) piece of concrete, was cast, with its face 8 in (203.2 mm) from the center line of the specimen. The specimen dimensions can be seen in Figure 2.2.

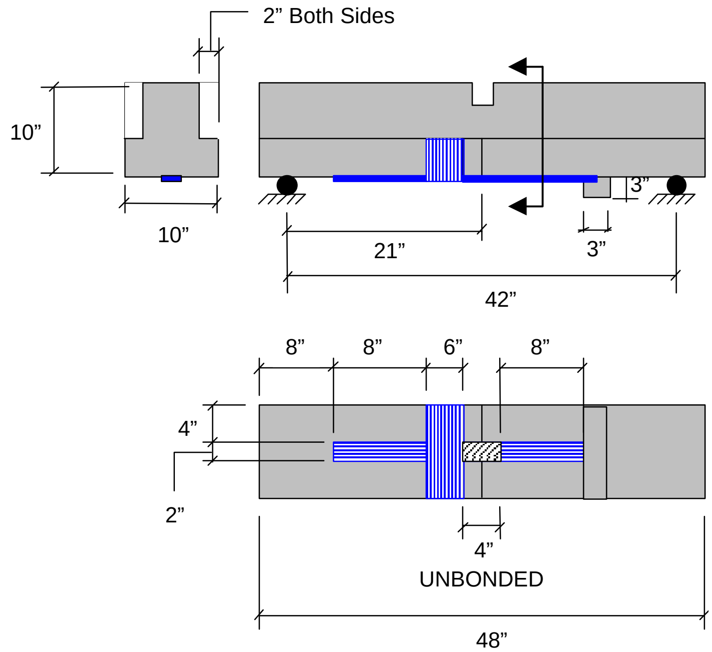

Figure 2.2. Dimensions and orientation of CFRP on beam with bump up (1 in = 25.4 mm)

2.2 CARBON FIBER SHEET

The MBrace Carbon system (MBrace, 1998) was used for this project. The type of sheet used in the testing was the MBrace CF-130. The manufacturer provided the information on the properties of this, unidirectional fiber sheet; they can be seen in Table 2.1. (Mbrace, 1998)

Table 2.1. Properties of Fiber Sheet

Fiber Tow Sheet	Ultimate Strength (ksi)	Design Strength (ksi)	Tensile Modulus (ksi)	Thickness (in)
High Tensile Carbon C130	620	550	33,000	0.0065

(Note: 1 ksi = 6.89 MPa; 1 in = 25.4 mm)

2.3 RESINS

There are three different resins used in the application of CFRP sheets to concrete, primer, putty, and saturant. The physical properties of these resins can be seen in Table 2.2 (MBrace, 1998). For this project, the method of mixing the resins was by volume. The properties of the resins in tension are shown in Table 2.3. The values shown are the theoretical values obtained from the manufacturer.

Table 2.2. Physical Properties of Epoxy Resins

Properties	Primer	Putty	Saturant
Color			
Part A	Amber	Tan	Blue
Part B	Clear	Charcoal	Clear
Mixed	Amber	Tan	Blue
Mix Ratio by Volume Part A/Part B	3/1	3/1	3/1
Mix Ratio by Mass Part A/Part B	100/30	100/30	100/34
Working Time at 77°F (25°C)	20 minutes	40 minutes	45 minutes

Table 2.3. Tension: Neat Resin Properties ASTM D-638

	Primer	Putty	Saturant
Maximum Stress psi (MPa)	2500 (17.2)	2200 (15.2)	8000 (55.2)
Stress at Yield psi (MPa)	2100 (14.5)	1900 (13.1)	7800 (53.8)
Stress at Rupture psi (MPa)	2500 (17.2)	2100 (14.5)	7900 (54.5)
Strain at Max. Stress	0.400	0.060	0.030
Strain at Yield	0.040	0.020	0.025
Strain at Rupture	0.400	0.070	0.035
Elastic Modulus psi (MPa)	104,000 (715)	260,000 (1790)	440,000 (3035)
Poisson's Ratio	0.48	0.48	0.40

2.4 COMPOSITE SYSTEM

Figure 2.1 shows the order of application in which the materials are applied. As can be seen, the first layer applied is the primer. It can be applied either by a brush or roller. The next layer is the putty, which is applied using a trowel. A layer of saturant is then placed on top of the putty. Next, the tow sheet is placed on the saturant followed by another layer of saturant. Normally, a protective coating is then placed on top, however; this is not necessary in the lab.

The thickness of each layer of resin and fiber sheet was determined in previous work conducted at the University of Missouri-Rolla (Tumialan, 1998). The method for determining the thickness of each layer was by a Scanning Electron Microscope (SEM). The SEM is a microscope that uses electrons rather than light to form an image. By employing a SEM, more control in the amount of magnification can be obtained. Figure 2.2 shows the resulting thicknesses obtained from the SEM.

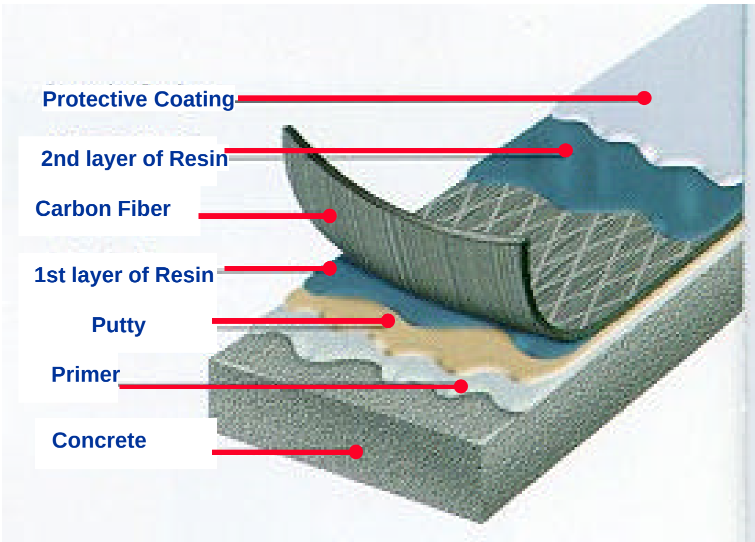

Figure 2.3. Application of FRP Sheets

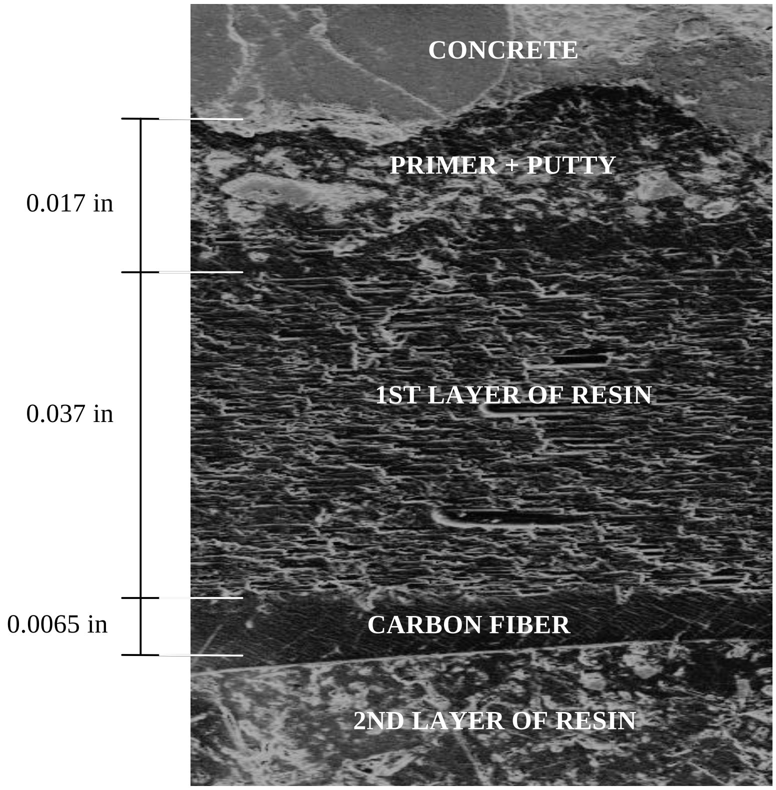

(Note: 1 in. = 25.4 mm)

Figure 2.4. Thickness of each Layer of Composite System

2.5 GLASS FRP ROD

GFRP deformed rods No. 3 and No. 4 commercially known with the name of C-Bar™ were supplied by Marshall Industries Composites Inc. These rebars are manufactured through the hybrid pultrusion/compression molding process. The outer core is composed of a sheet molding compound with chopped fiber mats embedded in urethane modified vinyl ester. The inner core is composed of unidirectional E-glass fibers embedded in recycled PET resin material (Marshall, 1998). Table 2.4 reports some of the properties of C-Bar™ No. 3 and No. 4 as specified by the manufacturer.

Table 2.4. Properties of C-Bar™

Bar Size	Nominal Diameter (in)	Cross-Sectional Area (in^2)	Tensile Strength (ksi)	Tensile Modulus (Msi)	Ultimate Strain (%)	Poisson's Ratio
No. 3	0.375	0.110	121	6	2.00	0.27
No. 4	0.500	0.196	116	6	1.90	0.27

(Note: 1 in = 25.4 mm, 1 in^2 = 645.2 mm^2, 1 ksi = 6.89 MPa)

2.6 EPOXY PASTE

The material used to embed the NSM FRP reinforcement in the grooves was an epoxy-based paste commercially known as Concresive Paste LPL, manufactured by Master Builders Technologies. Table 2.5 reports the mechanical properties of the paste, as specified by the manufacturer.

Table 2.5. Properties of Concresive Paste LPL

Tensile Strength (ASTM D 638) (psi)	2000
Elongation at Break (ASTM D 638) (%)	4
Compressive Yield Strength (ASTM D 695) (psi)	8000
Compressive Modulus (ASTM D 695) (ksi)	$4.0 \cdot 10^2$

(Note: 1 ksi = 6.89 MPa)

3. METHODOLOGY

3.1 INTRODUCTION

This section will discuss the procedure of the experimental phase of the research. It includes the selection, the preparation, and the actual testing of the specimens.

3.2 SPECIMEN SELECTION

The specimen for this test was chosen based on previous work (Miller, 1999). There were slight modifications made to represent the anchorage after the corner.

3.3 SPECIMEN PREPARATION

The preparation of the specimens for testing included surface preparation, application of CFRP sheets, and application of strain gauges. Surface preparation and application of CFRP sheets was performed in accordance with recommendations made by the manufacturer.

3.3.1. Surface Preparation. After the beams had cured properly, the surface where the CFRP sheets were to be applied was sandblasted. This was done in order to remove the laittance that forms at the finished surface of concrete. The machine used for sandblasting had a 90 cfm (2548 liter/min) air requirement, and was operated at 100-psi (689 kPa) air pressure with a 350-lb (1557 N) sand pot. The beam was sandblasted approximately 0.06 in (1.5 mm), which was just until the aggregate began to be exposed.

The beam was also saw cut at mid-span to create a weakened plane at which the beam would crack. The nominal depth of this cut was 2 inches (51 mm).

3.3.2. Groove Preparation. To create the groove for the anchor, a concrete saw was used to cut the concrete. A cut was made on each side of the groove, and then the material between was chiseled out. A grinder was then used to smooth the inside of the groove as well as to round the corner between the bonded length of FRP and the groove, this was done to limit the stress concentration at that point.

3.3.3. Application of the CFRP Sheet. There are three steps to applying a CFRP sheet. First, primer is applied to the concrete surface. Next, putty is used to level the surface. Then, a saturant layer, followed by the carbon sheet and another layer of saturant is applied.

The primer was applied, using a small paintbrush, to the area where the CFRP sheets were to be. The primer is used to fill the microscopic holes in the concrete. Next, putty was applied with a trowel to fill the larger holes and also to level the surface of the concrete. It was not necessary to allow the primer to dry before the putty was applied, but the putty was allowed to dry until it was tack free, before continuing the process.

After the putty had dried, a layer of saturant was rolled on top of the putty. The carbon sheet was then placed on the beam, and pressed into place. A plastic roller was then rolled over the surface to remove any air trapped under the sheet and to impregnate the saturant into the sheet. At this point it was imperative that the sheet in the anchor area was pushed by hand into the groove. A second layer of saturant was then rolled on the sheet and the plastic roller was used again to impregnate the saturant into the sheet.

3.3.4. Application of Anchorage System. Once the bonded region of the sheet was in place, the anchor had to be prepared. The groove was filled half way with concresive paste and then a glass FRP bar was pushed, firmly, by hand into the groove. Another layer of concresive paste was then placed in the groove and the surface was leveled off.

3.3.5. Application of Strain Gauges. After the CFRP sheet had been allowed to cure for at least three days, strain gauges were applied. The layout can be seen in Figure 3.1.

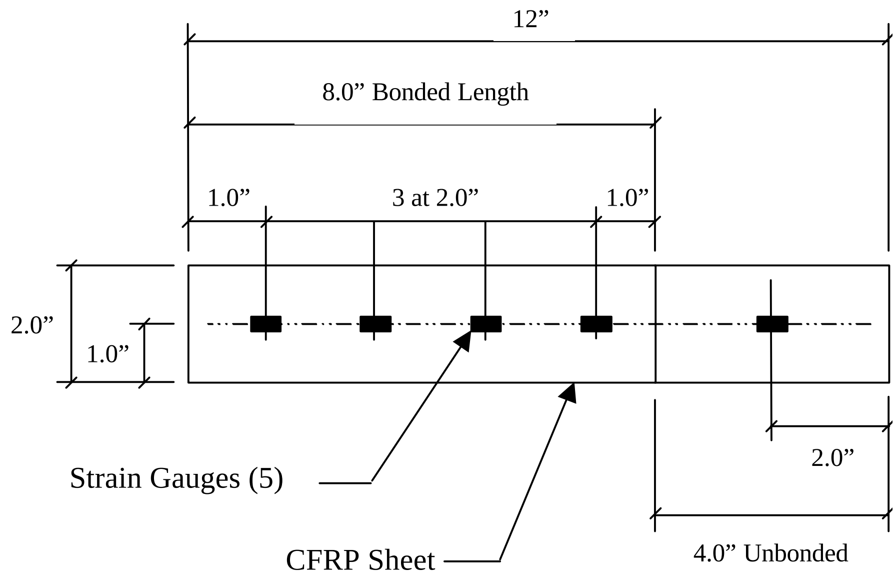

Figure 3.1. Placement of strain gauges (1 in = 25.4 mm)

3.4 TEST PROCEDURE

The FRP system was allowed to cure for a minimum of eleven (11) days prior to testing. The testing of the beams was performed on a Tinius-Olsen testing machine. An LVDT was used to measure the deflection at the center of the beam. The load, deflection and strain were all recorded at one-second intervals by a Labtech data acquisition system. A picture of the test setup can be seen Figure 3.2.

The testing was performed by first loading the beam until a crack formed at mid-span of the beam, and then unloaded to 500 lbs (2.22 kN). Load was then applied until failure resulted.

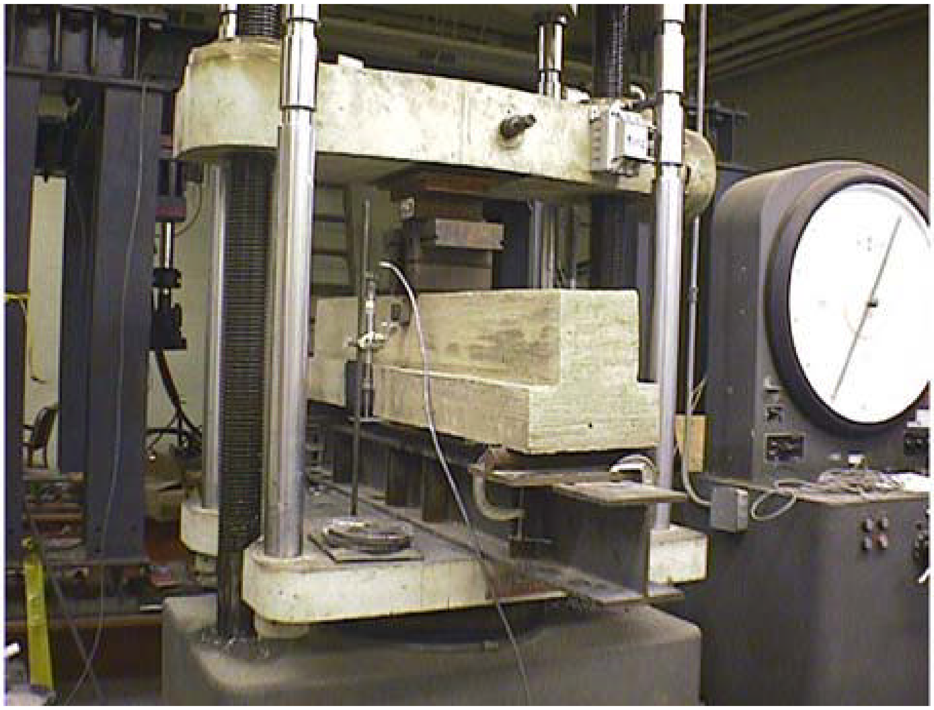

Figure 3.2. Picture of Test setup

3.5 SUMMARY OF TEST SPECIMENS

There was a total of sixteen (16) specimens tested, Table 3.1 shows the parameters of each specimen. Each specimen had a target concrete compressive strength of 3000 psi (20.67 MPa). Bar sizes are standard US bar sizes, a No. 3 bar has a 3/8 in (9.53 mm) diameter. Groove size is based either on 1.5 or 2.5 times the bar diameter.

The specimens are labeled based on their parameter, for example the A-0-1 is anchored after the corner, has no bar, and a groove size of 9/16 in (14.29 mm). The specimen labeled B-3-2 is anchored before the corner, has a No. 3 bar, and a groove size of 15/16 in (23.81 mm). If the label has a lower case 'a' after the last number, it is a repeat test. The specimen labels ending in 'u' have an unbonded length, only the anchor is bonded.

Table 3.1. Test Matrix of Specimens

Specimen No.	Anchor Location	Bar Size (#)	Groove Size (in)	Special Conditions
A-0-1	After the Groove	0	9/16	
A-3-1		3	9/16	
A-3-2		3	15/16	
A-4-3		4	3/4	
A-4-3a		4	3/4	retest
A-3-1-u		3	9/16	Unbonded length
A-3-2-u		3	15/16	Unbonded length
A-3-1-4		3	9/16	4” anchor bar
B-0-1	Before the Groove	0	9/16	
B-0-1a		0	9/16	retest
B-3-1		3	9/16	
B-3-2		3	15/16	
B-4-3		4	3/4	
B-4-3a		4	3/4	retest
B-3-1-u		3	9/16	Unbonded length
B-3-2-u		3	15/16	Unbonded length

(Note: 1in = 25.4 mm)

The target compressive strength for the beams was 3000 psi (20.67 MPa), Table 3.2 shows the actual compressive strengths of the specimens.

Table 3.2. Compressive Strength of Concrete Beams

Specimen	Compressive Strength (psi)		Specimen	Compressive Strength (psi)	
	Target	Actual		Target	Actual
B-0-1	3000	4220	A-0-1	3000	5475
B-3-1			A-3-1		
B-3-2			A-3-2		
B-4-3			A-4-3		
B-0-1a	3000	4010	A-4-3a	3000	4460
B-4-3a			A-3-1-u		
B-3-1-u			A-3-2-u	3000	4320
B-3-2-u			A-3-1-4		

(Note: 1 psi = 6.89 kPa)

4. EXPERIMENTAL RESULTS

4.1 INTRODUCTION

This section will discuss the results of the laboratory tests. The data plots will be discussed first, followed by tables showing the ultimate load of each test, and the failure mode.

4.2 LOAD VS DEFLECTION GRAPHS

The load versus deflection was plotted for each test; this shows the vertical displacement with change in load. Figure 4.1 is a typical plot, with the load in pounds on the vertical axis and the deflection in milli inches plotted on the horizontal axis. The deflection is as recorded from the LVDT and does not account for settlement.

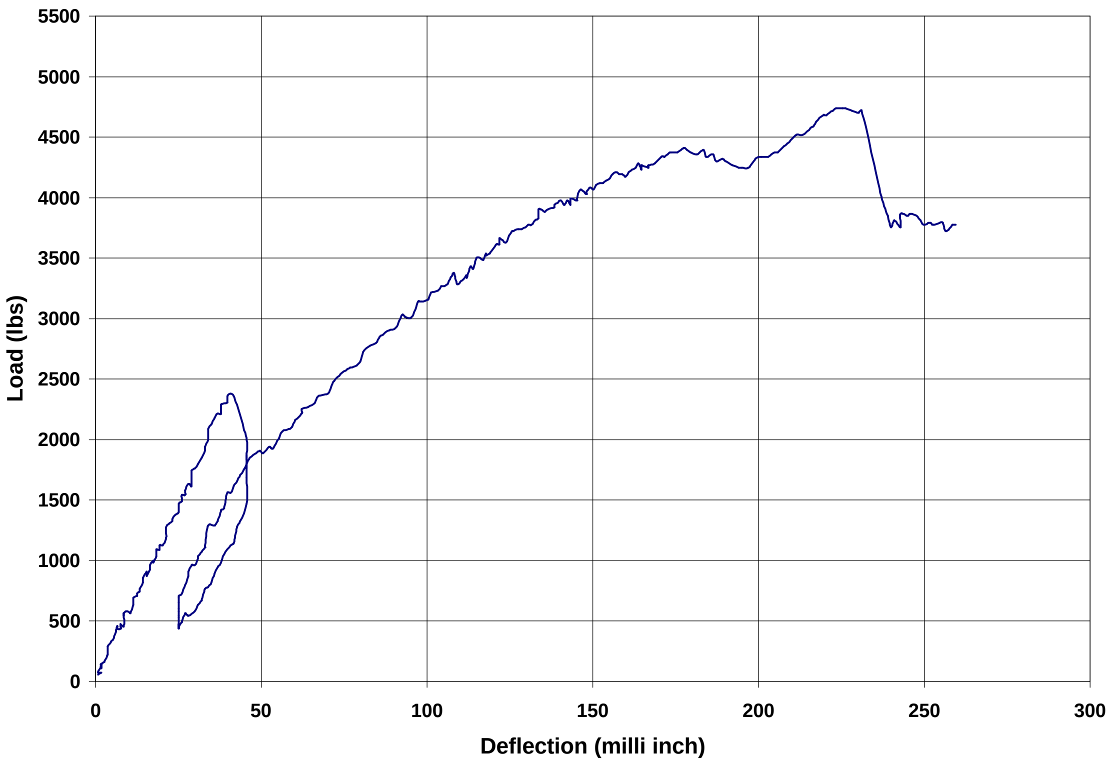

Figure 4.1. Typical Load vs. Deflection plot (B-3-1)
(1 in = 25.4 mm, 1 lb = 4.448 N)

4.3 LOAD VS STRAIN GRAPHS

The second plot, is the load versus the strain in each strain gauge; a typical plot is shown in Figure 4.2. On most plots, there are five curves which represent the five strain gauges on each specimen. Strain 1 is the values for strain gauge 1 which is located at the saw cut, as strain numbers increase so does their distance from the saw cut. For every specimen but those ending in ‘u’, strain 2 is 3 in (76.2 mm) from the saw cut, 1 in (25.4 mm) into the bonded region, and each following strain is 2 in (50.8 mm) from the proceeding gauge, this can be seen in Figure 3.1. The specimens ending in ‘u’ have only two gauges, so strain 2 is 8.5 in (215.9 mm) from the saw cut.

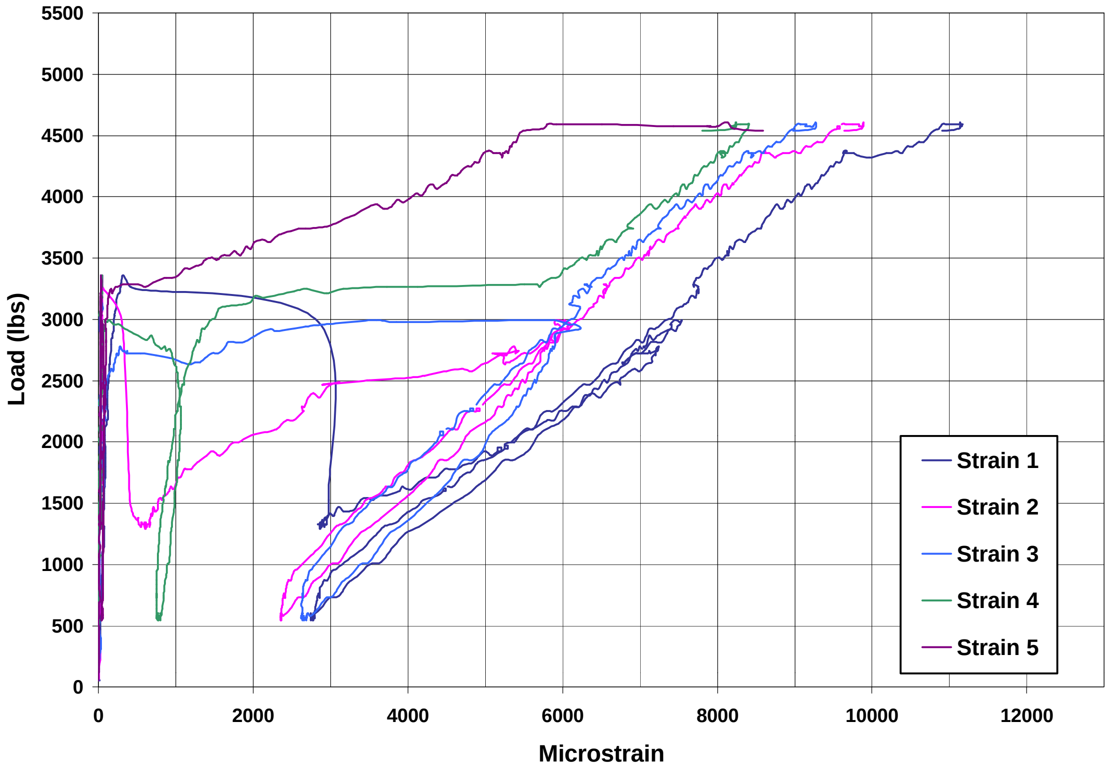

Figure 4.2. Typical Load vs. Strain plot (A-0-1)
(1 lb = 4.448 N)

4.4 STRAIN VS POSITION GRAPHS

The final plot is that of strain versus position of the gauge, Figure 4.3 show a typical plot. The stress distribution along the length of the FRP sheet can be seen from these plots. If the end of the sheet was not anchored, the strain at the end of the sheet would be zero (0), but with the anchor, it can be seen that strain develops throughout the entire length of the sheet. The first curve is for a 1000 lb (4.448 kN) load, followed by the 2000 lb (8.896 kN) load and proceeding as shown in the graphs legend.

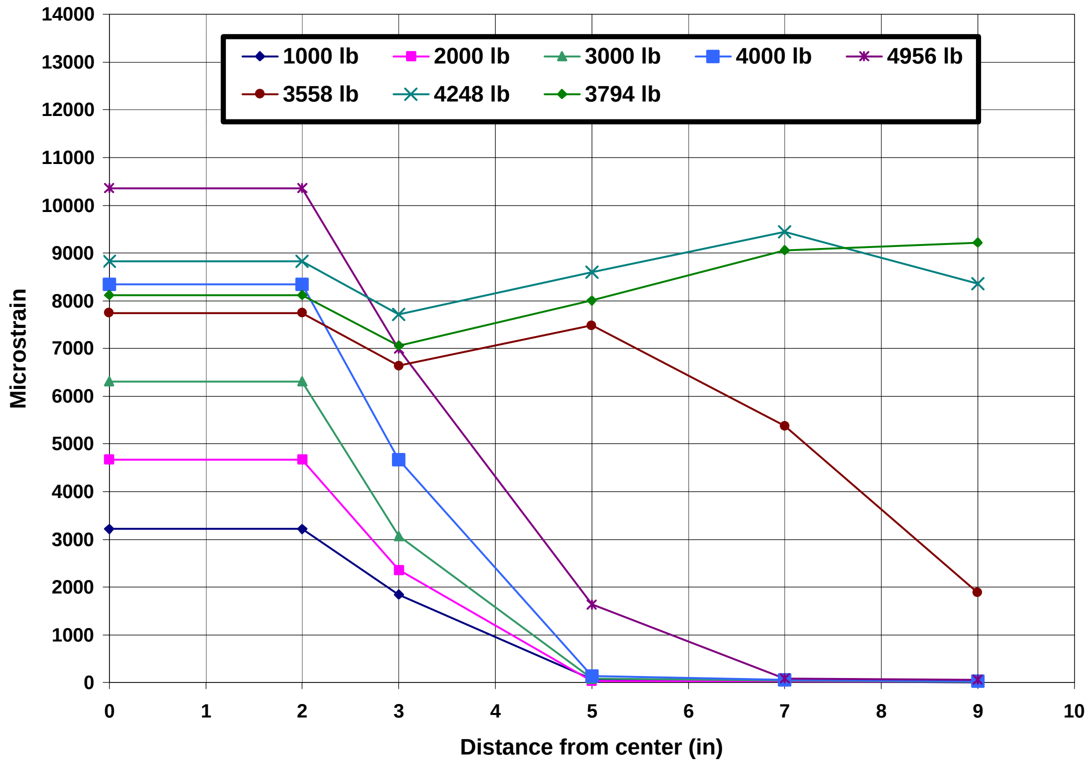

Figure 4.3. Typical Strain vs. Position plot (B-3-2)
(1 in = 25.4 mm, 1 lb = 4.448 N)

4.5 TEST RESULTS

The following tables show the results of the tests. Table 4.1, shows the ultimate load and the failure mode for each test.

Table 4.1. Ultimate Load and Failure Mode Results Table

Specimen	Ultimate Load (lbs)	**Failure Mode**
A-0-1	4611	anchor pullout
A-3-1	3976	anchor pullout
A-3-2	4756	anchor pullout
A-4-3	4012	FRP rupture at anchor
A-4-3a	4248	FRP rupture 4” from center
A-3-1-u	2778	anchor pullout
A-3-2-u	3522	anchor pullout
A-3-1-4	5555	FRP rupture 6” from center
B-0-1	5301	FRP rupture at cross wrap
B-0-1a	4937	FRP rupture 3” from center
B-3-1	4738	anchor pullout
B-3-2	4956	anchor pullout
B-4-3	5337	FRP rupture at anchor
B-4-3a	5591	FRP rupture at cross wrap
B-3-1-u	3958	anchor pullout
B-3-2-u	4248	FRP rupture at anchor
3-1-8-1	4450	*Test results from B. Miller tests*
3-1-8-2	2920	*Used as no anchor reference*

(Note: 1 lb = 4.448 N)

5. COMPARISON OF RESULTS

This section will compare the results of the laboratory tests, presented in section 4, in order to evaluate the influence of the variables on the anchor system. Anchorage location, groove size, and bar size will all be compared with each other and comparison to previous tests will also be considered. The fundamental issue of these results is that the anchor does not stop peeling, but is responsible for holding the system in place after peeling takes place along the bonded region. Another fact to keep in mind is the ultimate strength of the FRP sheet alone which is 7150 lb (31.80 kN).

5.1 ANCHOR VS NO ANCHOR

The purpose of this project was to see if the anchorage system would increase the capacity of the FRP system. The tests were compared to previous tests which had an average capacity of 3700 lb (16.47 kN) (Miller, 1999). Table 5.1 shows the test results for this project and the increase in capacity, which was determined by subtracting 3700 lb (16.47 kN) from the results of this test, and then dividing by the results of this test.

Table 5.1. Ultimate Load Compared to Previous Tests

Specimen	Ultimate Load (lbs)	*Percent increase in capacity over no anchor*		Specimen	Ultimate Load (lbs)	*Percent increase in capacity over no anchor*
A-0-1	4611	*24.6*		B-0-1	5301	*38.4*
-----				B-0-1a	4937	
A-3-1	3976	*7.5*		B-3-1	4738	*28.1*
A-3-2	4756	*28.5*		B-3-2	4956	*33.9*
A-4-3	4012	*11.6*		B-4-3	5337	*47.7*
A-4-3a	4248			B-4-3a	5591	
A-3-1-4	5555	*55.1*		-----		

(Note: 1 lb = 4.448 N)

5.2 ANCHORAGE LOCATION

The location of the anchor shows to have a significant impact on the ultimate load. Table 5.2, shows the capacities of specimens with the same groove and bar variables but differing anchor locations and the increase in capacity of the anchor. The table shows that placing the anchor after the corner can increase the capacity of the FRP system by up to 40 percent.

Table 5.2. Comparison of Anchorage Location

Specimen	Ultimate Load (lbs) *a*		Specimen	Ultimate Load (lbs) *b*	*Percent increase in capacity (b-a)/a*
A-0-1	4611		B-0-1	5301	*11.0*
-----			B-0-1a	4937	
A-3-1	3976		B-3-1	4738	*19.2*
A-3-2	4756		B-3-2	4956	*4.2*
A-4-3	4012		B-4-3	5337	*32.3*
A-4-3a	4248		B-4-3a	5591	
A-3-1-U	2778		B-3-1-U	3958	*42.5*
A-3-2-U	3522		B-3-2-U	4248	*20.6*

(Note: 1 lb = 4.448 N)

5.3 GROOVE SIZE

The size of the grove shows an increase in capacity for the specimens that had their groove size relative to the bar diameter changed. Specimens A-3-1 and B-3-1 had a groove size of 9/16 in (14.29 mm), which is 1.5 times the bar diameter for a #3 rebar; specimens A-3-2 and B-3-2, had an increase groove size of 15/16 in (23.81 mm), which is 2.5 times the bar diameter. Table 5.3, shows the increase in capacity for the specimens.

Table 5.3. Comparison of Groove Size

Specimen	Ultimate Load (lbs) *a*		Specimen	Ultimate Load (lbs) *b*	*Percent increase in capacity (b-a)/a*
A-3-1	3976		A-3-2	4756	*19.6*
B-3-1	4738		B-3-2	4956	*4.6*

(Note: 1 lb = 4.448 N)

5.4 BAR SIZE VS GROOVE DIMENSION

When comparing the specimens with a bar size to groove dimension ratio the same, the results show that the capacity is about the same for the "A" specimens, but increases for the "B" specimens. Table 5.4, shows the comparison of the specimens and the increase in capacity of the '4-3' specimens over the '3-1' specimens.

Table 5.4. Comparison of Bar Size, Groove Dimension Ratio

Specimen	Ultimate Load (lbs) *a*		Specimen	Ultimate Load (lbs) *b*	*Percent increase in capacity (b–a)/a*
A-3-1	3976		A-4-3	4130(avg)	*3.9*
B-3-1	4738		B-4-3	5464(avg)	*15.3*

(Note: 1 lb = 4.448 N)

5.5 BAR VS NO BAR PRESENT

Two specimens for each location case, have the same parameters except for the bar being present or not. The comparison for these specimens (A-0-1 vs. A-3-1 and B-0-1 vs. B-3-1) can be seen in Table 5.5; it shows that the presence of the bar decreases the capacity of the anchor system.

Table 5.5. Comparison of Bar Present vs. Not Present

Specimen	Ultimate Load (lbs) *a*		Specimen	Ultimate Load (lbs) *b*	*Percent increase in capacity (b–a)/a*
A-3-1	3976		A-0-1	4611	*16.0*
B-3-1	4738		B-0-1	5119(avg)	*8.0*

(Note: 1 lb = 4.448 N)

5.6 MISCELLANEOUS SPECIMENS

Several specimens were tested to analyze some additional variables. Specimens A-3-1-u, A-3-2-u, B-3-1-u, and B-3-2-u were tested to see the capacity of just the anchor, therefore the length of the FRP strip was left unbonded to the concrete. These results can be seen in Table 5.6. When compared to the tests without an anchor, but an 8 in (203.2 mm) bonded length, the specimens with anchor after the corner have ultimate loads less than the 3770 lb (16.77 kN). The specimens with the anchor present before the corner show a greater ultimate load than those specimens without the anchor.

Table 5.6. Ultimate Load of Unbonded Specimens

Specimen	Ultimate Load (lbs)	Specimen	Ultimate Load (lbs)
A-3-1-u	2778	B-3-1-u	3958
A-3-2-u	3522	B-3-2-u	4248

(Note: 1 lb = 4.448 N)

The other special test was A-3-1-4, in this specimen a 4 in (101.6 mm) long bar was used instead of a 2 in (50.8 mm) bar like in the other tests. The result of this test is shown in Table 5.7, along with the result of specimen A-3-1, which had a 2 in (50.8 mm) bar.

Table 5.7. Ultimate load of A-3-1-4 and A-3-1

Specimen	Ultimate Load (lbs) *a*	Specimen	Ultimate Load (lbs) *b*	*Percent increase in capacity (b–a)/a*
A-3-1	3976	A-3-1-4	5555	*39.7*

(Note: 1 lb = 4.448 N)

5.7 SUMMARY

From all of the above sections it can be seen that the anchorage system does increase the capacity of the FRP system. The length of the anchor bar seems to have the greatest impact, followed by the anchor location, the groove size, and then the bar size.

When compared to the ultimate strength of a single CFRP sheet, of 7150 lb (31.80 kN), the results of these tests show a lower capacity. Of the tests which failure by FRP rupture occurred, the results ranged from 56.1% to 78.2% of ultimate. This is due to stress concentrations along the sheet, and also testing difference. Testing of the ultimate strength of the sheet was done by pulling the sheet along a linear plane, the loading of the sheet for this test was not linear because the testing of the sheet was done in flexure.

6. CONCLUSION

From the results of all the tests it can be seen that the use of the anchorage system does increase the capacity of the FRP system. The location of the anchor has a significant impact on the capacity, shown by the greater capacity of the specimens with the anchor placed before the corner of the turn, as opposed to after. The test show that there is an increase in strength with increasing groove size, but the trade off's are increased labor and the chance that the reinforcing steel of the beam will be cut when making the grooves if they are made too deep. A slight increase can be achieve when increasing both the bar size and groove dimension, while keeping the ratio the same, but the problems with increasing the groove dimension presents themselves.

The results of the specimens with the anchor bar not present are of the same capacities of those with the anchor. However, constructibility is a concern here, because it is easier to install the anchorage system using the anchor rod. Using the bar is more effective when ensuring that the epoxy paste has completely filled the voids in the groove. The specimen with the 4 in (101.6 mm) bar has a higher capacity that the specimens with the 2 in (50.8 mm) bars, once again this is because the bar transfers the stress from the localized point and distributes it along the length of the bar. This is opposed to the previous discussion on the bar being present or not, but can be rationalized on the basis that the tests were carried out on narrow fiber widths where the bar width is the same as the loaded area. In the case of the 4 in (101.6 mm) bar, the sheet width was half of the bar, so the load was able to be distributed out from the loaded region.

The ultimate capacity increases from the A-3-1 to A-3-1-4 specimen, because the longer bar transfers the load from the two (2) inch wide sheet over twice the distance. The represents the case of a T-beam, where the load may be concentrated at one point or one region, but the FRP runs the entire length of the beam. If the anchor is over the length of the beam, the anchor rod will transfer the load away from where it is concentrated, thus reducing the stress concentration and increasing the capacity.

REFERENCES

Annaiah, R., Myers, J., Nanni, A., "In-Situ Shear and Flexure Strengthening of Reinforced Concrete Members with Advanced Composites," Report CIES 99-11, Center for Infrastructure Engineering Studies, University of Missouri-Rolla, Rolla, MO

Khalifa, A., Alkhradaji, T., Nanni, A., and Lansburg, S., (1999). "Anchorage of Surface Mounted FRP Reinforcement," *Concrete International*, Vol. 21, No. 10, pp 49-54

Marshall Industries Composites, Inc., (1998) "C-Bar Reinforcing Rods for Concrete Reinforcement," Jacksonville, FL

MBrace Composite Strengthening System Engineering Design Guidelines Second Edition, (1998). Master Builders, Inc. and Structural Preservation Systems

Miller, B. D., (1999). "Bond Between Carbon Fiber Reinforced Polymer Sheets and Concrete." MSc Thesis, Department of Civil Engineering, University of Missouri-Rolla, Rolla, MO

Nanni, A., Gold, W., Alkhrdaji, T., and Blaszak, G., (1998) "FRP Reinforcement: A New Alternative to Steel in Concrete Construction," Concrete Construction

Sato, Y., Katsumata, H., and Kobatake, Y., (1997), "Shear Strengthening of Existing Reinforced Concrete Beams CFRP Sheet," *Proceeding of the Third International Symposium on Non-Metallic (FRP) Reinforcement for Concrete Structures (FRPRCS-3)*, Japan Concrete Institute, Sapporo, Japan, Vol. 1, pp. 507-514

Tumialan, J. G., (1998). "Concrete Cover Delamination in Reinforced Concrete Beams Strengthened with CFRP Sheets," MSc Thesis, Department of Civil Engineering, University of Missouri-Rolla, Rolla, MO

APPENDIX A.

DIAGRAMS AND PHOTOGRAPHS FOR SPECIMENS

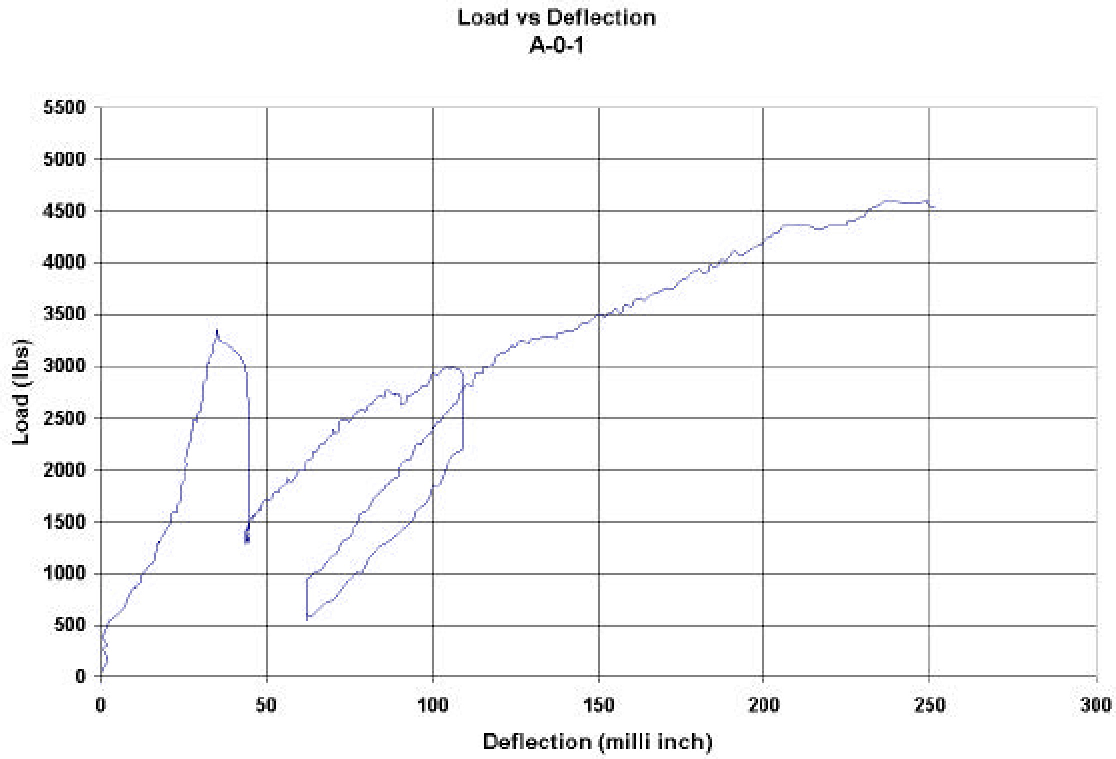

Figure A.1. Load vs. Deflection plot for A-0-1 (1 in = 25.4 mm, 1 lb = 4.448 N)

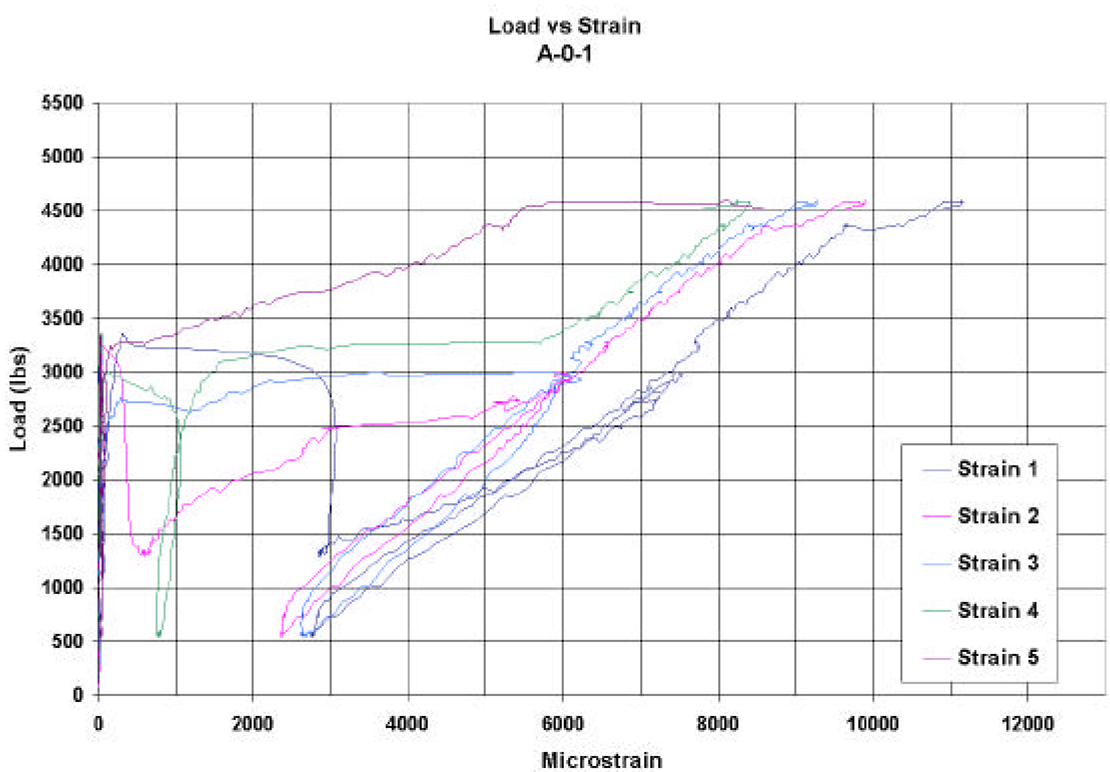

Figure A.2. Load vs. Strain plot for A-0-1 (1 lb = 4.448 N)

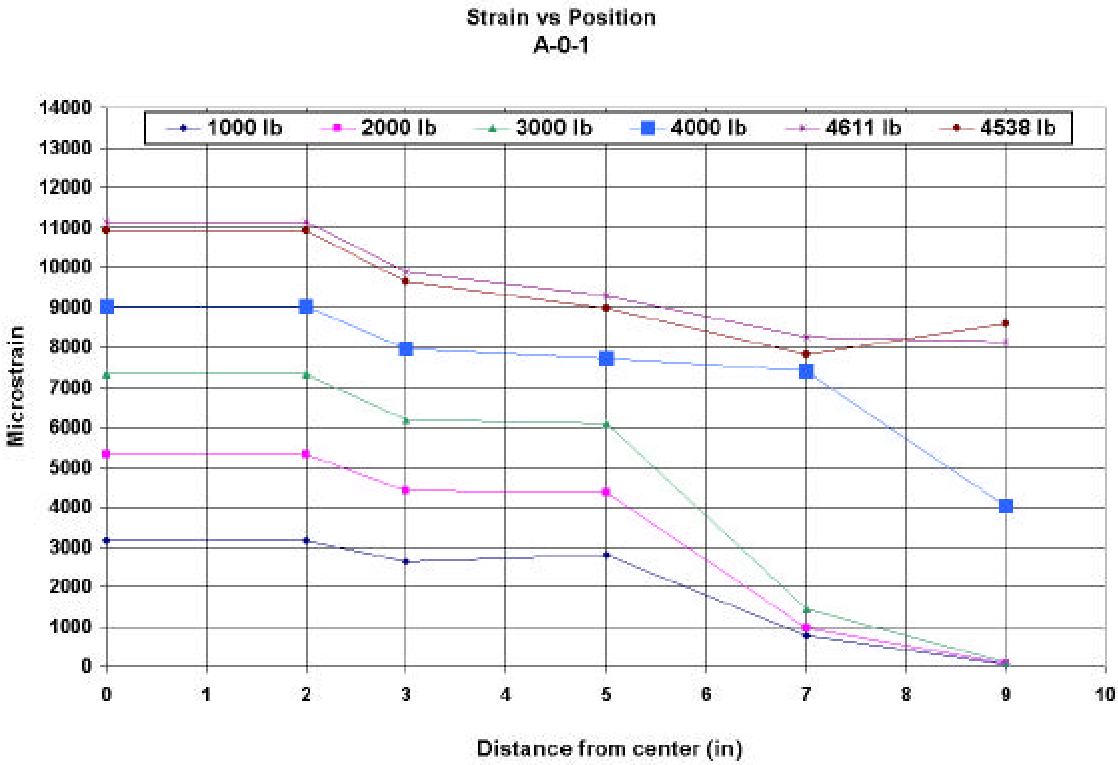

Figure A.3. Strain vs. Position plot for A-0-1 (1 in = 25.4 mm, 1 lb = 4.448 N)

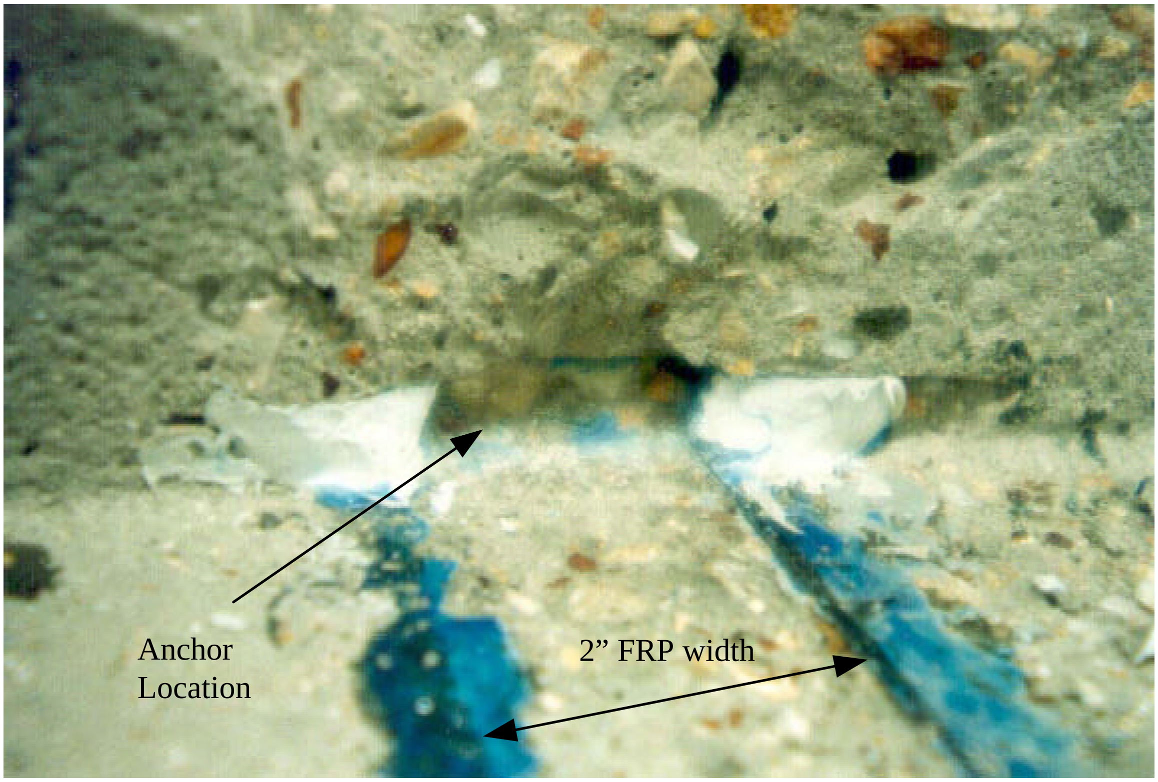

Figure A.4. Picture of failure location for A-0-1 (1 in = 25.4 mm)

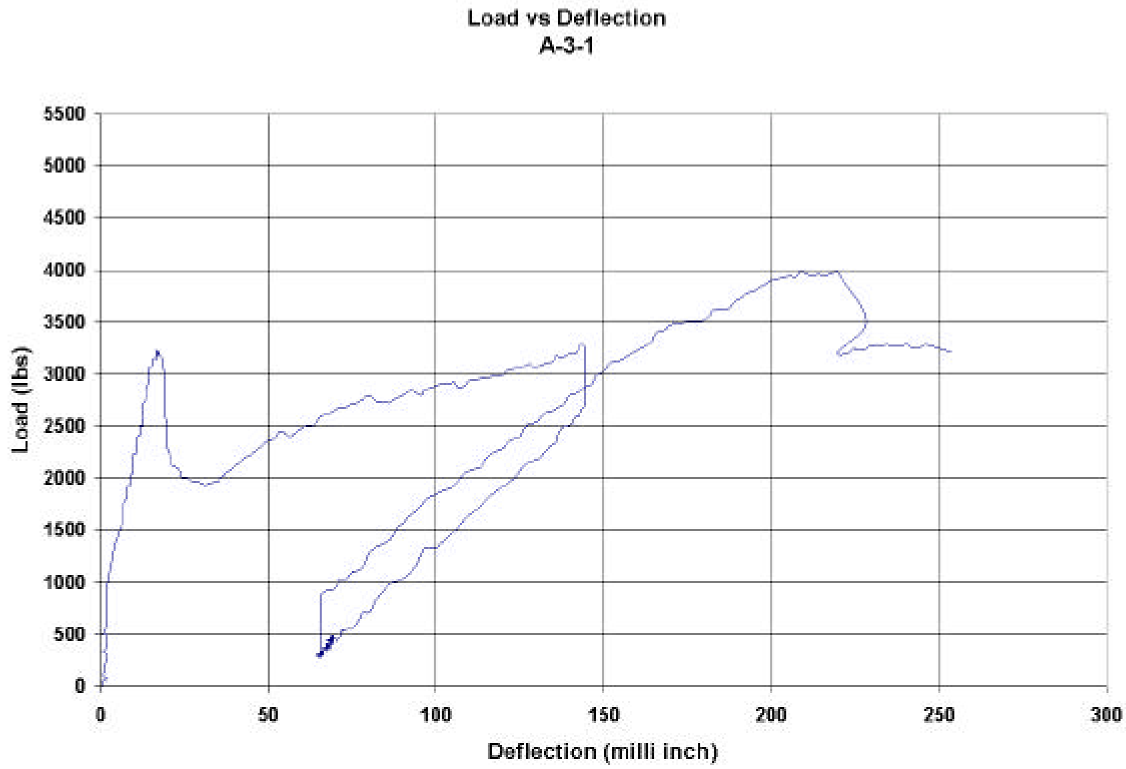

Figure A.5. Load vs. Deflection plot for A-3-1 (1 in = 25.4 mm, 1 lb = 4.448 N)

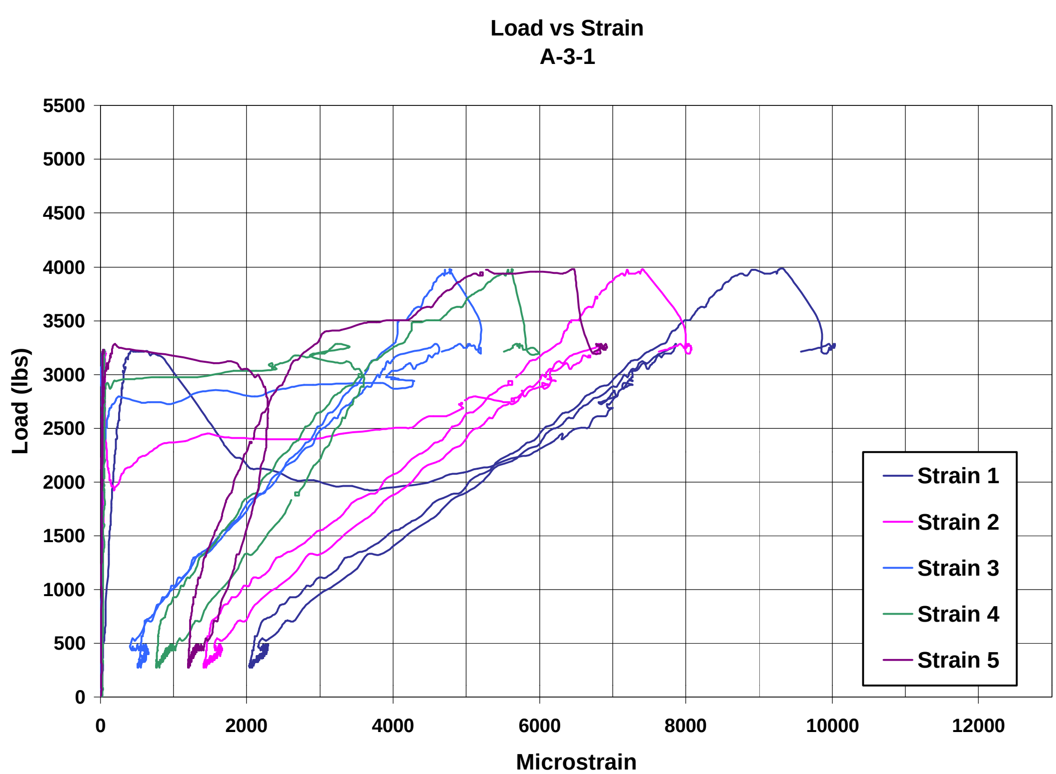

Figure A.6. Load vs. Strain plot for A-3-1 (1 lb = 4.448 N)

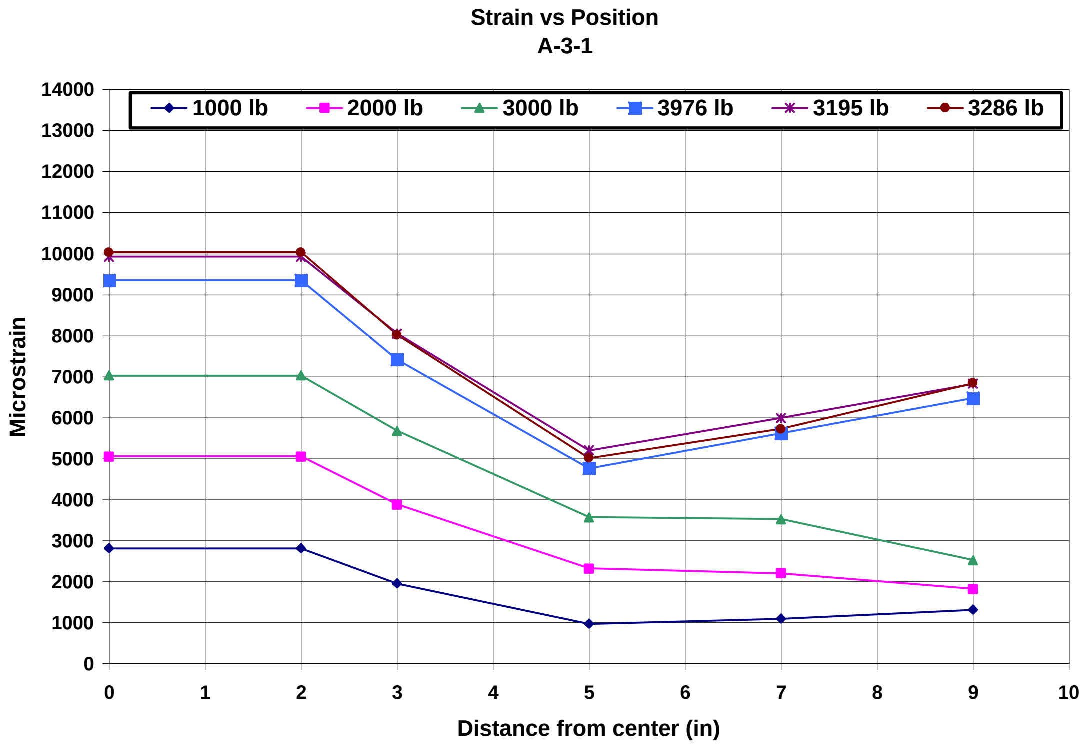

Figure A.7. Strain vs. Position plot for A-3-1 (1 in = 25.4 mm, 1 lb = 4.448 N)

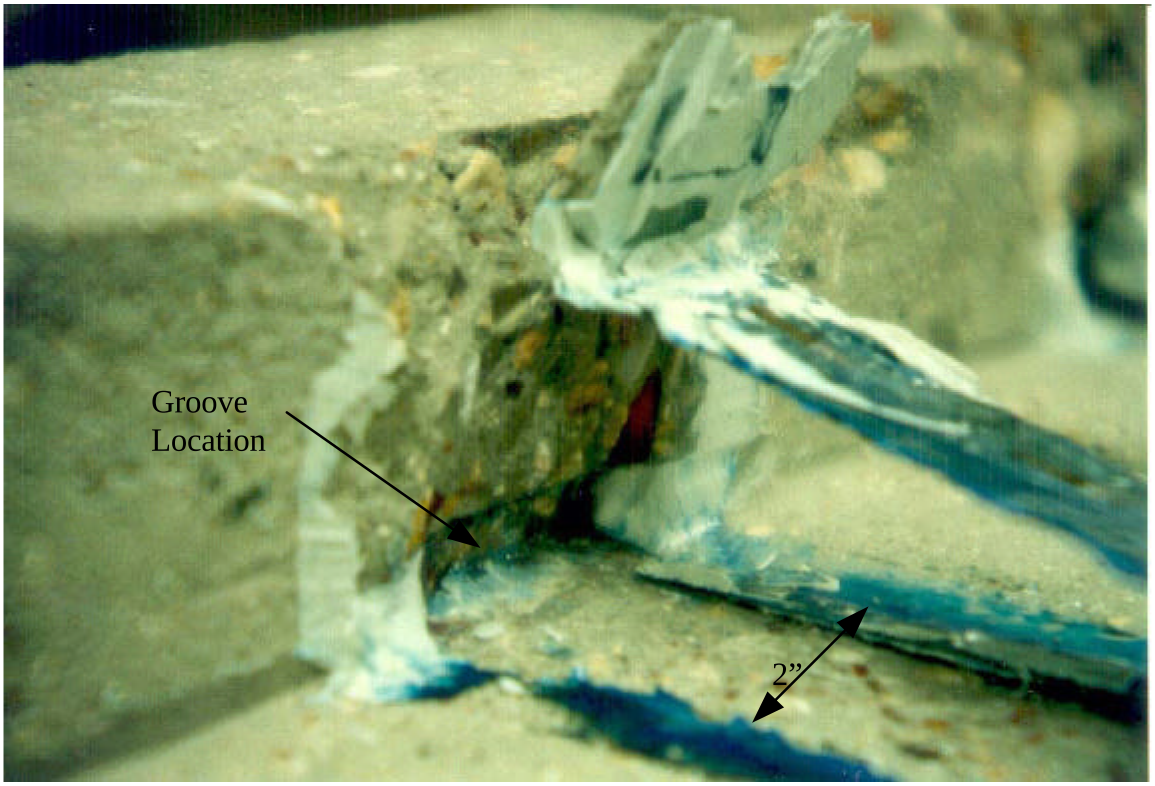

Figure A.8. Picture of failure location for A-3-1 (1 in = 25.4 mm)

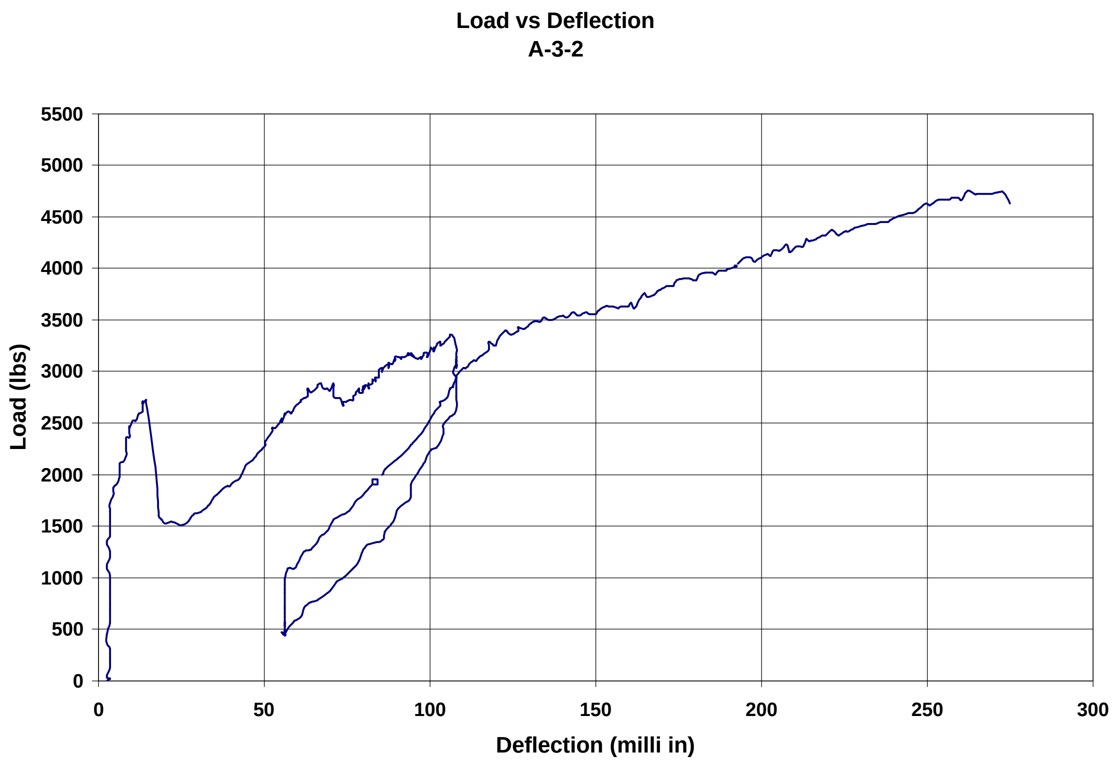

Figure A.9. Load vs. Deflection plot for A-3-2 (1 in = 25.4 mm, 1 lb = 4.448 N)

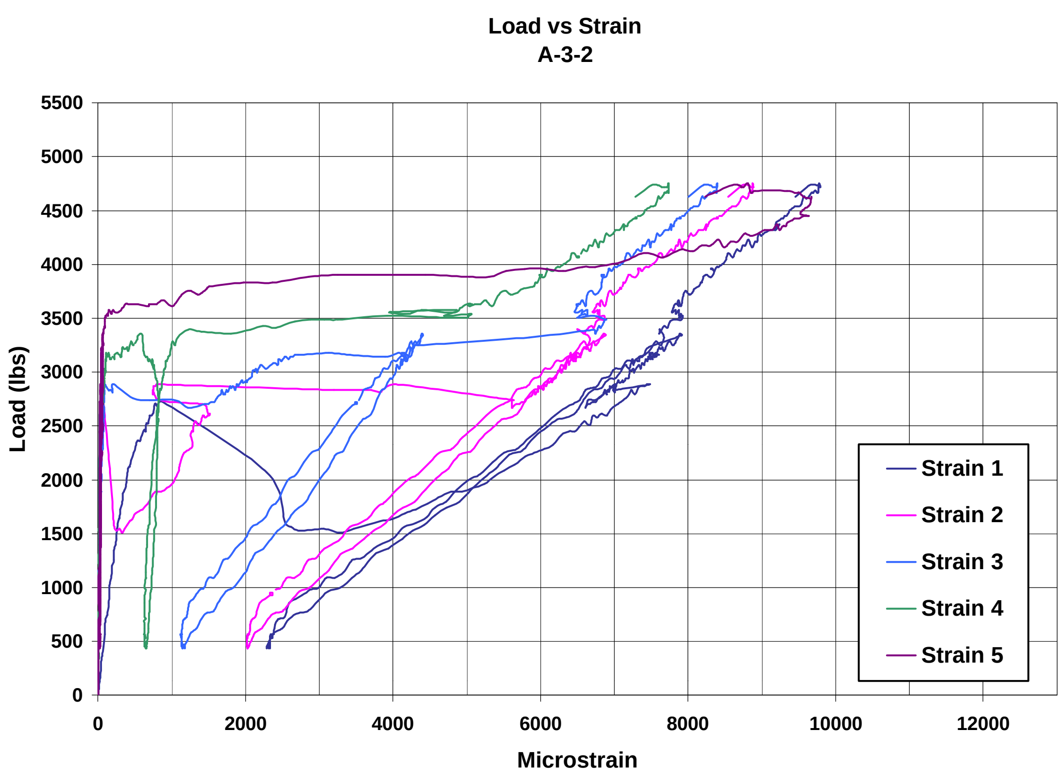

Figure A.10. Load vs. Strain plot for A-3-2 (1 lb = 4.448 N)

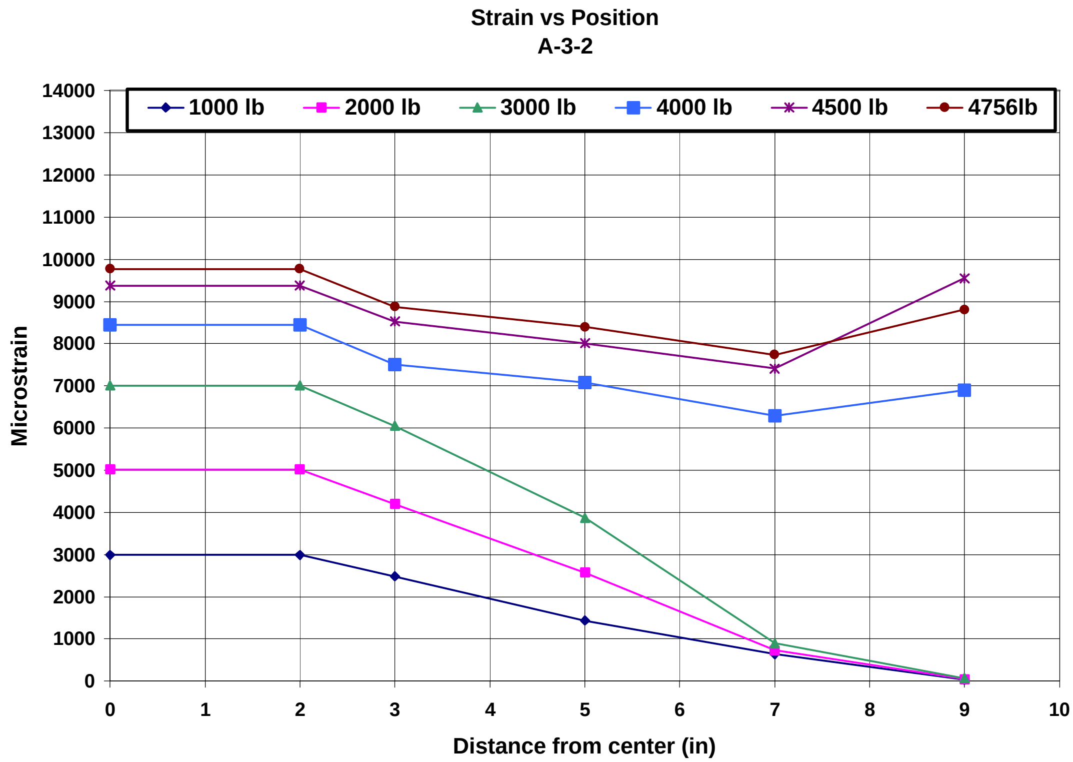

Figure A.11. Strain vs. Position plot for A-3-2 (1 in = 25.4 mm, 1 lb = 4.448 N)

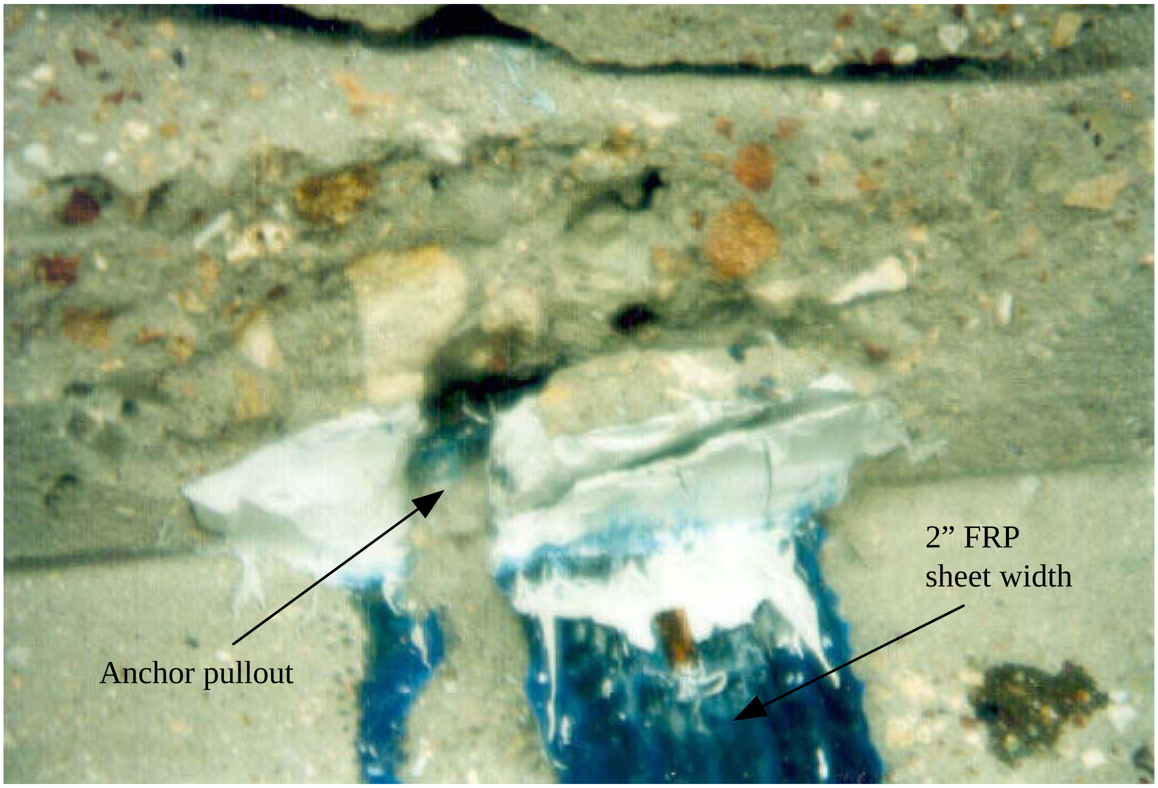

Figure A.12. Picture of failure location for A-3-2 (1 in = 25.4 mm)

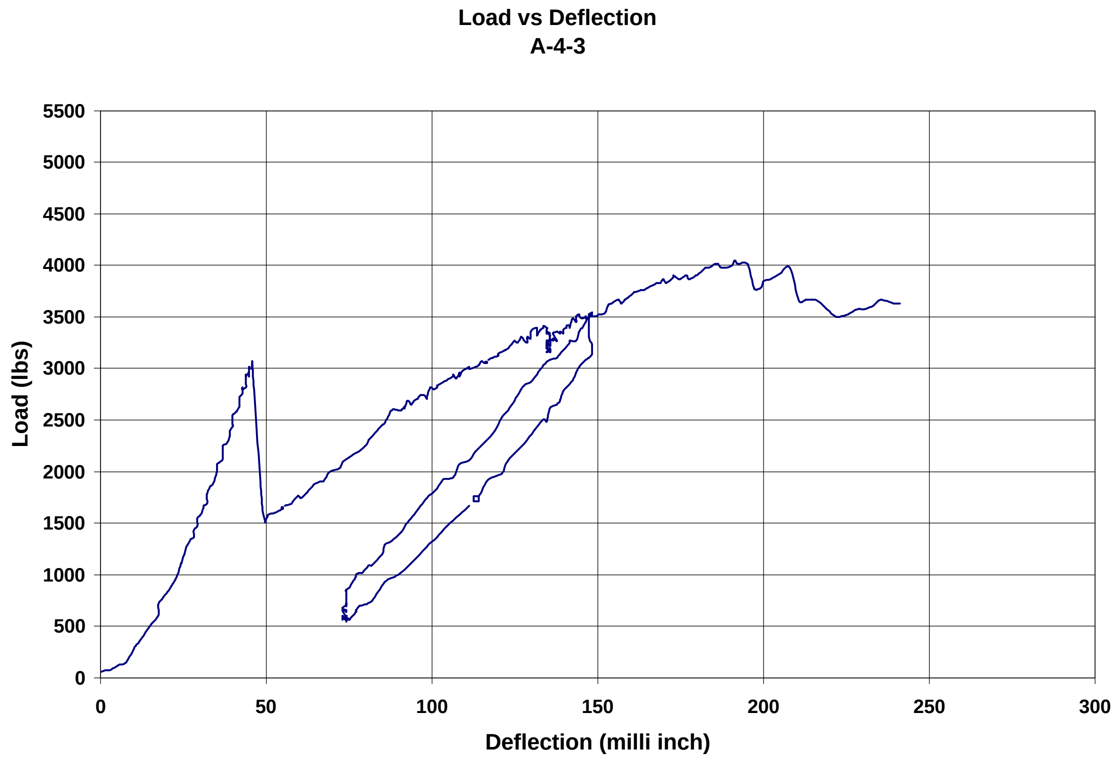

Figure A.13. Load vs. Deflection plot for A-4-3 (1 in = 25.4 mm, 1 lb = 4.448 N)

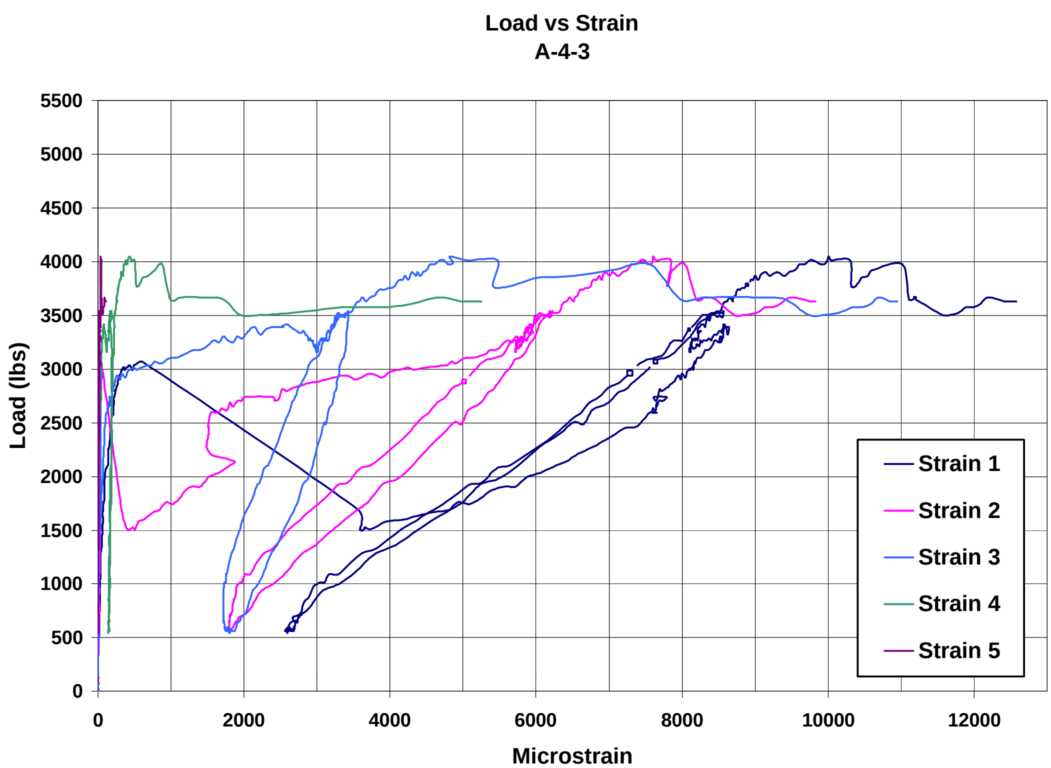

Figure A.14. Load vs. Strain plot for A-4-3 (1 lb = 4.448 N)

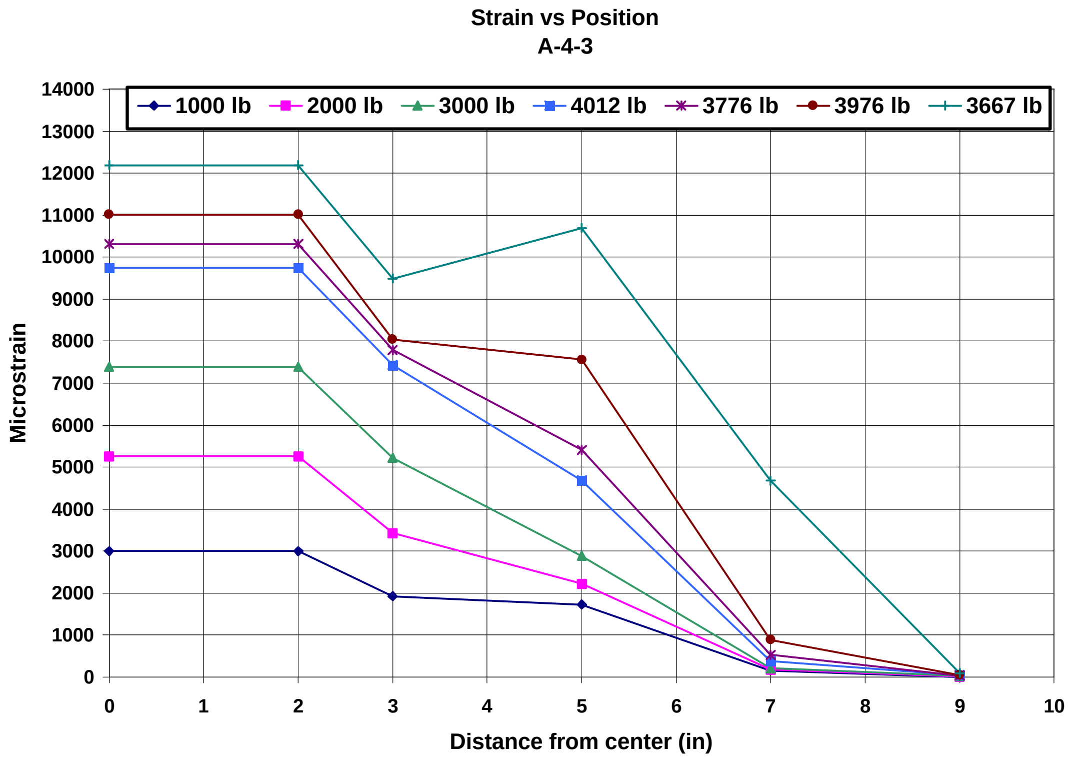

Figure A.15. Strain vs. Position plot for A-4-3 (1 in = 25.4 mm, 1 lb = 4.448 N)

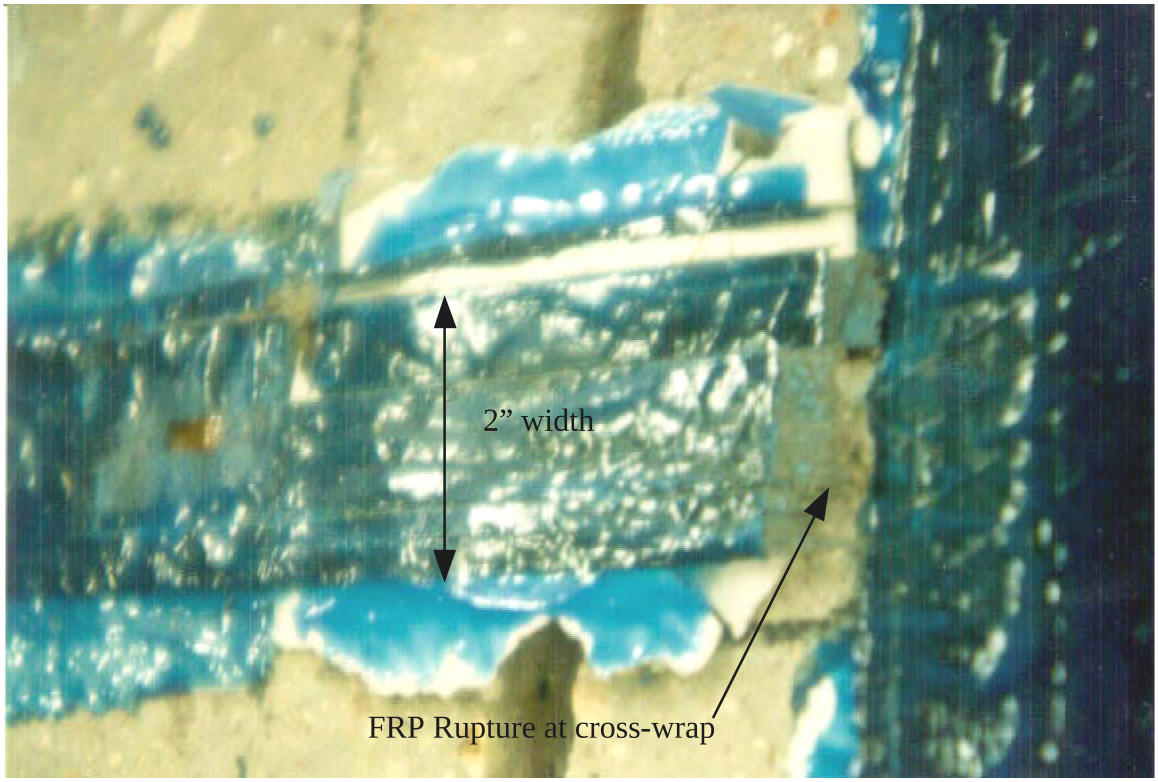

Figure A.16. Picture of failure location for A-4-3 (1 in = 25.4 mm)

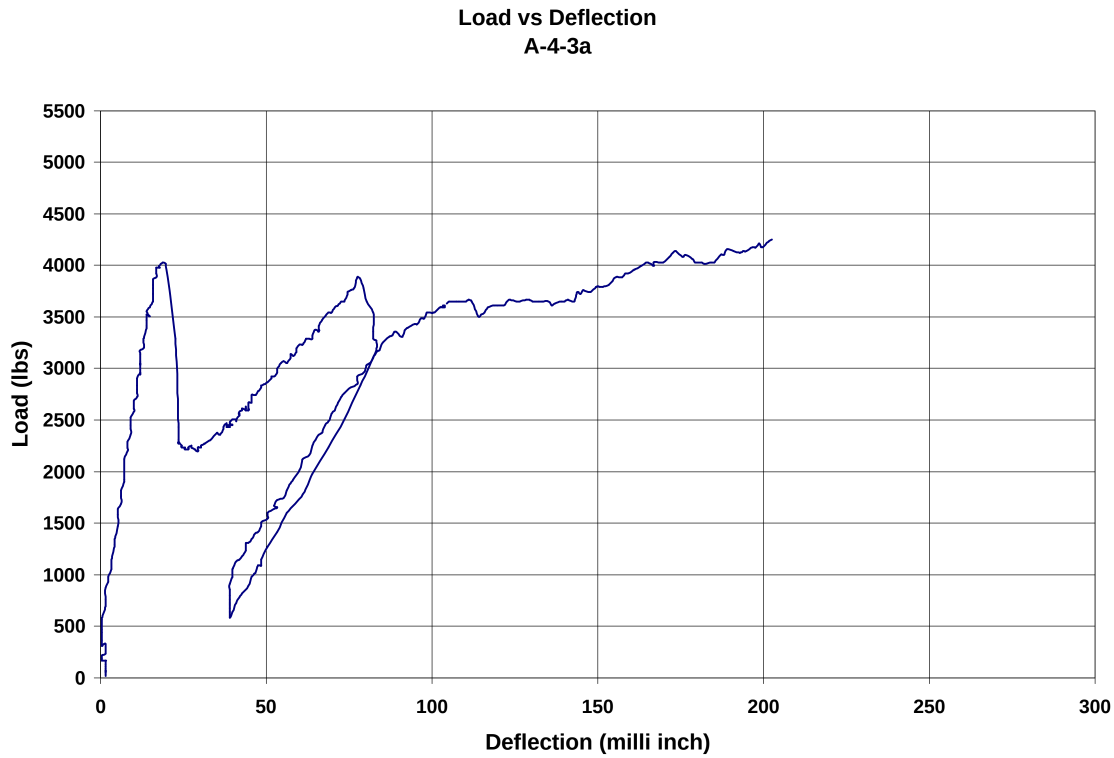

Figure A.17. Load vs. Deflection plot for A-4-3a (1 in = 25.4 mm, 1 lb = 4.448 N)

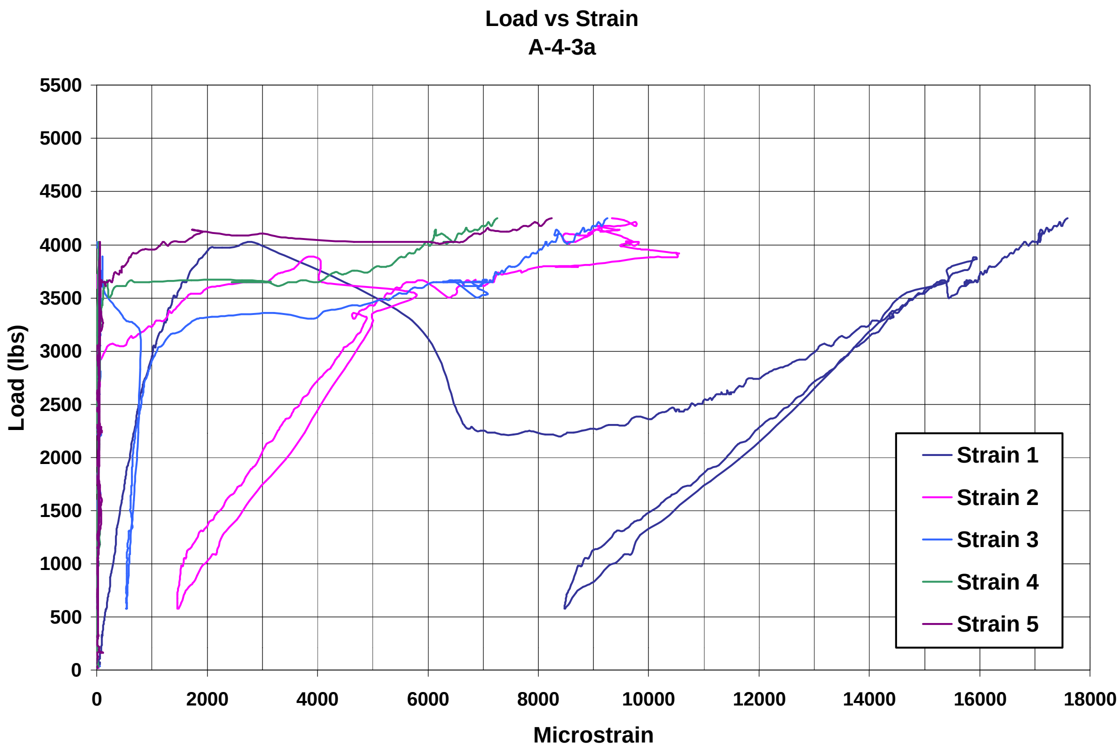

Figure A.18. Load vs. Strain plot for A-4-3a (1 lb = 4.448 N)

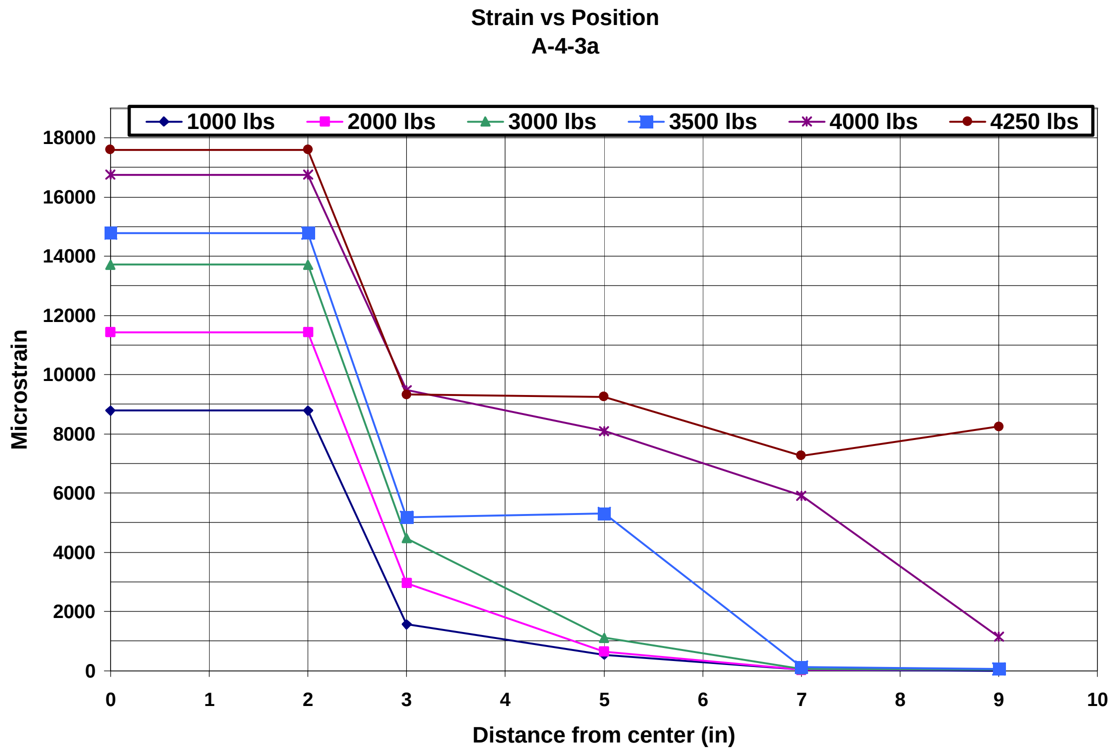

Figure A.19. Strain vs. Position plot for A-4-3a (1 in = 25.4 mm, 1 lb = 4.448 N)

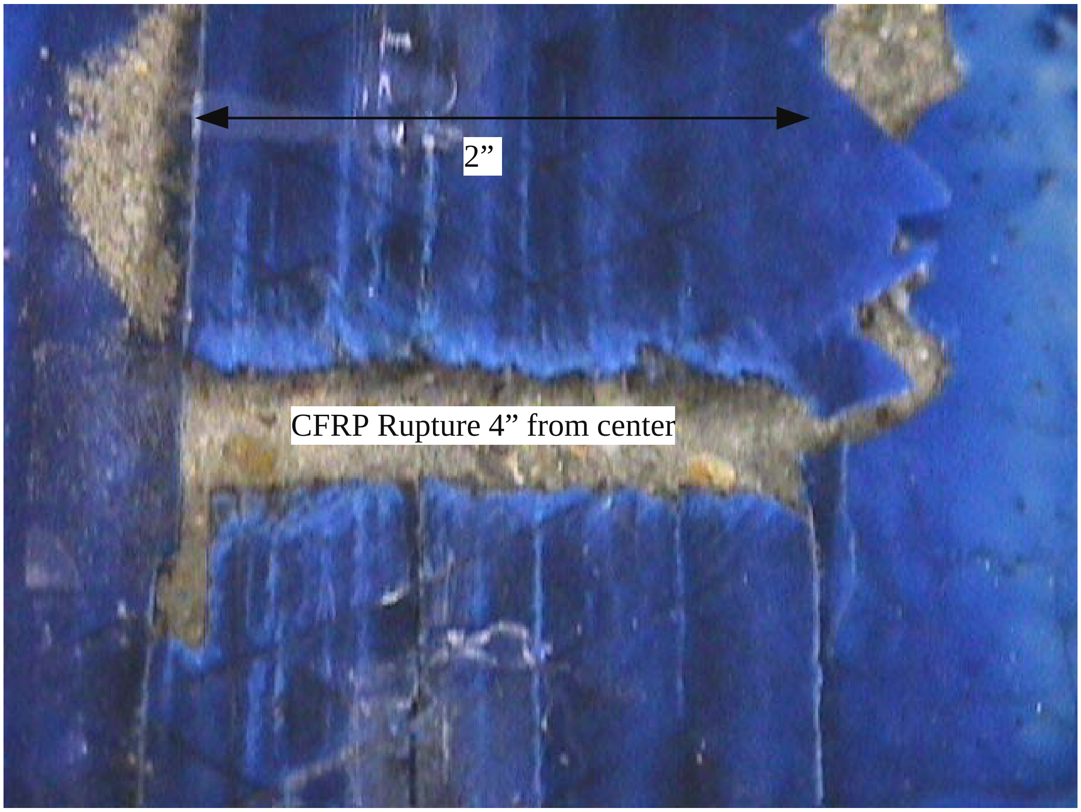

Figure A.20. Picture of failure location for A-4-3a (1 in = 25.4 mm)

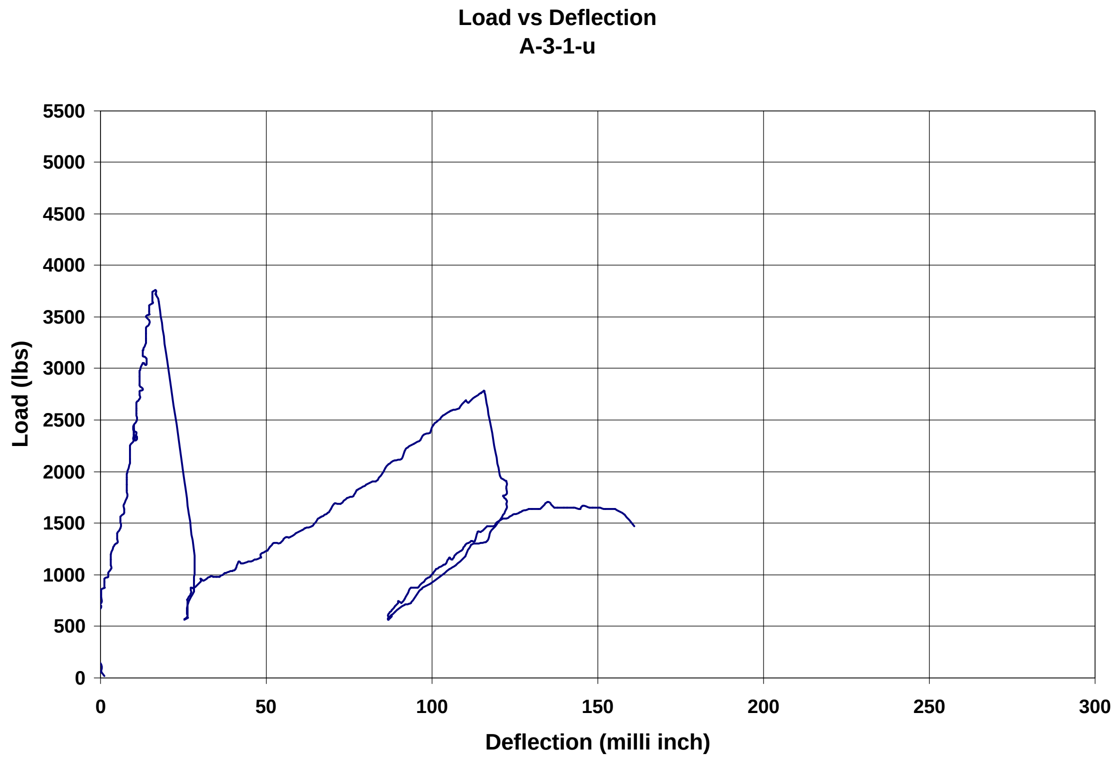

Figure A.21. Load vs. Deflection plot for A-3-1-u (1 in = 25.4 mm, 1 lb = 4.448 N)

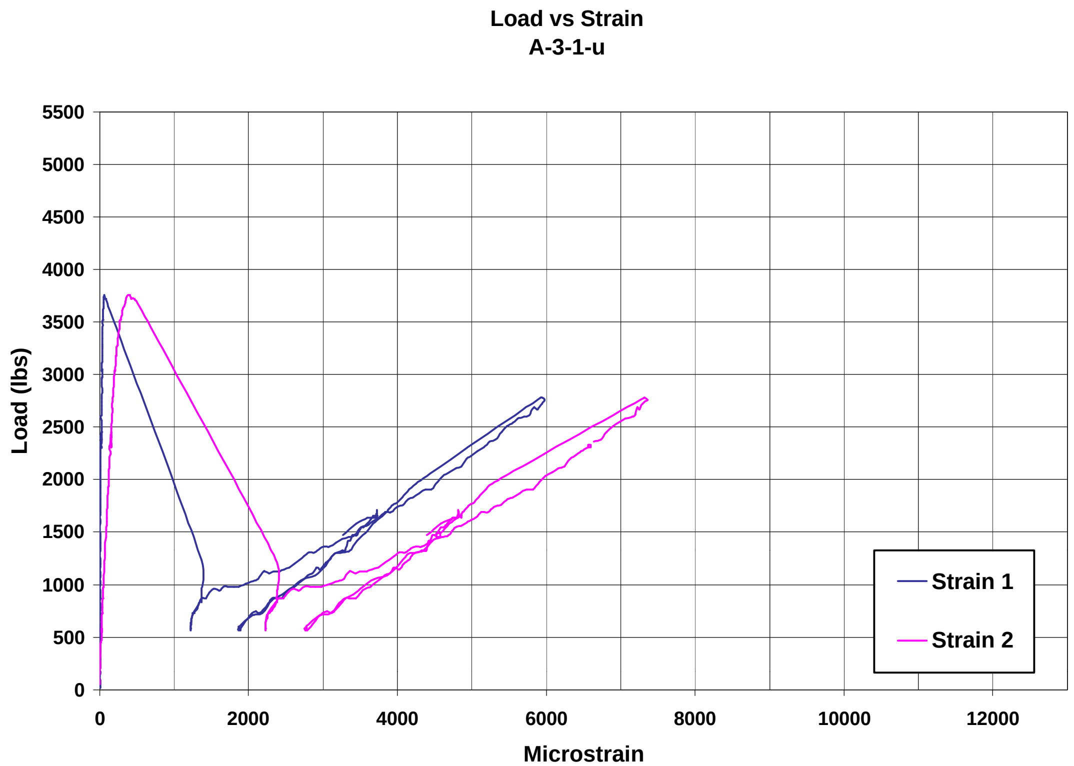

Figure A.22. Load vs. Strain plot for A-3-1-u (1 lb = 4.448 N)

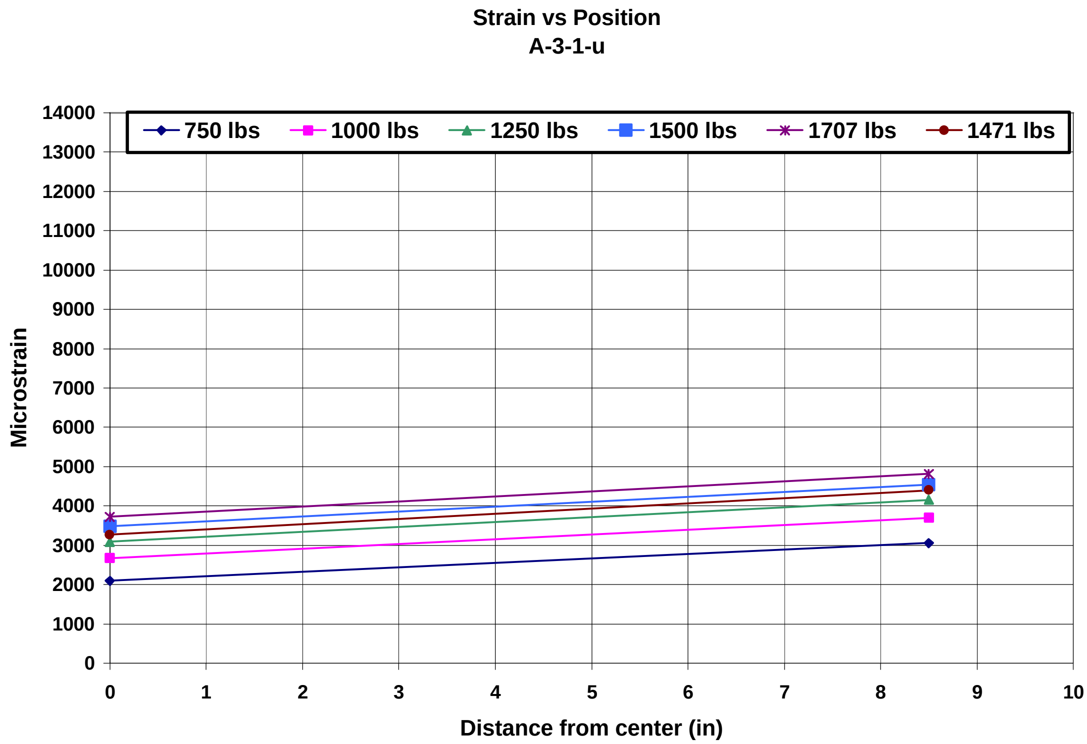

Figure A.23. Strain vs. Position plot for A-3-1-u (1 in = 25.4 mm, 1 lb = 4.448 N)

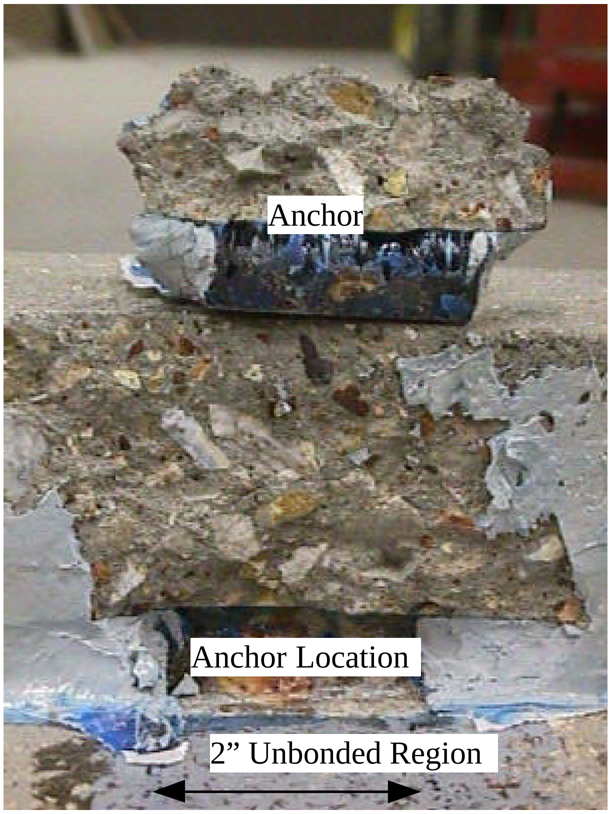

Figure A.24. Picture of failure location for A-3-1-u (1 in = 25.4 mm)

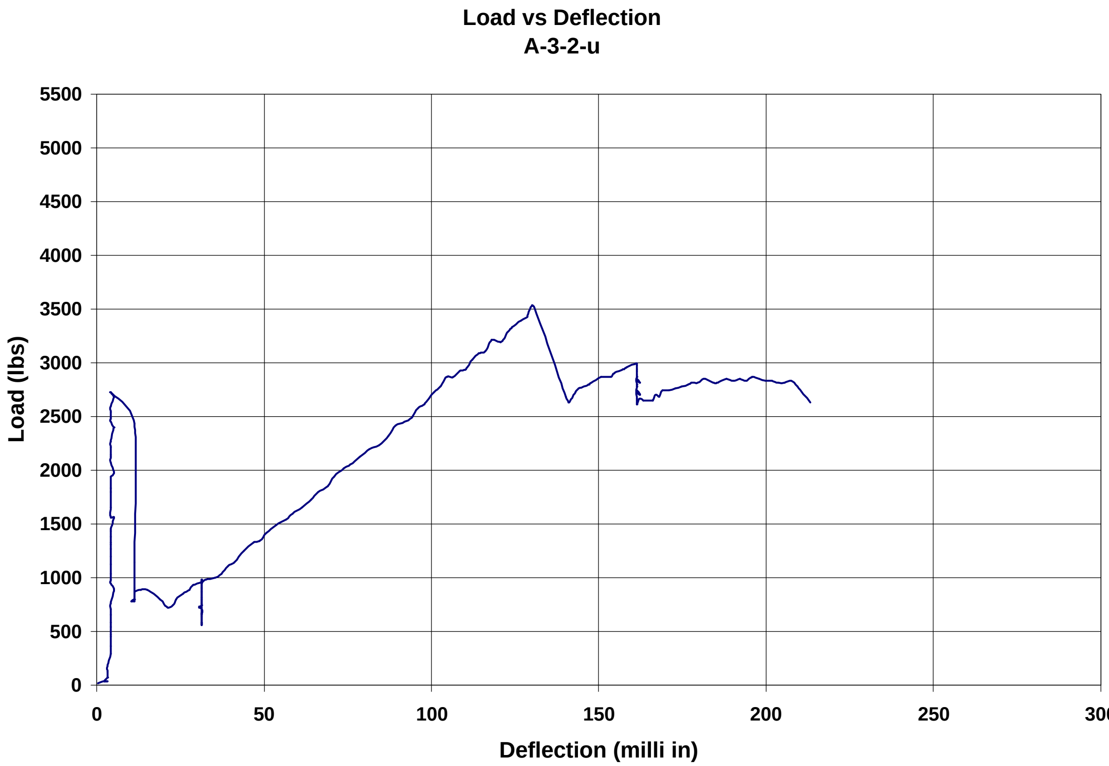

Figure A.25. Load vs. Deflection plot for A-3-2-u (1 in = 25.4 mm, 1 lb = 4.448 N)

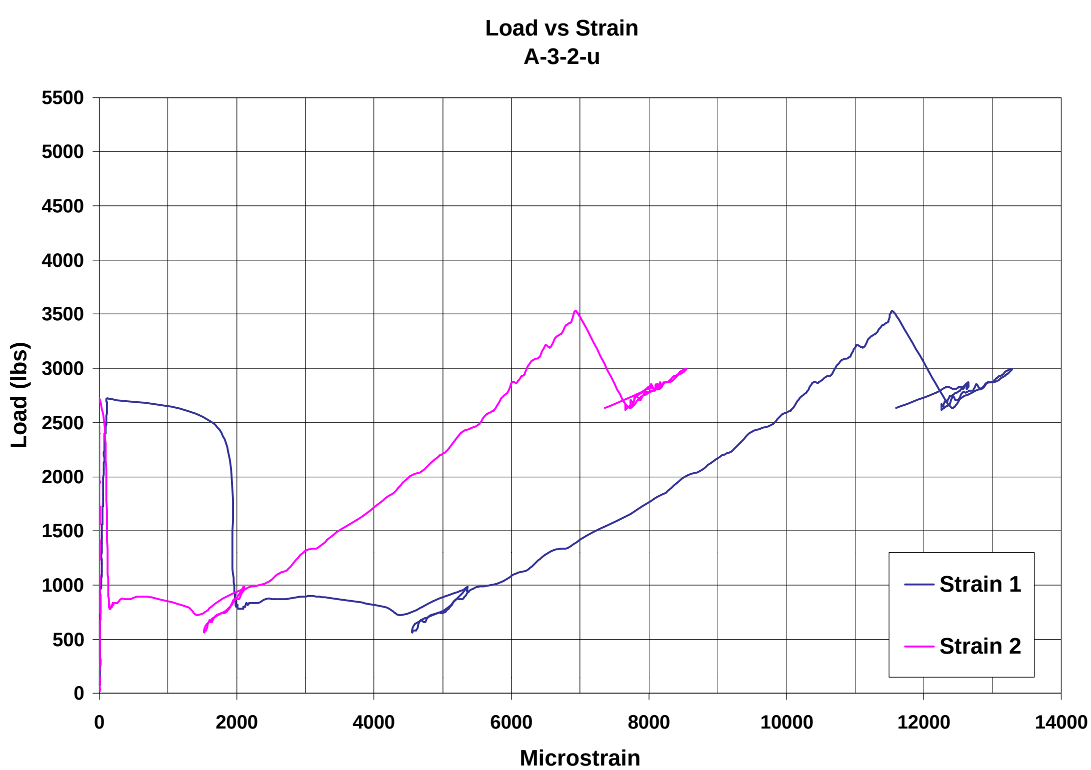

Figure A.26. Load vs. Strain plot for A-3-2-u (1 lb = 4.448 N)

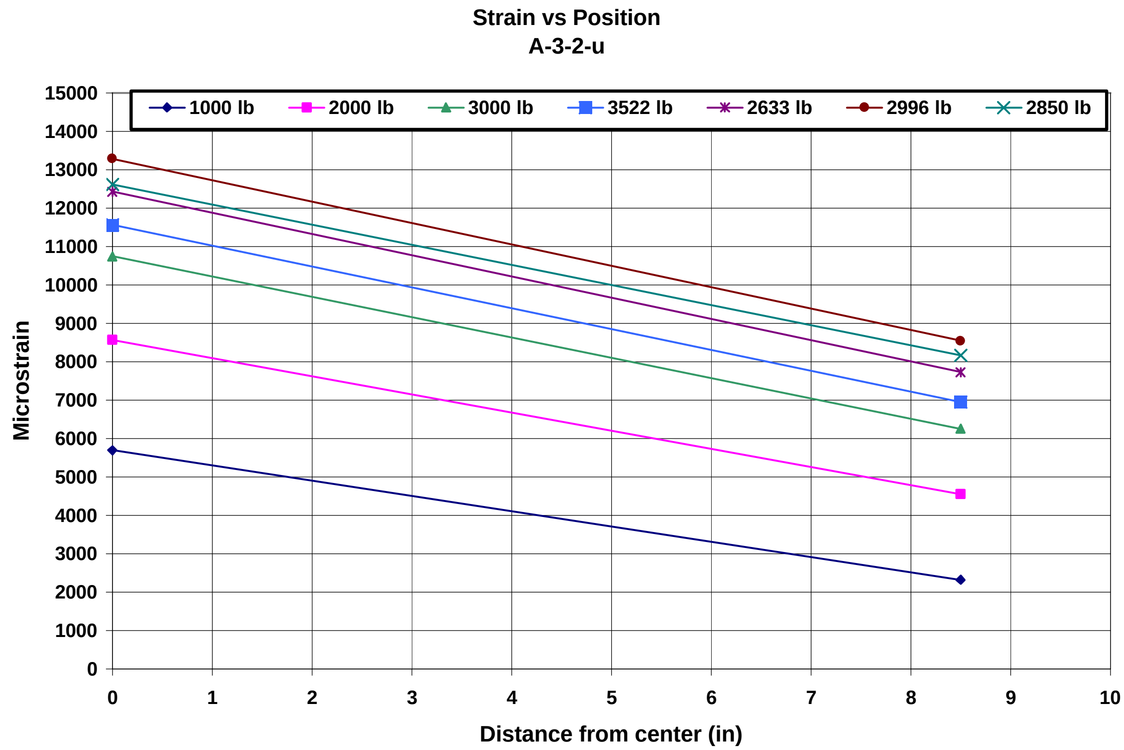

Figure A.27. Strain vs. Position plot for A-3-2-u (1 in = 25.4 mm, 1 lb = 4.448 N)

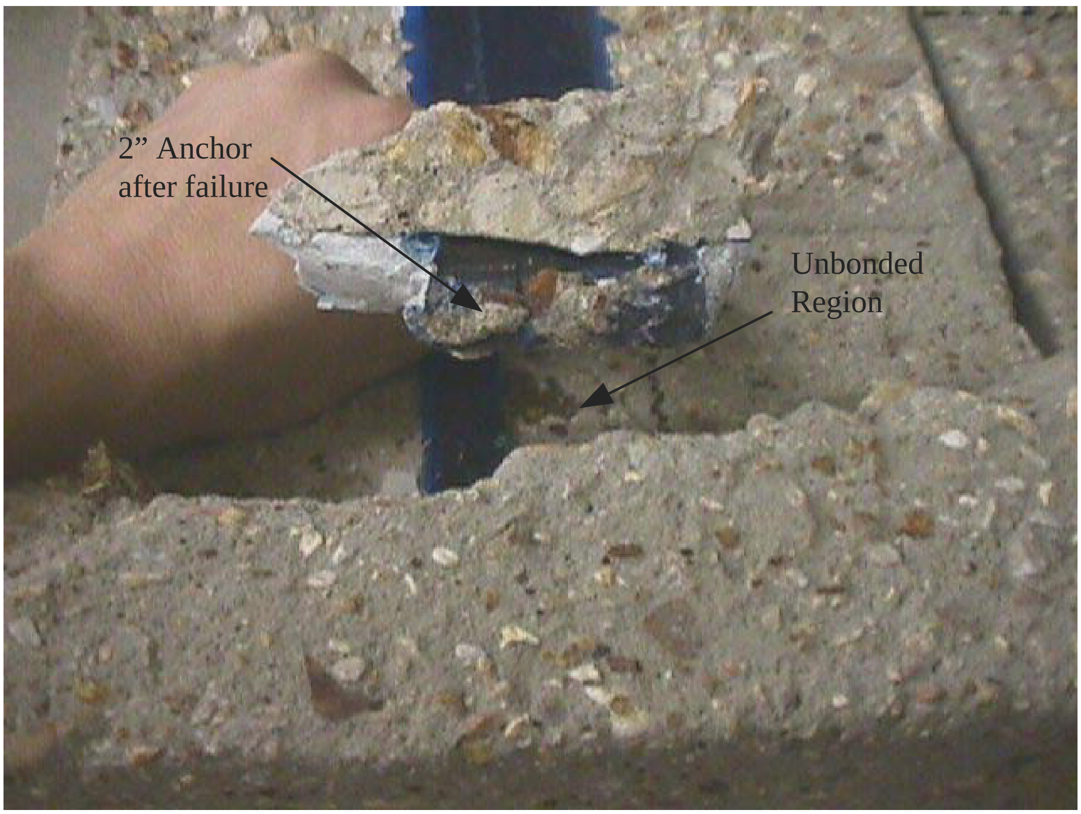

Figure A.28. Picture of failure location for A-3-2-u (1 in = 25.4 mm)

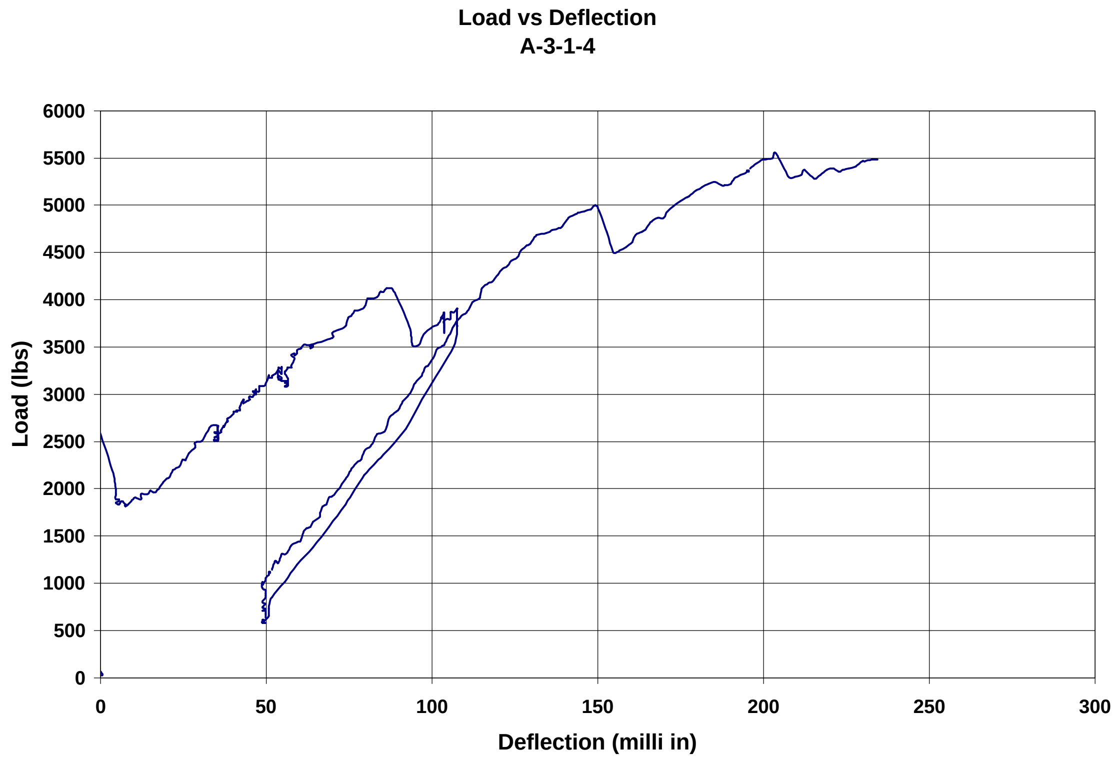

Figure A.29. Load vs. Deflection plot for A-3-1-4 (1 in = 25.4 mm, 1 lb = 4.448 N)

Figure A.30. Load vs. Strain plot for A-3-1-4 (1 lb = 4.448 N)

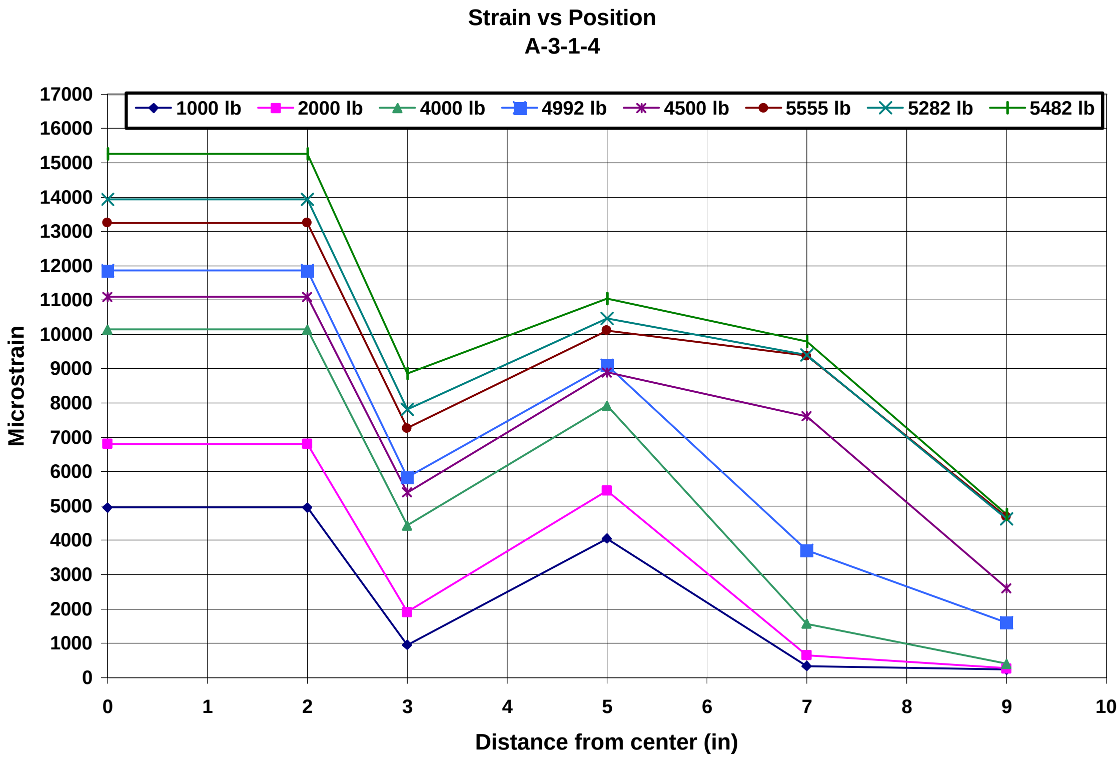

Figure A.31. Strain vs. Position plot for A-3-1-4 (1 in = 25.4 mm, 1 lb = 4.448 N)

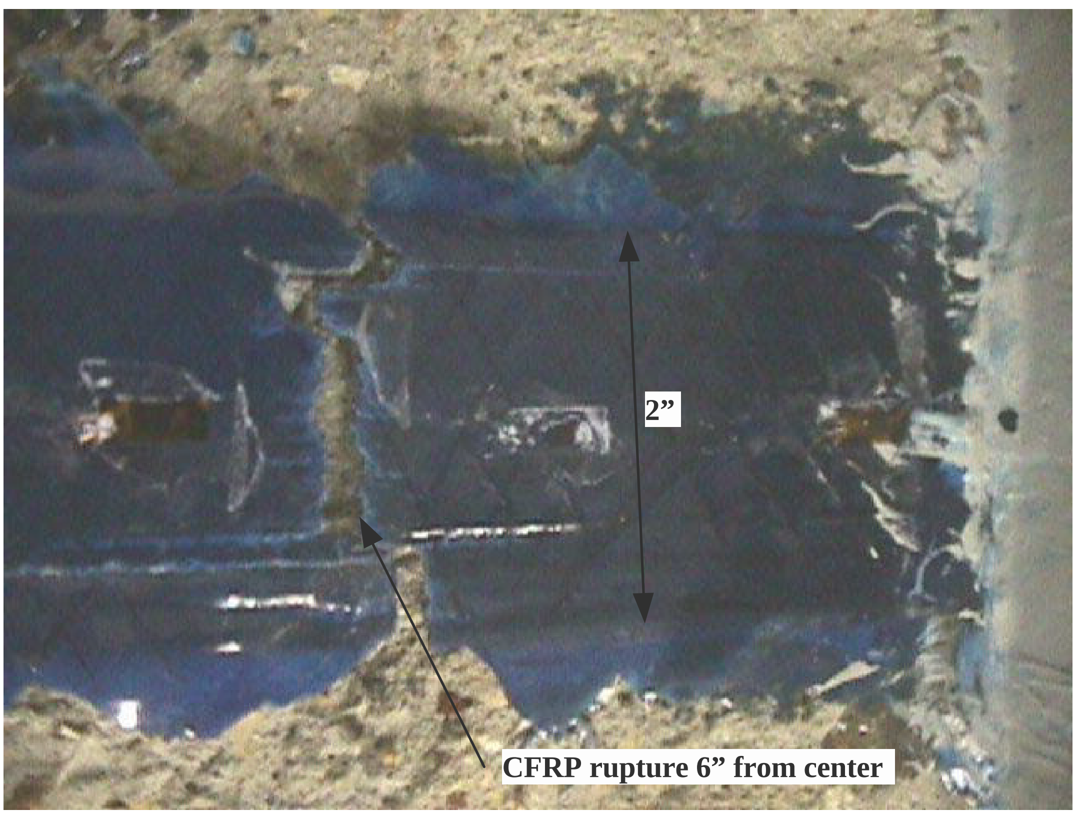

Figure A.32. Picture of failure location for A-3-1-4 (1 in = 25.4 mm)

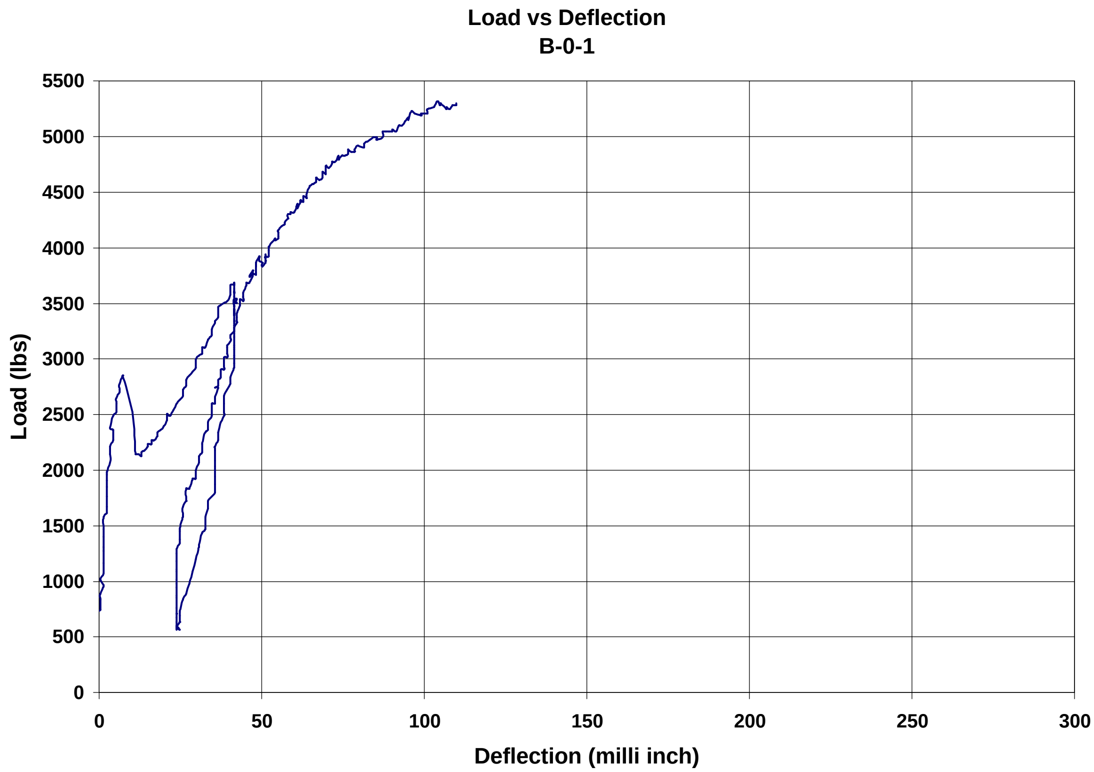

Figure A.33. Load vs. Deflection plot for B-0-1 (1 in = 25.4 mm, 1 lb = 4.448 N)

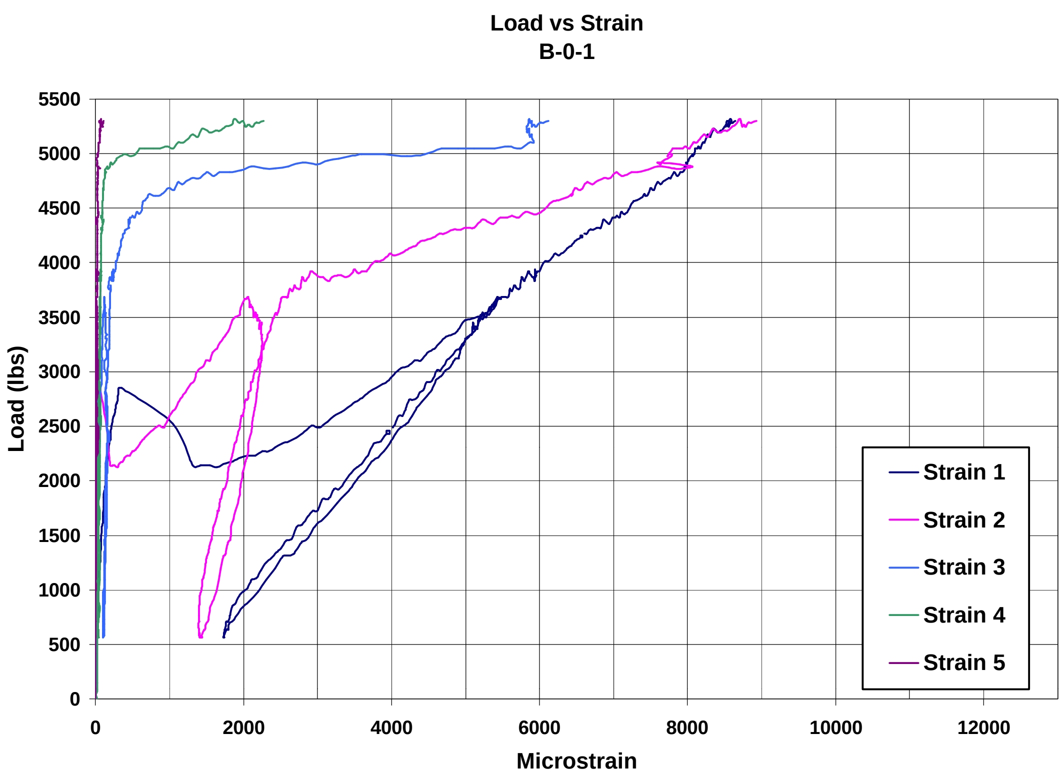

Figure A.34. Load vs. Strain plot for B-0-1 (1 lb = 4.448 N)

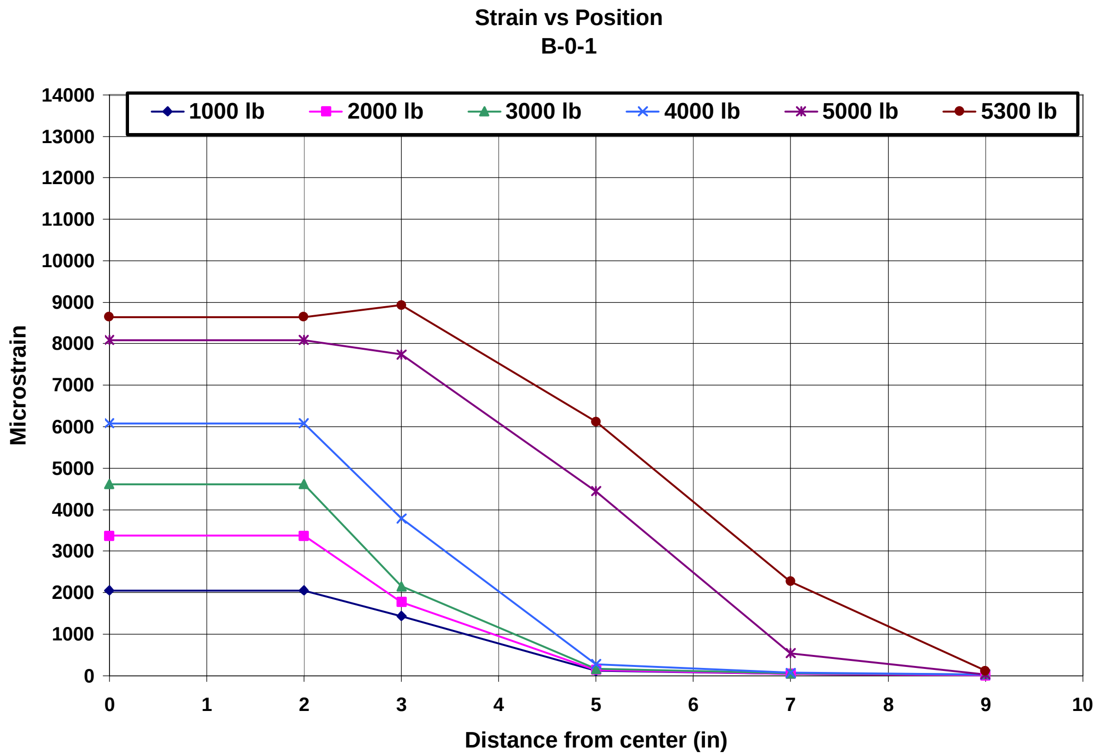

Figure A.35. Strain vs. Position plot for B-0-1 (1 in = 25.4 mm, 1 lb = 4.448 N)

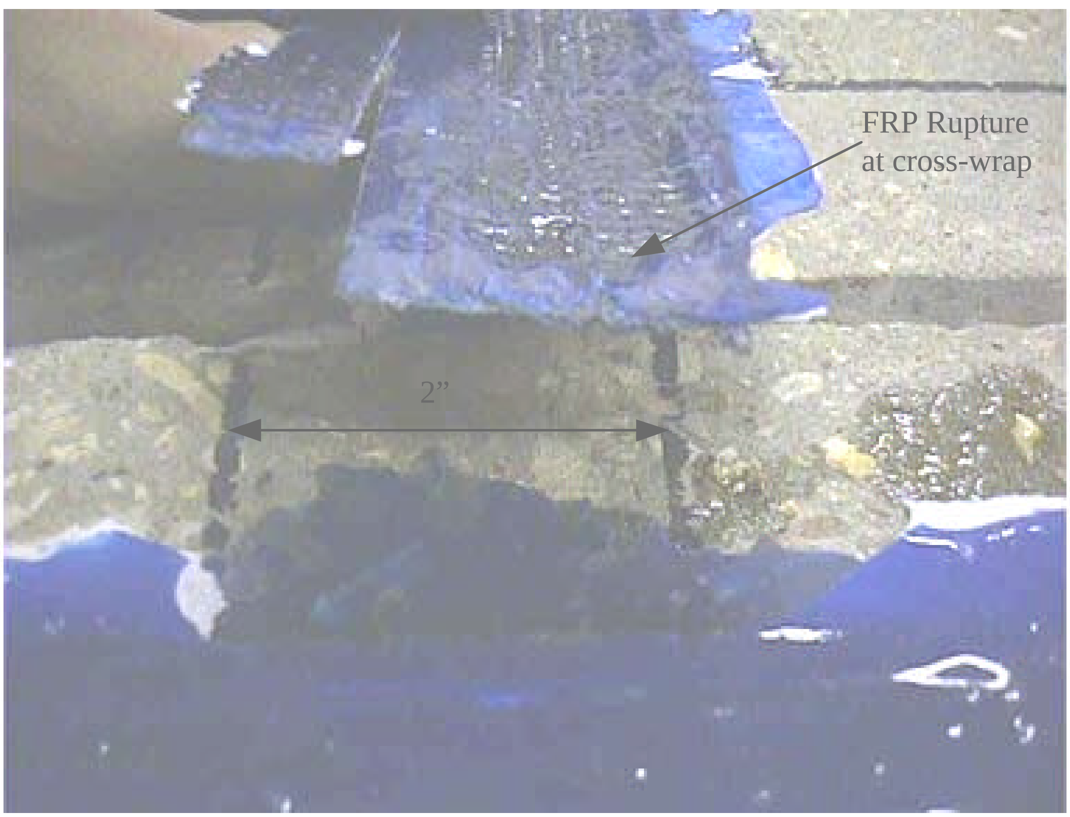

Figure A.36. Picture of failure location for B-0-1 (1 in = 25.4 mm)

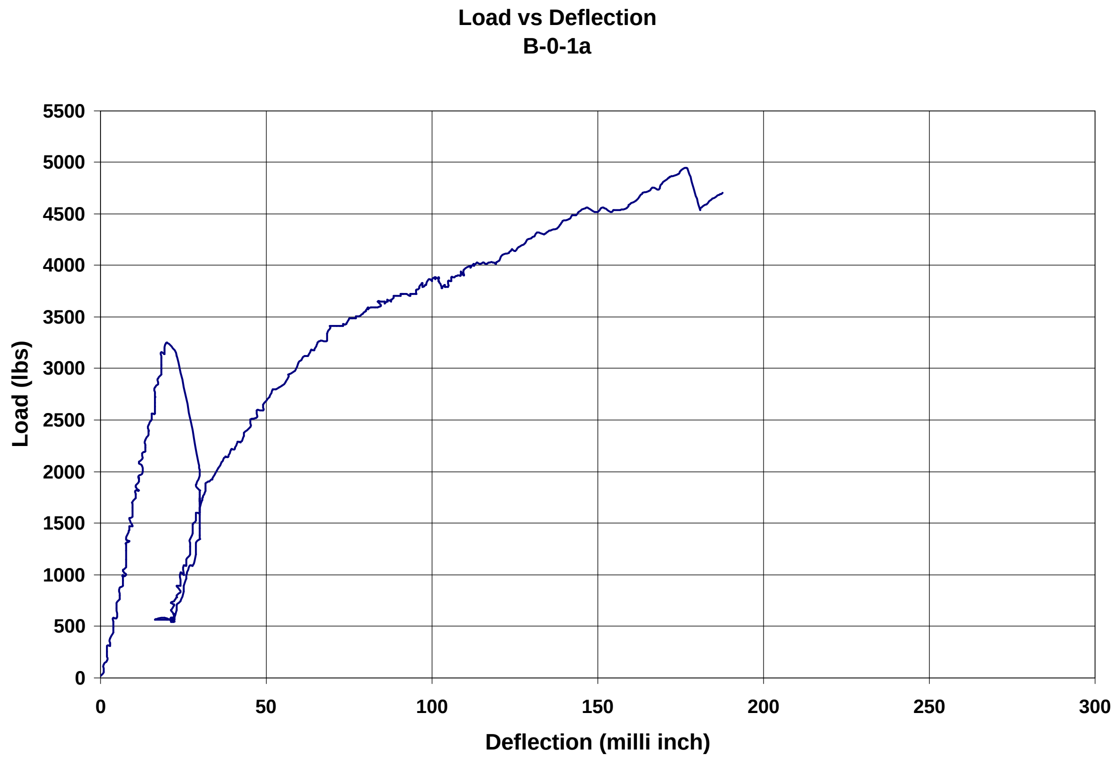

Figure A.37. Load vs. Deflection plot for B-0-1a (1 in = 25.4 mm, 1 lb = 4.448 N)

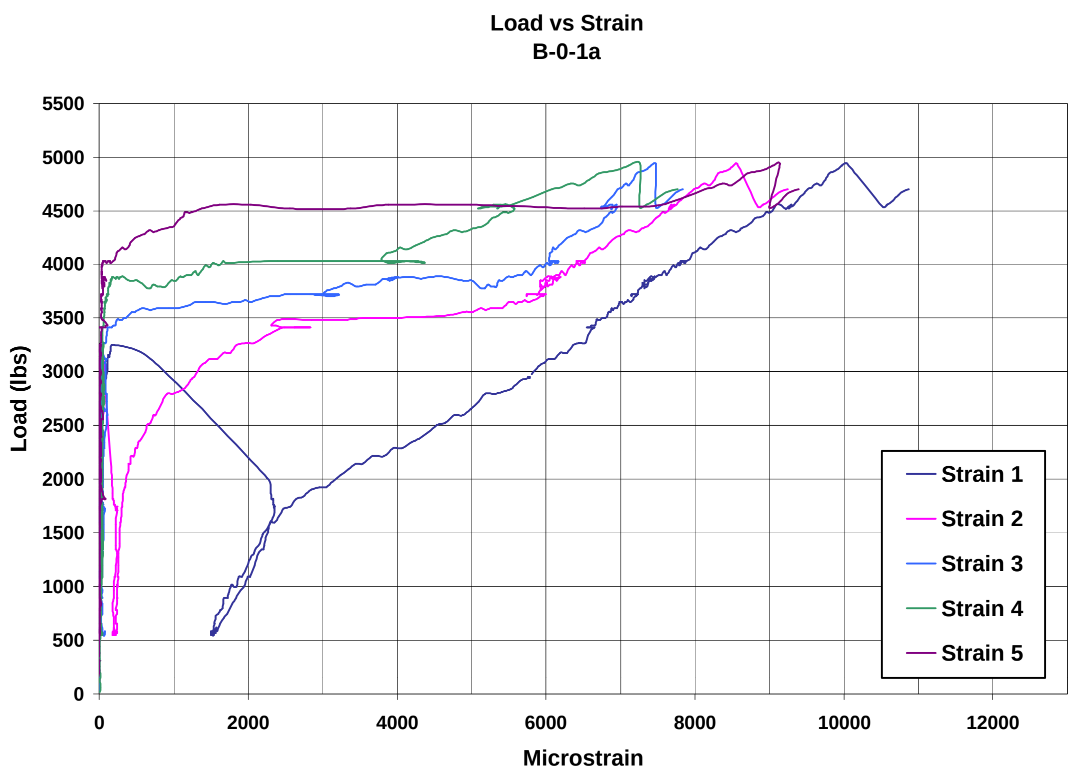

Figure A.38. Load vs. Strain plot for B-0-1a (1 lb = 4.448 N)

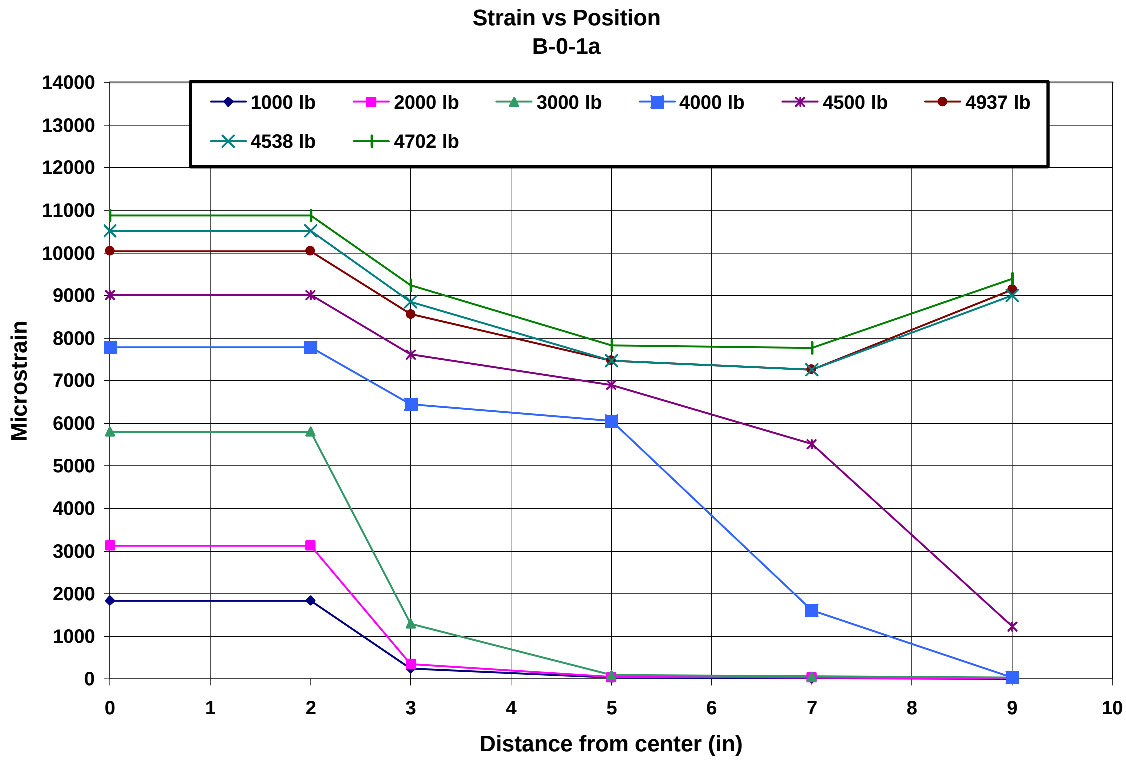

Figure A.39. Strain vs. Position plot for B-0-1a (1 in = 25.4 mm, 1 lb = 4.448 N)

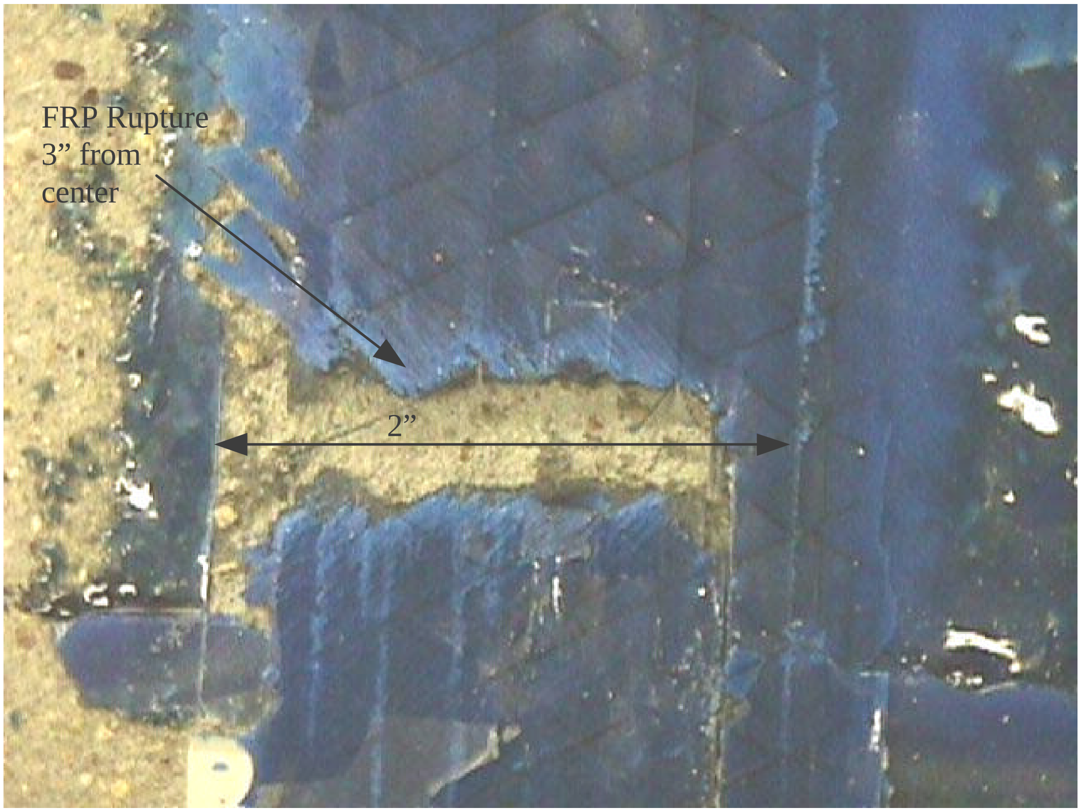

Figure A.40. Picture of failure location for B-0-1a (1 in = 25.4 mm)

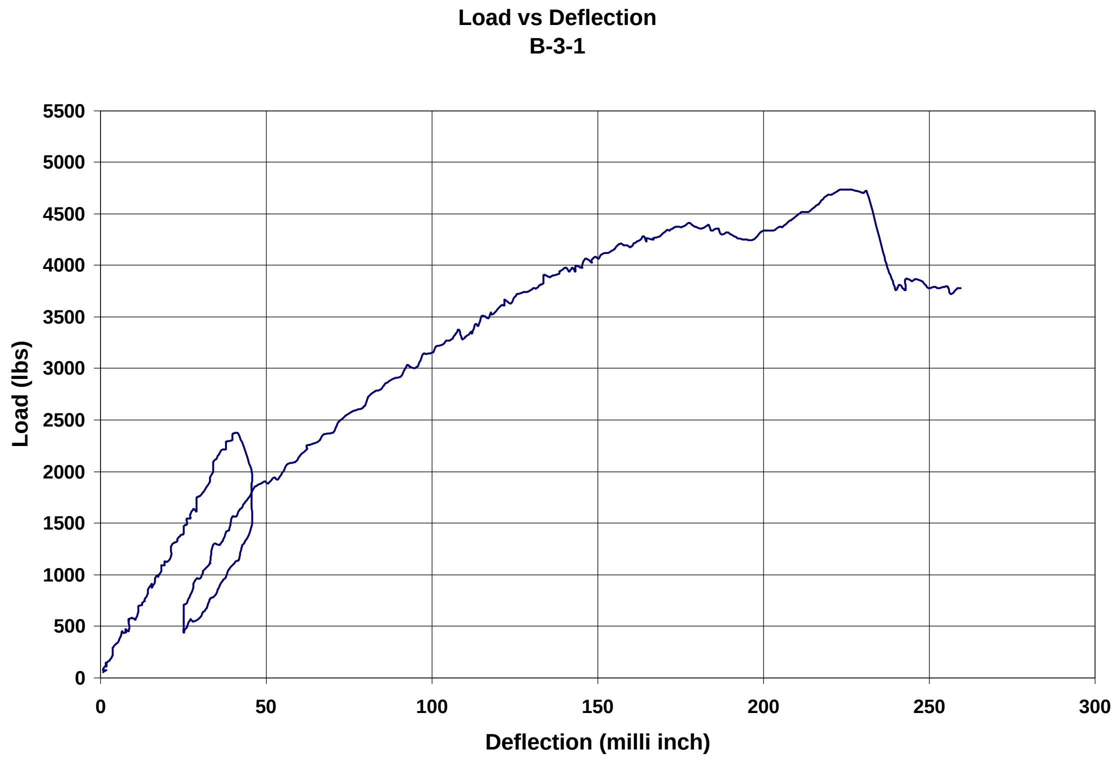

Figure A.41. Load vs. Deflection plot for B-3-1 (1 in = 25.4 mm, 1 lb = 4.448 N)

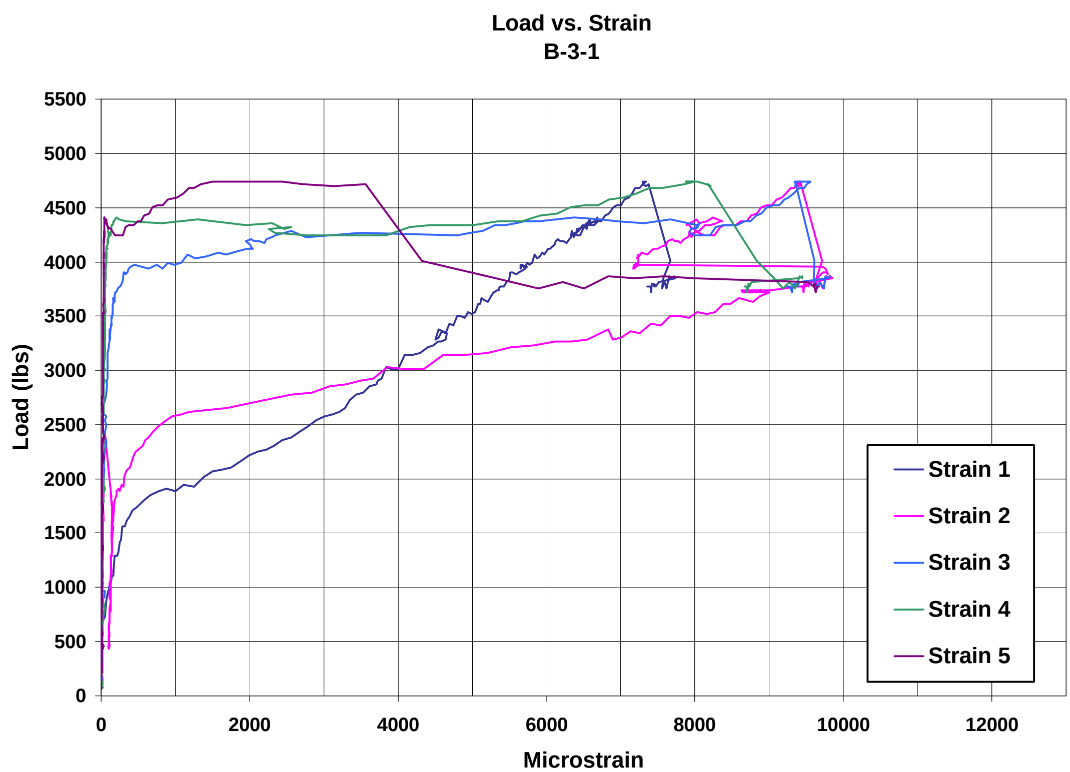

Figure A.42. Load vs. Strain plot for B-3-1 (1 lb = 4.448 N)

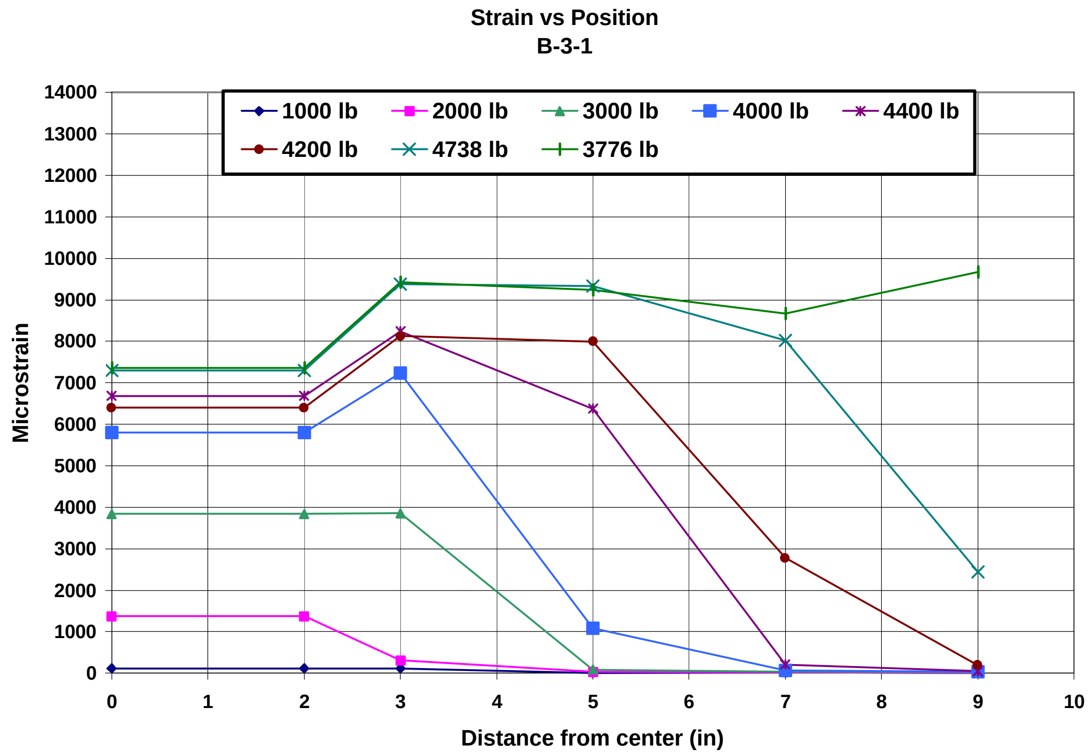

Figure A.43. Strain vs. Position plot for B-3-1 (1 in = 25.4 mm, 1 lb = 4.448 N)

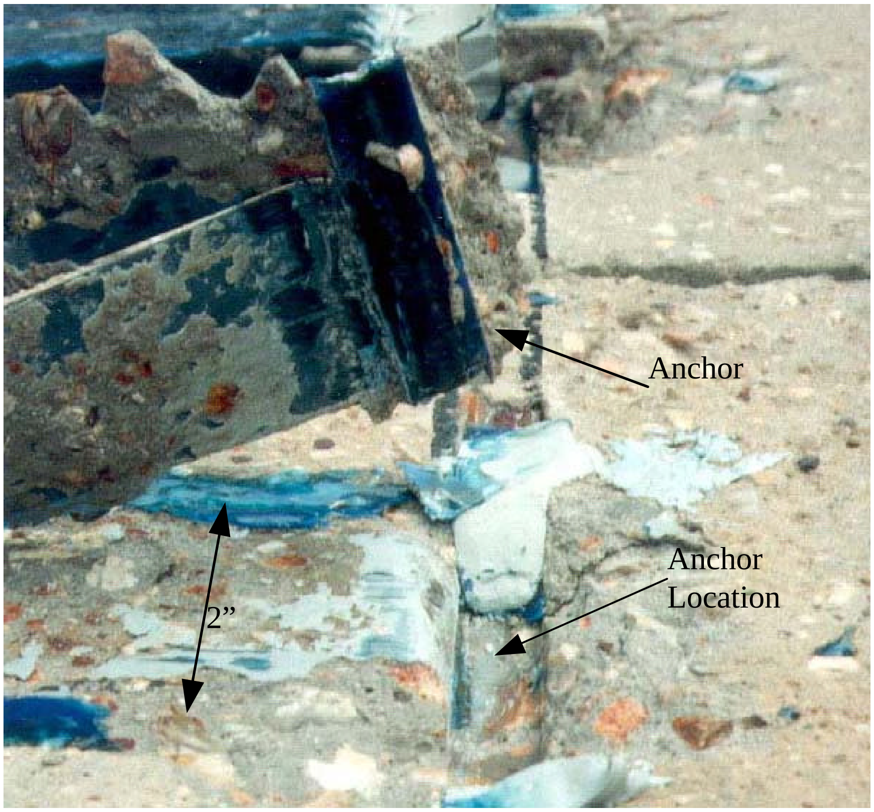

Figure A.44. Picture of failure location for B-3-1 (1 in = 25.4 mm)

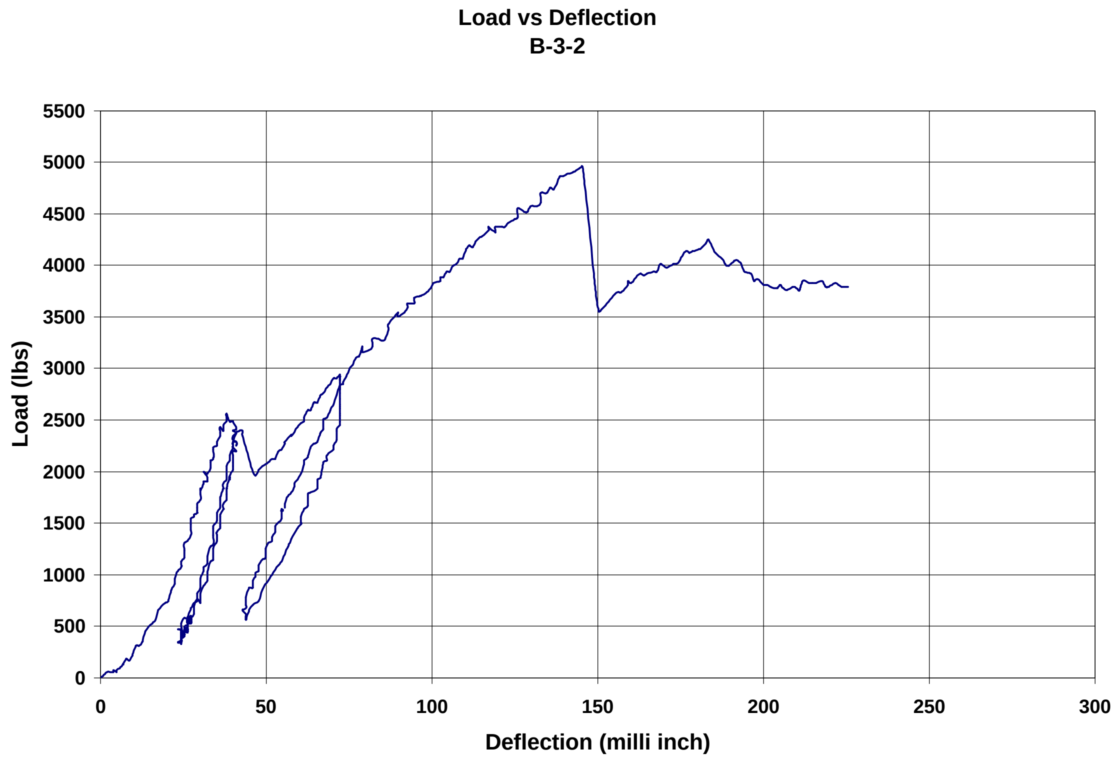

Figure A.45. Load vs. Deflection plot for B-3-2 (1 in = 25.4 mm, 1 lb = 4.448 N)

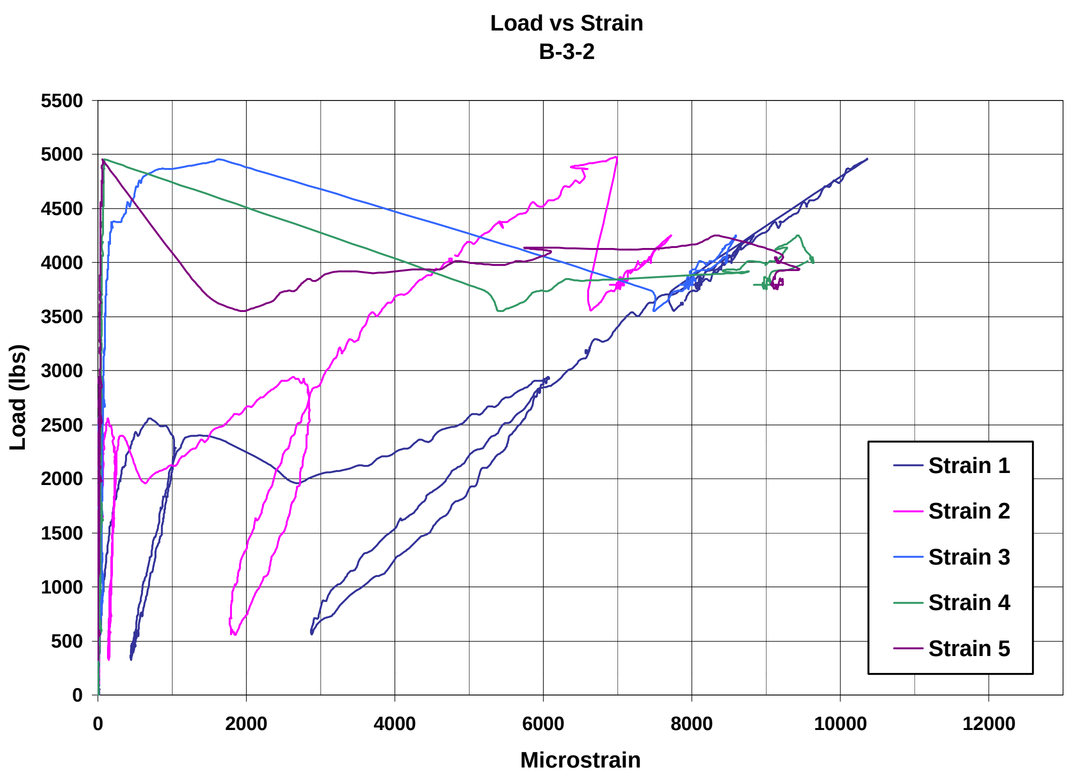

Figure A.46. Load vs. Strain plot for B-3-2 (1 lb = 4.448 N)

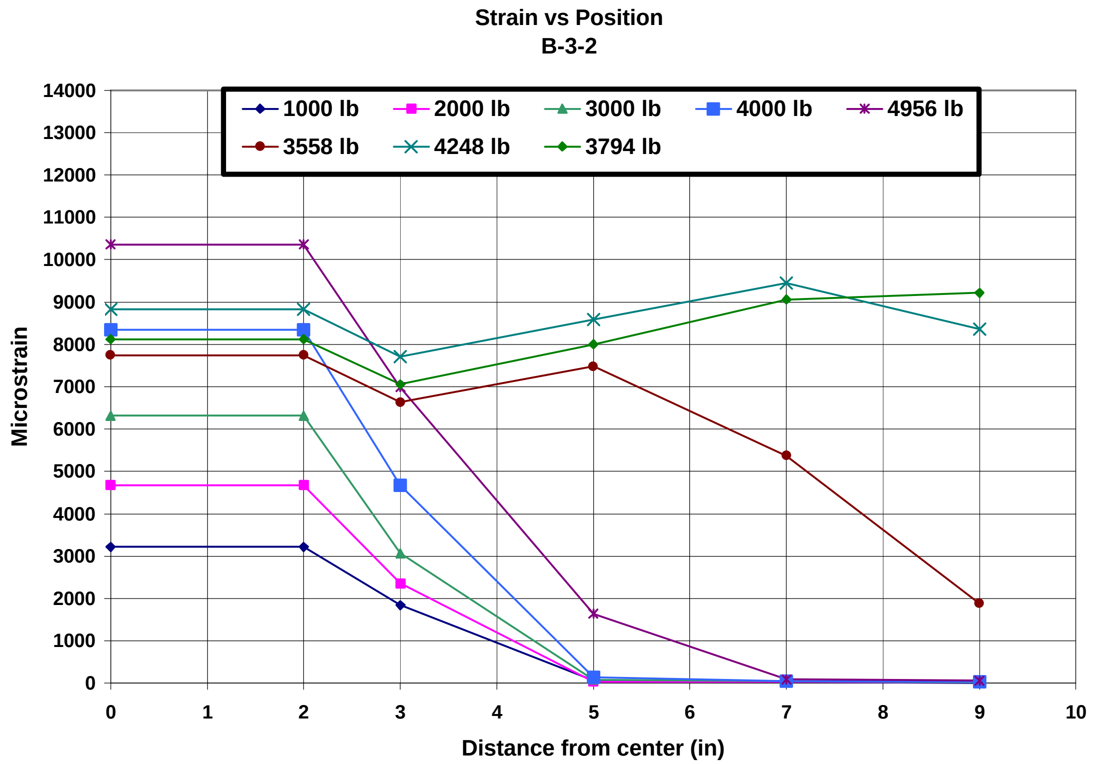

Figure A.47. Strain vs. Position plot for B-3-2 (1 in = 25.4 mm, 1 lb = 4.448 N)

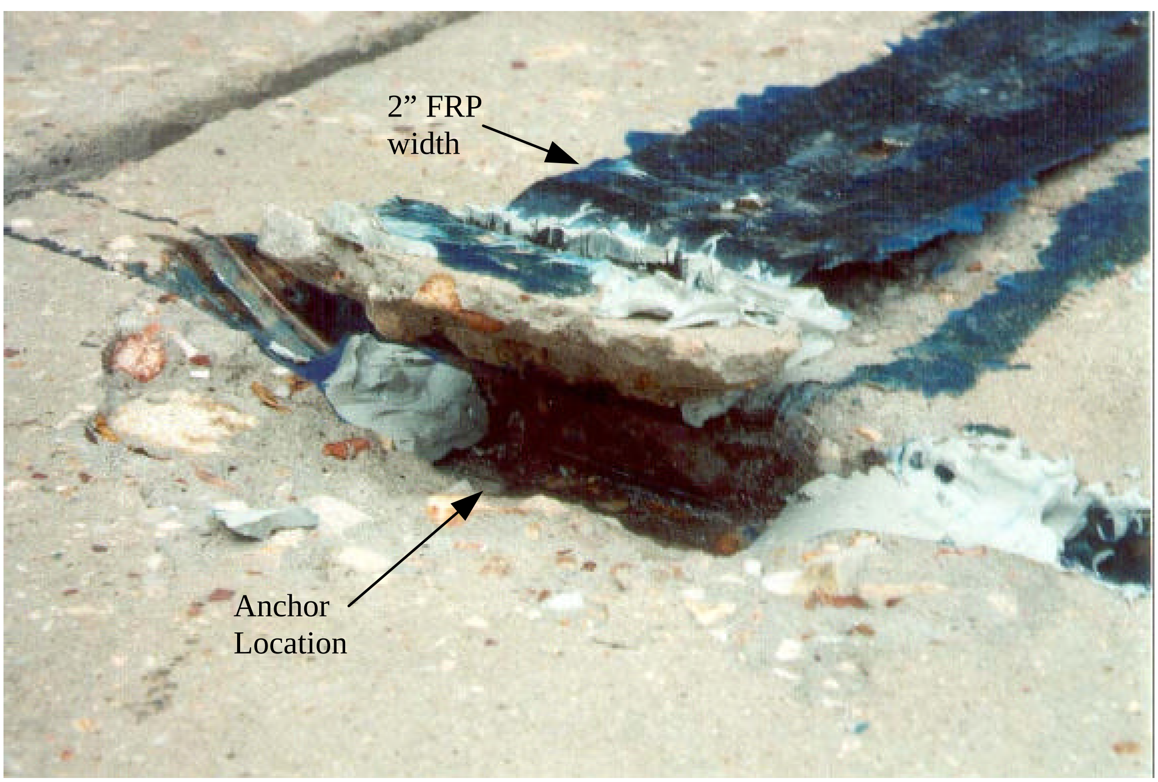

Figure A.48. Picture of failure location for B-3-2 (1 in = 25.4 mm)

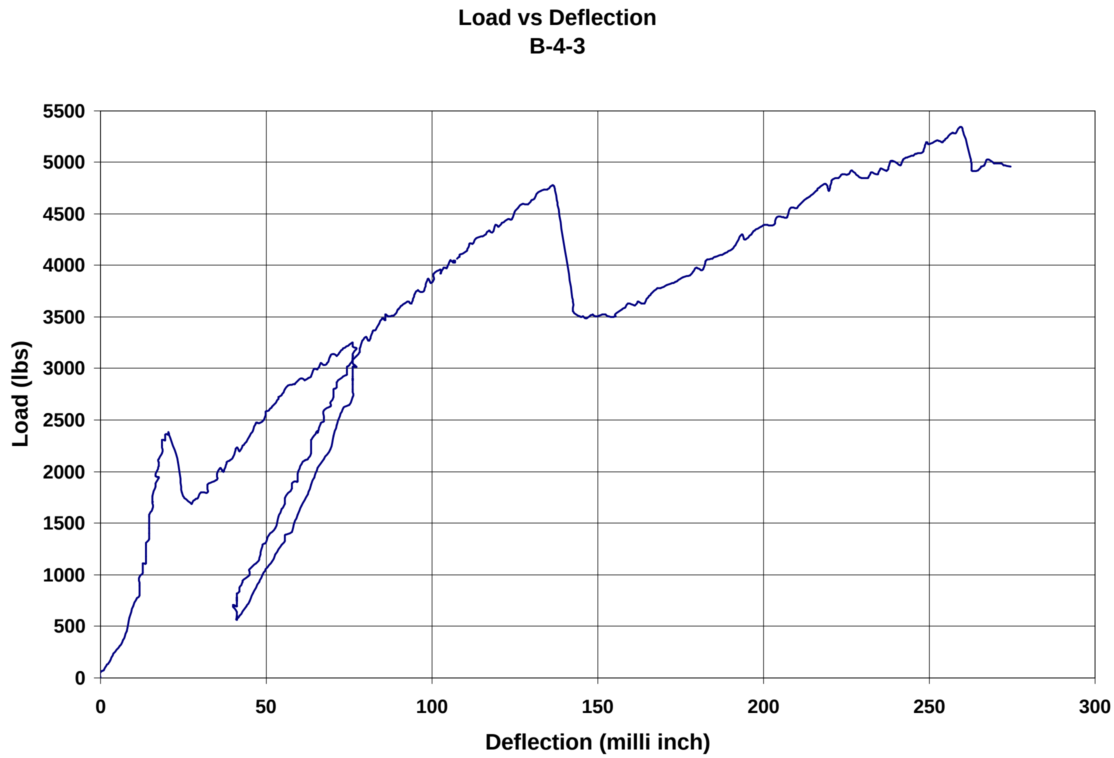

Figure A.49. Load vs. Deflection plot for B-4-3 (1 in = 25.4 mm, 1 lb = 4.448 N)

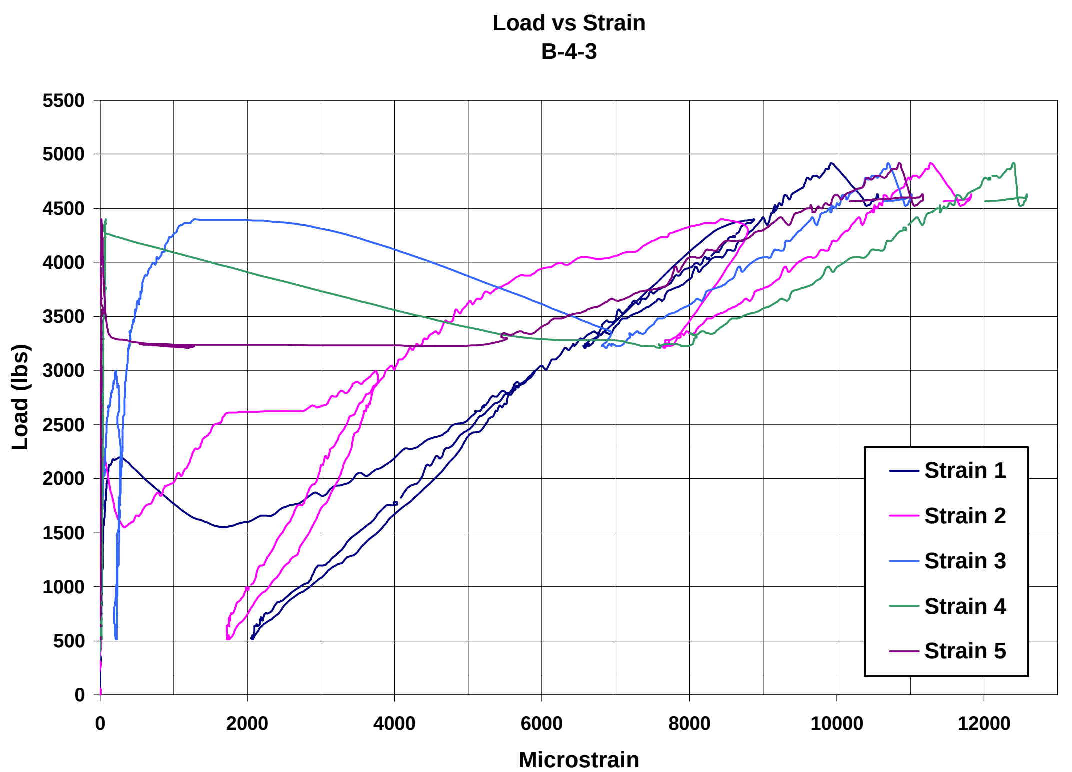

Figure A.50. Load vs. Strain plot for B-4-3 (1 lb = 4.448 N)

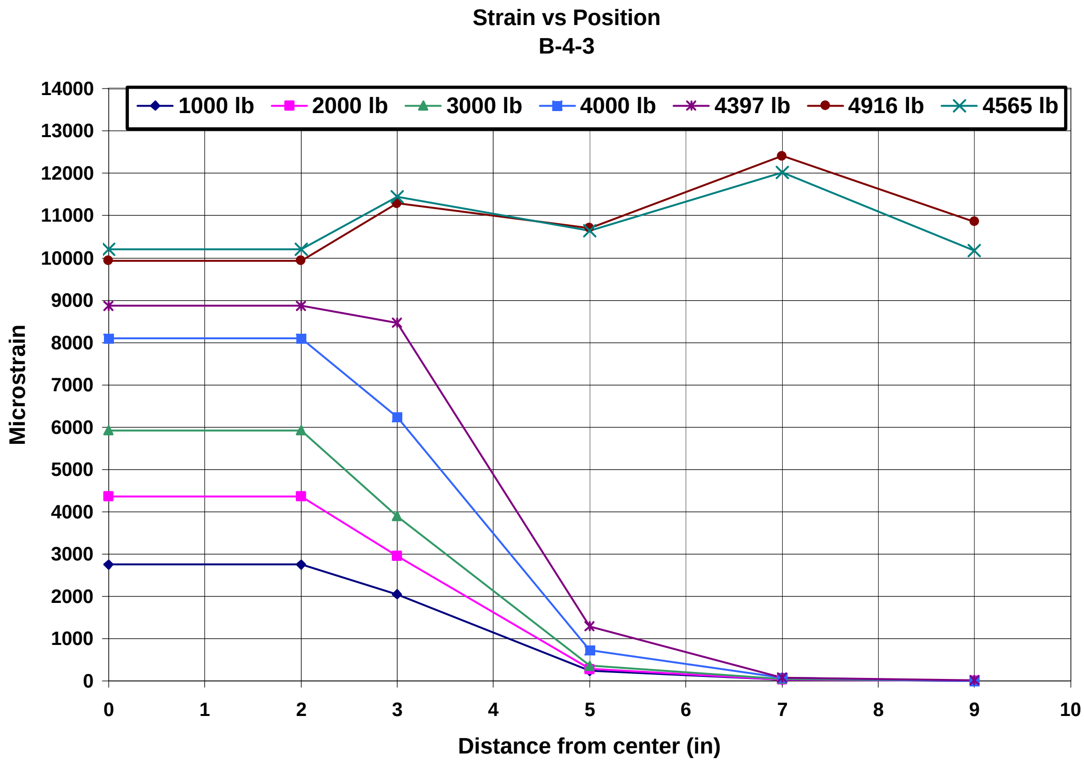

Figure A.51. Strain vs. Position plot for B-4-3 (1 in = 25.4 mm, 1 lb = 4.448 N)

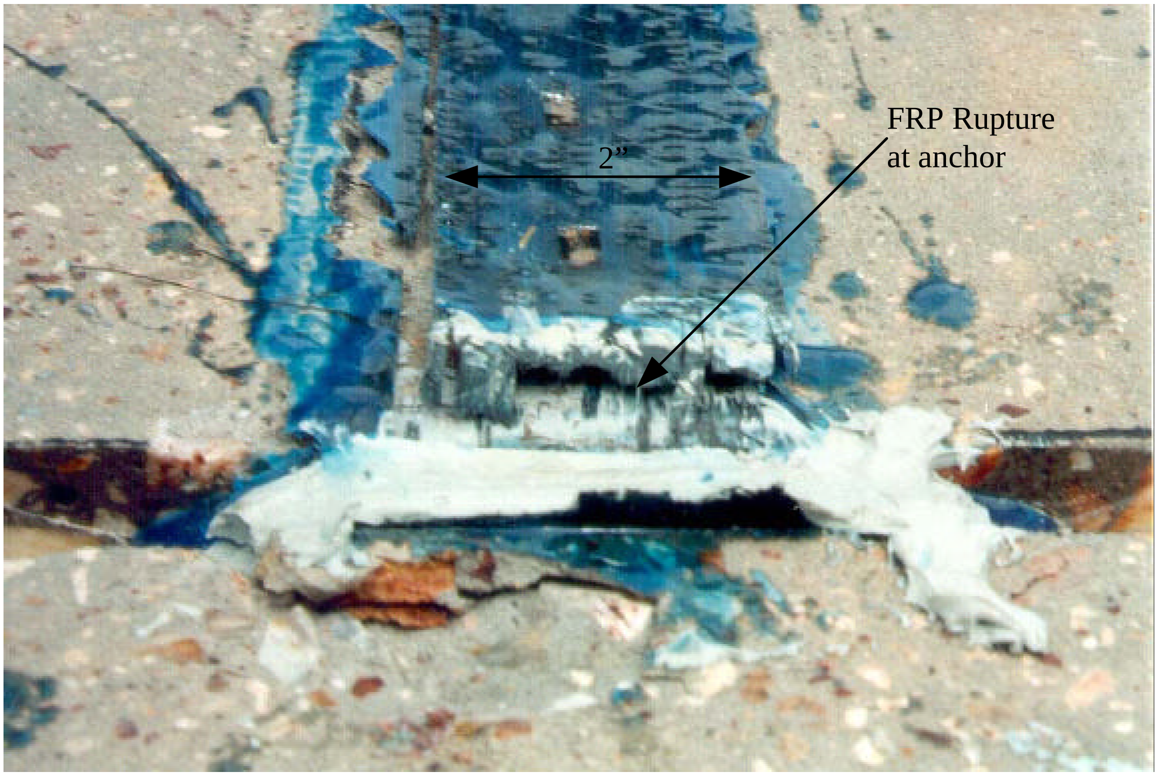

Figure A.52. Picture of failure location for B-4-3 (1 in = 25.4 mm)

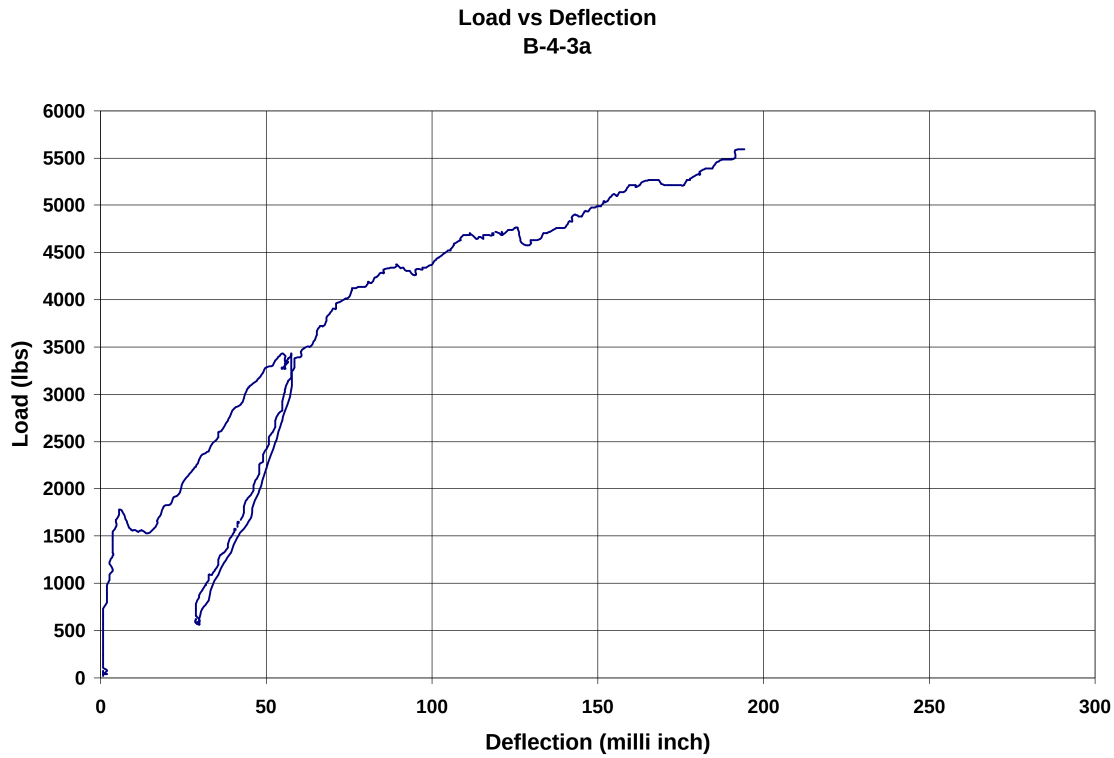

Figure A.53. Load vs. Deflection plot for B-4-3a (1 in = 25.4 mm, 1lb = 4.448 N)

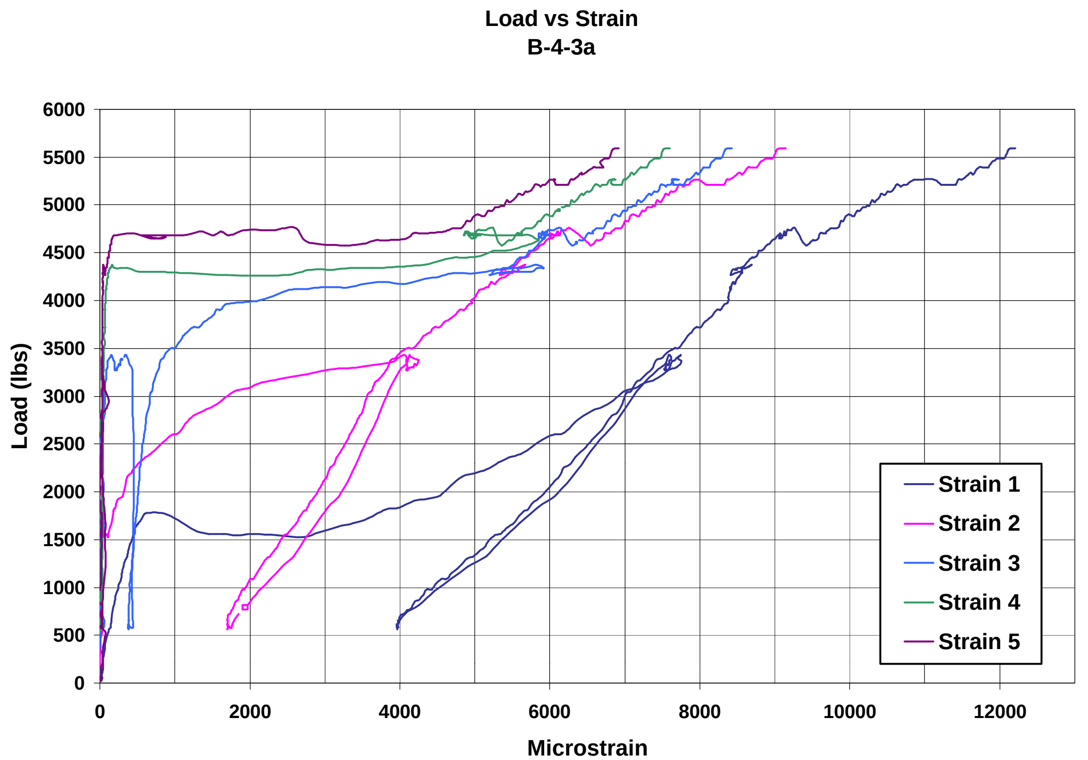

Figure A.54. Load vs. Strain plot for B-4-3a (1lb = 4.448 N)

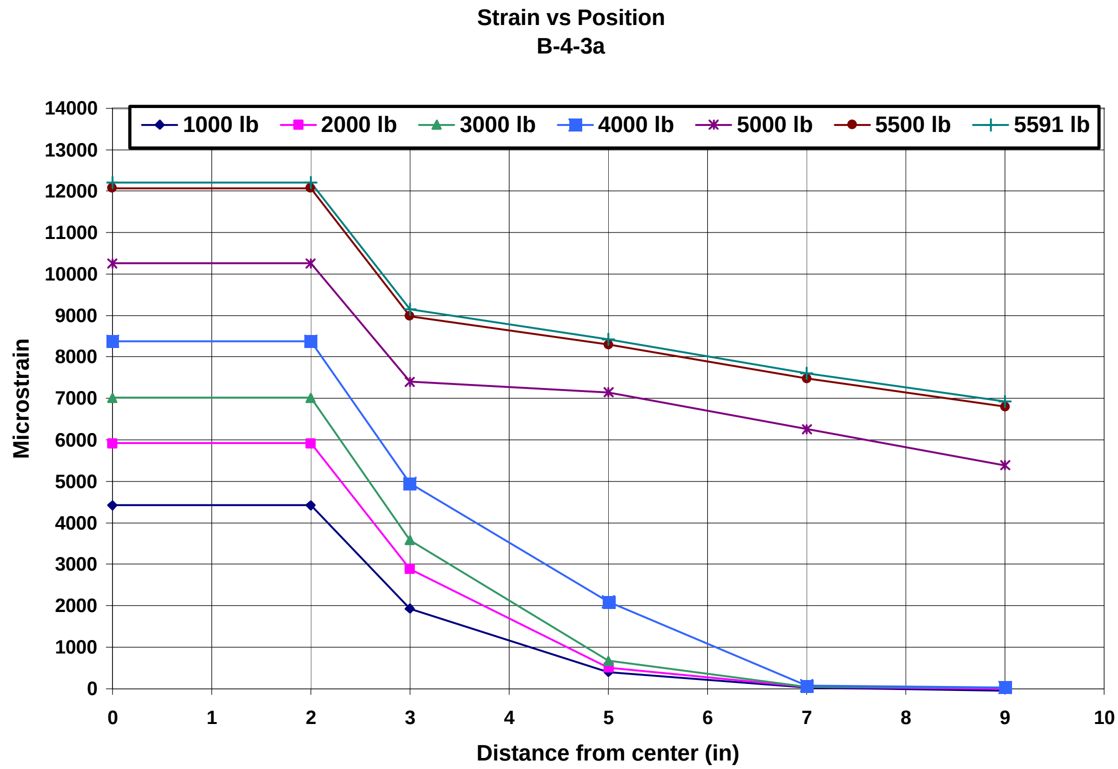

Figure A.55. Strain vs. Position plot for B-4-3a (1 in = 25.4 mm, 1lb = 4.448 N)

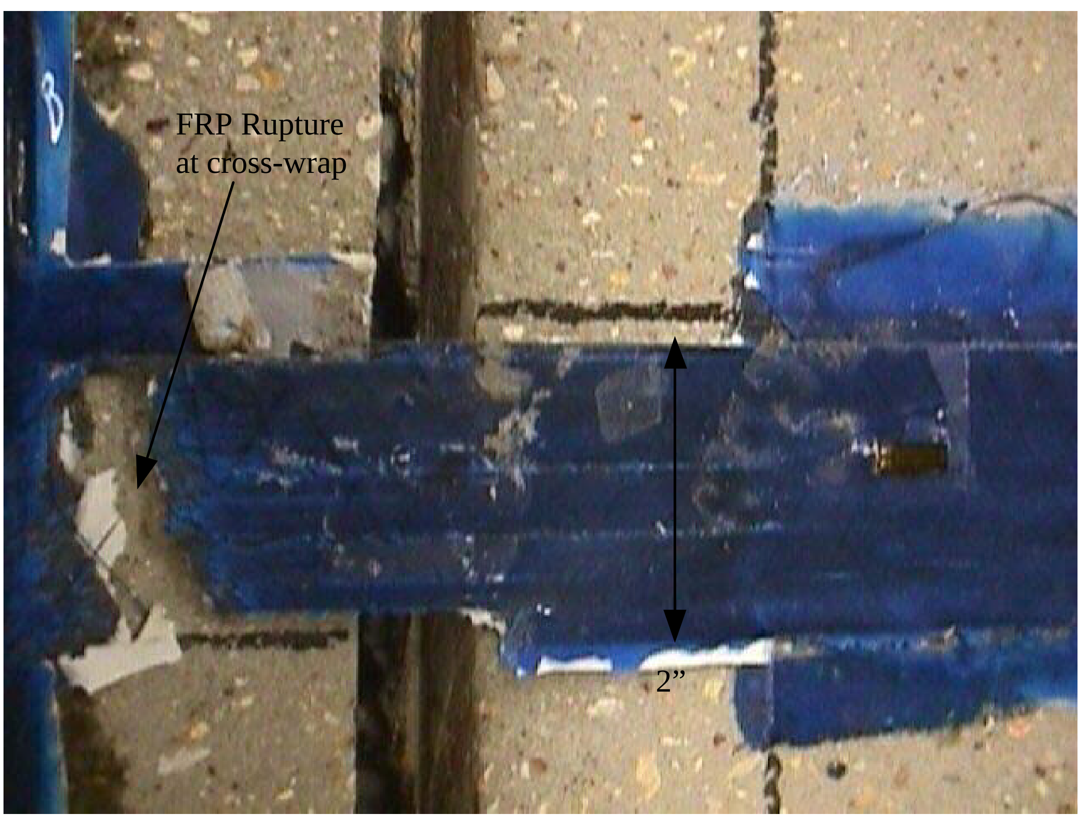

Figure A.56. Picture of failure location for B-4-3a (1 in = 25.4 mm)

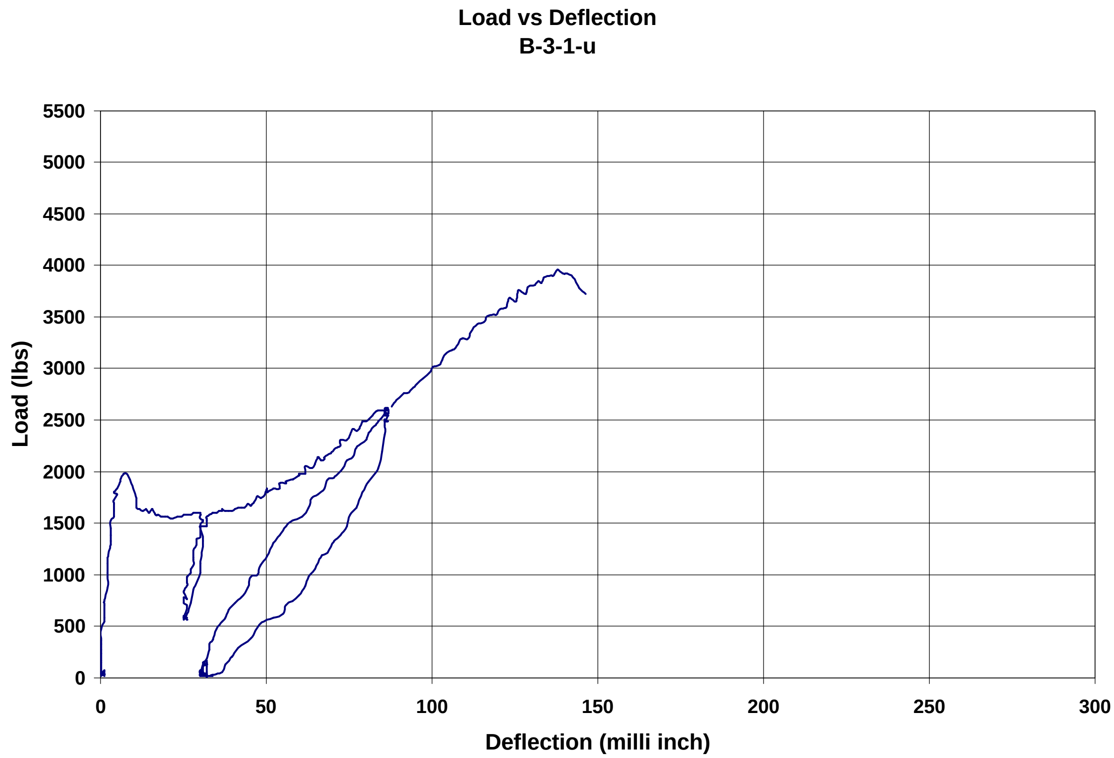

Figure A.57. Load vs. Deflection plot for B-3-1-u (1 in = 25.4 mm, 1 lb = 4.448 N)

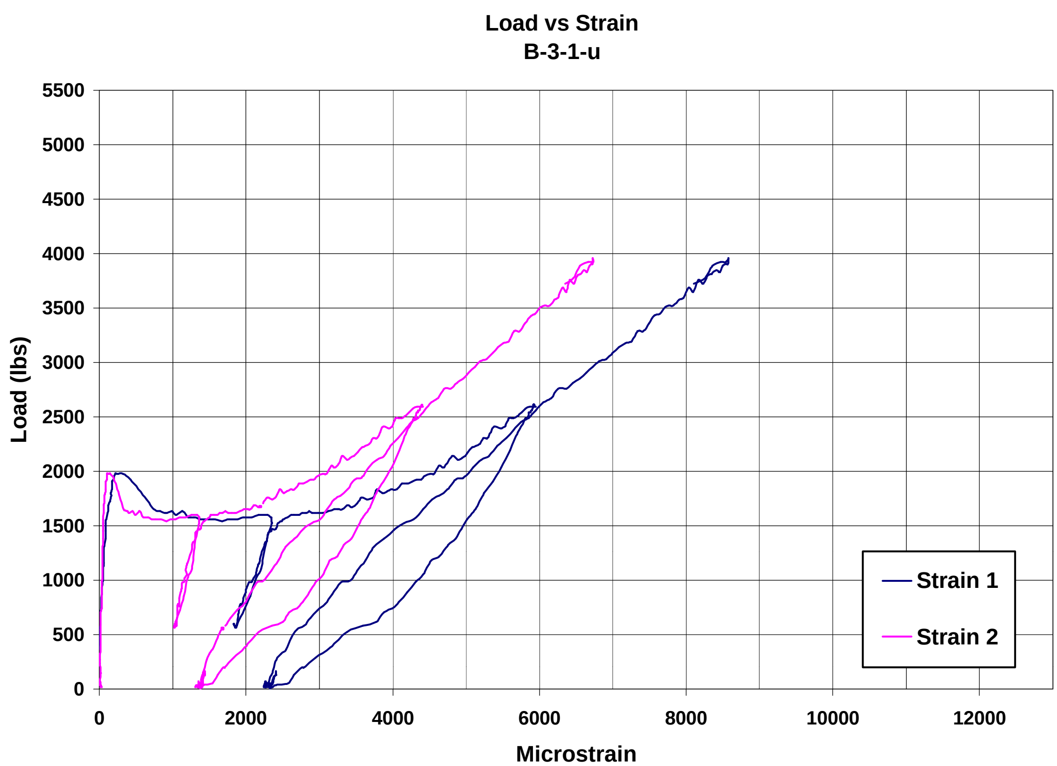

Figure A.58. Load vs. Strain plot for B-3-1-u (1 lb = 4.448 N)

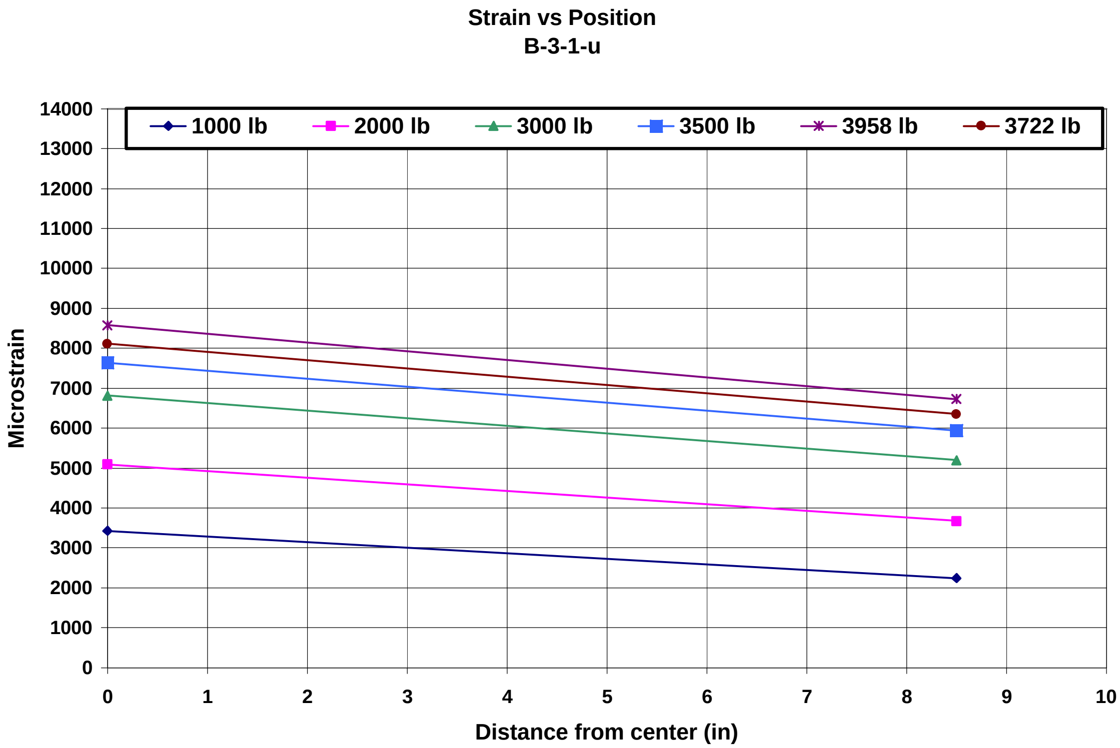

Figure A.59. Strain vs. Position plot for B-3-1-u (1 in = 25.4 mm, 1 lb = 4.448 N)

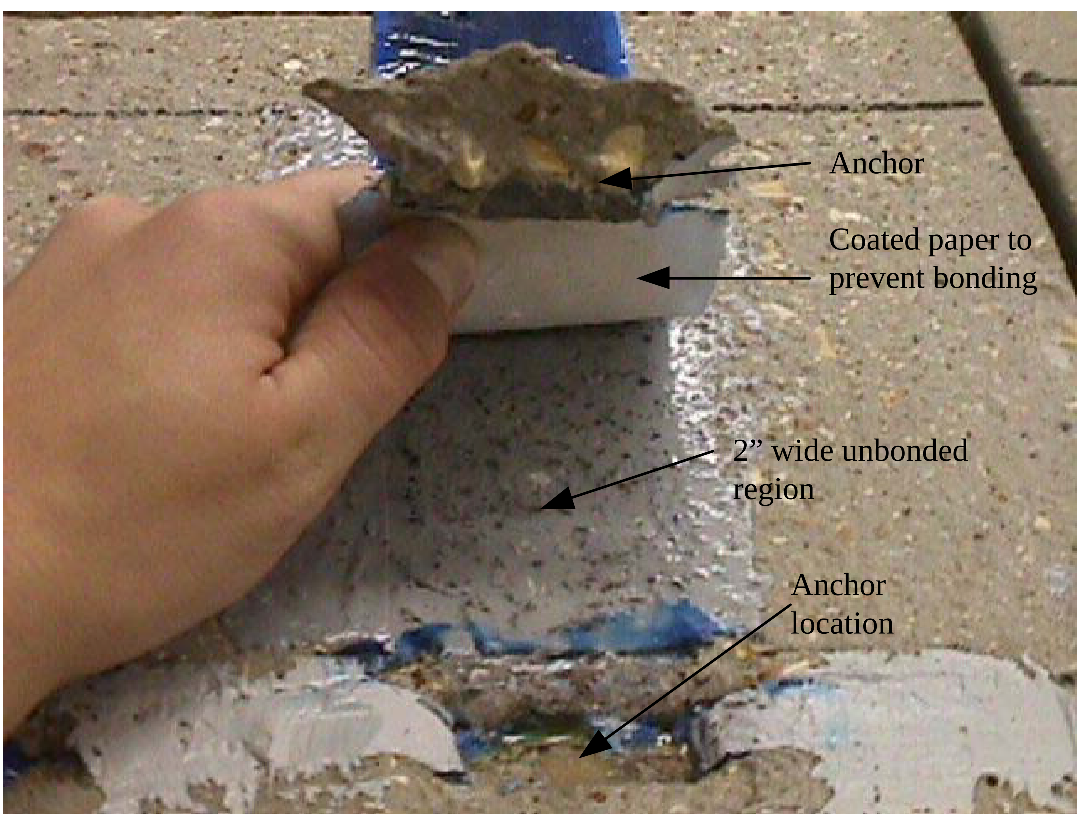

Figure A.60. Picture of failure location for B-3-1-u (1 in = 25.4 mm)

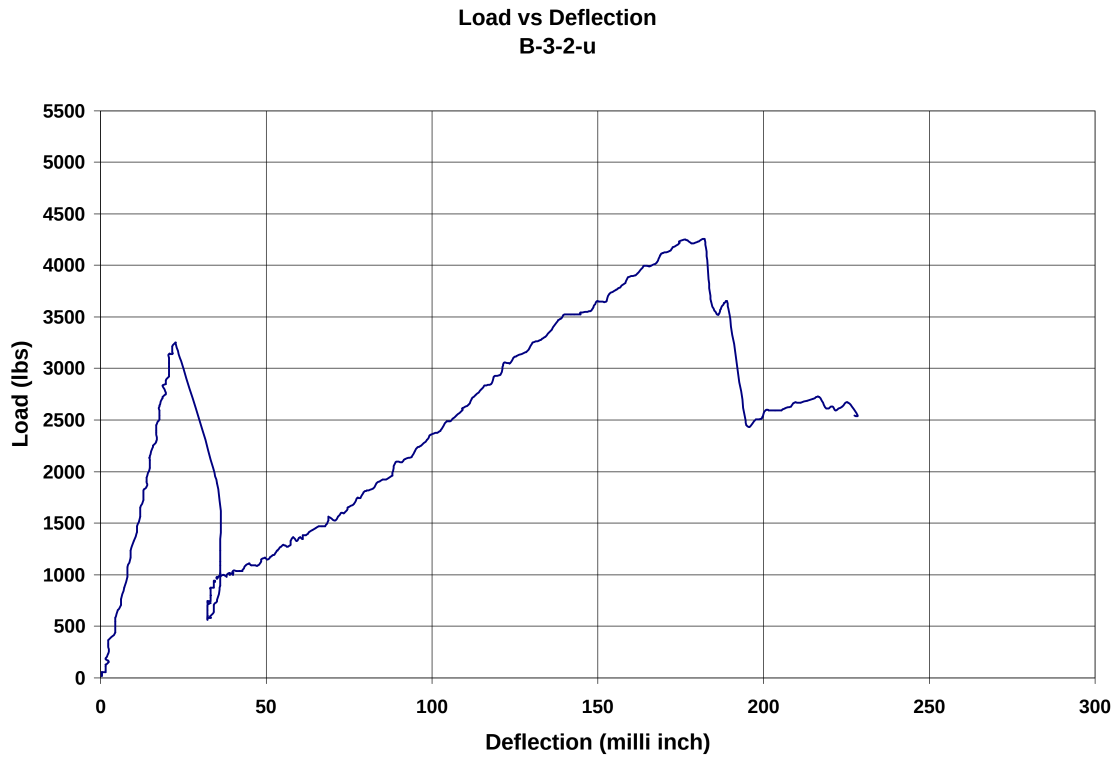

Figure A.61. Load vs. Deflection plot for B-3-2-u (1 in = 25.4 mm, 1 lb = 4.448 N)

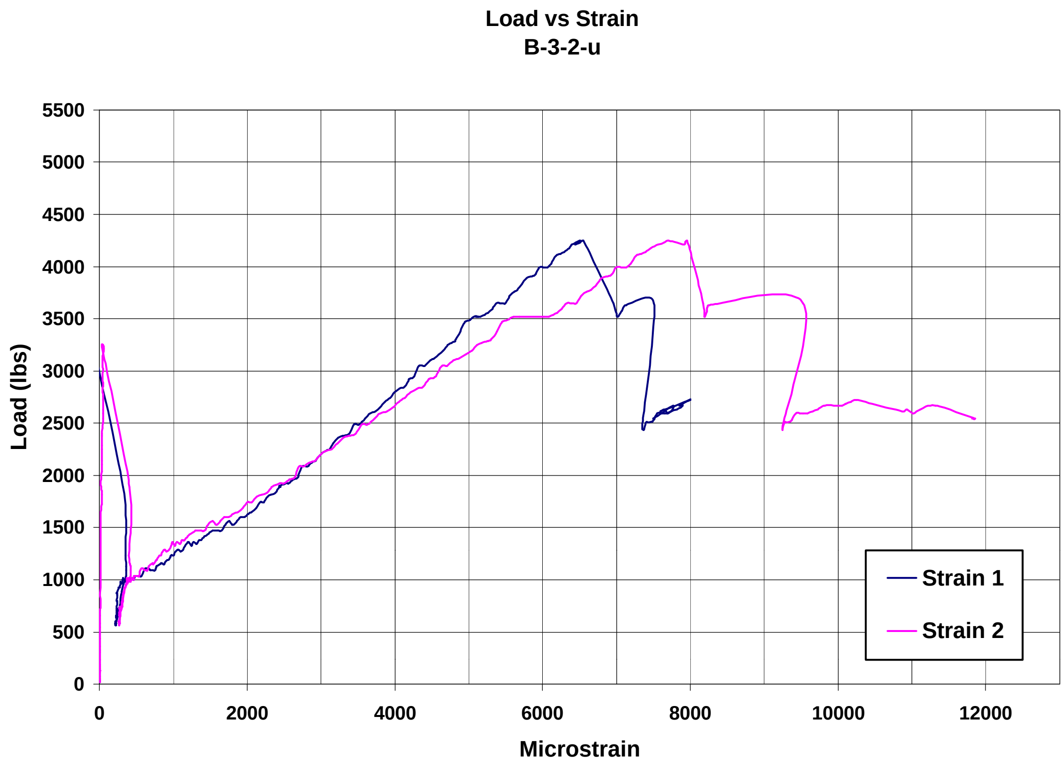

Figure A.62. Load vs. Strain plot for B-3-2-u (1 lb = 4.448 N)

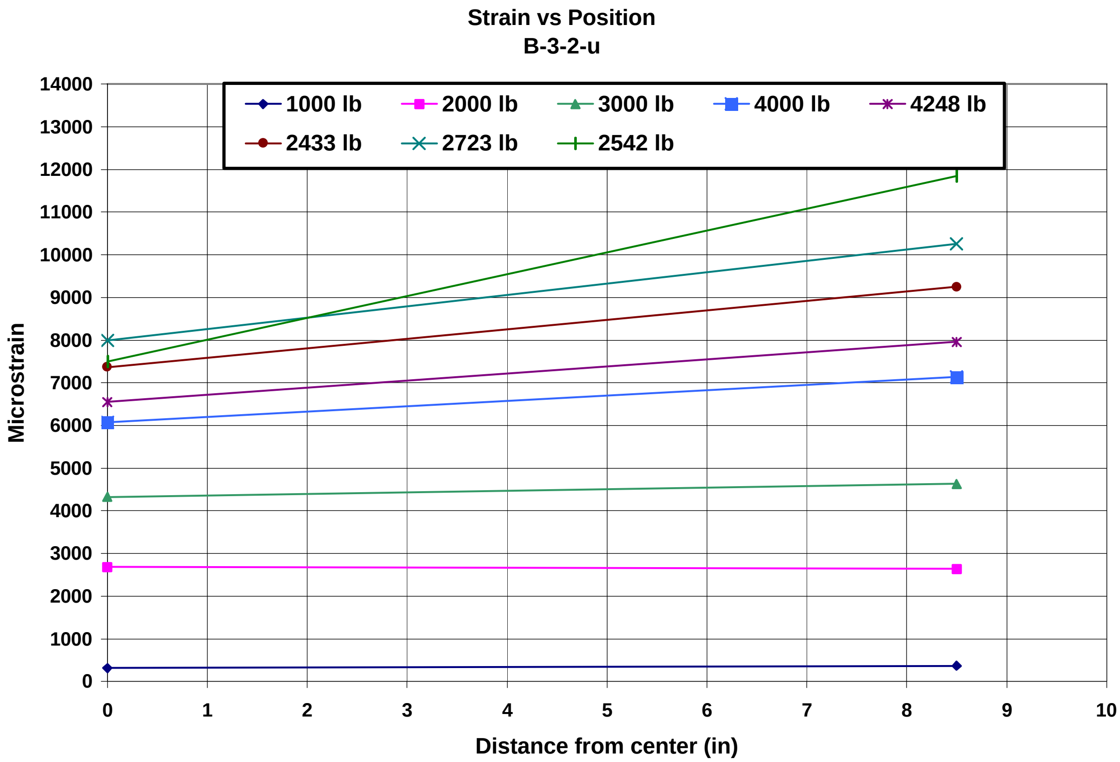

Figure A.63. Strain vs. Position plot for B-3-2-u (1 in = 25.4 mm, 1 lb = 4.448 N)

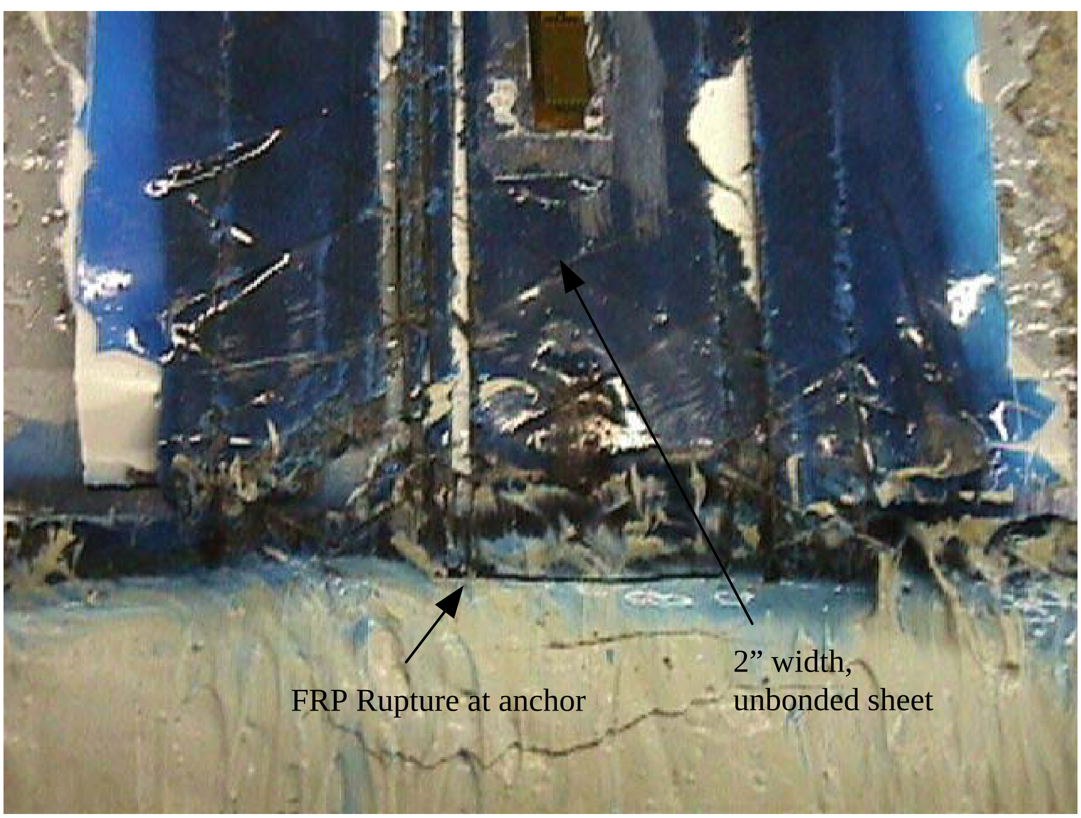

Figure A.64. Picture of failure location for B-3-2-u (1 in = 25.4 mm)